Electric Vehicles as Grid Resources

Mushfiqur R. Sarker

A dissertation
submitted in partial fulfillment of the
requirements for the degree of

Doctor of Philosophy

University of Washington

2016

Reading Committee:

Miguel Ortega-Vazquez, Chair

Daniel Kirschen

Baosen Zhang

Program Authorized to Offer Degree:
Electrical Engineering

University of Washington

Abstract

Electric Vehicles as Grid Resources

Mushfiqur R. Sarker

Chair of the Supervisory Committee:
Professor Miguel Ortega-Vazquez
Electrical Engineering

Electric vehicles (EV) are poised as environmentally-friendly alternatives to conventional combustion vehicles because of the internal battery which uses electricity for transportation. It is estimated the global EV penetration will hit upwards of 20 million on the road by 2020. Even with this technology available today, consumers' EV adoption is hindered due to the high upfront cost, lack of adequate charging infrastructure, range anxiety, and slow charging times. On the other hand, the potential revolution of the transportation sector will bring forth economic benefits to the operations of the power system.

The EV batteries allow flexibility in the amount of power and the specific time of day when they can charge and discharge. Such features enable the extraction of resources from these batteries in order to benefit the power system and EV owner's themselves. However, the challenge remains on how to reduce the issues of EV ownership while the power system extracts services from EVs that benefit operations. The main motivation behind this dissertation is to develop frameworks that take advantage of EVs as grid resources.

TABLE OF CONTENTS

VITA

Mushfiqur Sarker was born in Dhaka, Bangladesh in 1990 and has resided in Corvallis, Oregon, United States for the majority of his life. He received his BSc in Electrical Engineering from Oregon State University in Corvallis, Oregon on June 2012, with an emphasis in Power Systems. In September 2012, he joined the University of Washington in Seattle, Washington, United States to pursue a PhD.

He was awarded the University of Washington Clean Energy Institute's Graduate Fellowship (2013-2015) and also the Clean Energy Institutes Exploration Grant (2015-2016). In addition, he received the Vikram Jandhyala and Suja Vaidyanathan Endowed Innovation Award from the University of Washington.

ACKNOWLEDGMENTS

My utmost gratitude goes to my professor, Miguel A. Ortega-Vazquez, for providing excellent guidance. His professionalism and commitment is a trait I will continue to uphold in my career. I am also thankful to Professor Daniel S. Kirschen for providing excellent advice along the way. In addition, thanks to all my colleagues at the University of Washington's MOVES and REAL research groups that has assisted me throughout my PhD.

Most of all, this would not have been possible without the unconditional support throughout the years from my parents and my brother. They taught me with hardwork I can achieve whatever I desire, a teaching I will continue to follow in the years to come. In addition, the constant encouragement, support, and care I have received from my wife has allowed me to obtain my PhD successfully.

ACRONYMS

B2B: Battery-to-Battery

B2G: Battery-to-Grid

B2S: Battery-to-Station

BSS: Battery Swapping Station

CAISO: California Independent System Operator

CDF: Cumulative Distribution Function

DA: Day-ahead

DR: Demand Response

DSM: Demand Side Management

DSO: Distribution System Operator

DW: Dishwasher

EMS: Energy Management System

EMCHG: Energy Market Charge

EMDSG: Energy Market Discharge

ESOC: Energy State-of-Charge

ES: Energy Storage

EPA: Environmental Protection Agency

EV: EV

EVCS: Electric Vehicle Charging Stations

EWH: Electric Water Heater

G2B: Grid-to-Battery

G2V: Grid-to-Vehicle

HVAC: Heating, ventilation, and air conditioning

ICE: Internal Combustion Engine

LI-ION: Lithium-ion

MILP: Mixed Integer Linear Program

MC: Monte Carlo

NHTS: National Household Travel Survey

PEV: PEV

PJM: Pennsylvania-New Jersey-Maryland

PQP: Price-Quantity-Probability

PS: Pre-scheduling

PV: Photovoltaics

REF: Refrigerator

REGUP: Regulation Up

REGDN: Regulation Down

RES: Renewable Energy Resources

RO: Robust Optimization

RS: Re-scheduling

RT: Real-time

RTP: Real-Time Pricing

SO: System Operator

STOPCHG: Stop Charge

STOPDSG: Stop Discharge

SOS2: Special Ordered Sets of Type 2

TOU: Time-of-Use

UC: Unit commitment

V2G: Vehicle-to-Grid

V2H: Vehicle-to-Home

WM: Washing machine

LIST OF FIGURES

LIST OF TABLES

LIST OF PUBLICATIONS

Journal Publications

1. **Sarker, M. R.**; Murbach, M. D.; Schwartz, D. T., Ortega-Vazquez, M. A., "Optimal Energy Storage Management System: Trade-off between Grid Economics and Health," in IEEE Transactions on Smart Grid, *to be submitted August 2016*

2. **Sarker, M. R.**; Pandzic, H.; Sun, K., Ortega-Vazquez, M. A., "Optimal Market Participation of Aggregated Electric Vehicle Charging Stations Considering Uncertainty," in IEEE Transactions on Smart Grid, *to be submitted August 2016*

3. Contreras Ocaña, J. E.; **Sarker, M. R.**; Ortega-Vazquez, M. A.,"Decentralized Coordination of a Building Manager and an Electric Vehicle Aggregator," in IEEE Transactions on Smart Grid, *Revise and resubmit July 2016*

4. Olsen, D. J.; **Sarker, M. R.**; Ortega-Vazquez, M. A., "Optimal Penetration of Home Energy Management Systems in Distribution Networks Considering Transformer Aging," in IEEE Transactions on Smart Grid, *Revise and resubmit June 2016*

5. **Sarker, M. R.**; Olsen, D. J.; Ortega-Vazquez, M. A., "Co-Optimization of Distribution Transformer Aging and Energy Arbitrage Using Electric Vehicles," in IEEE Transactions on Smart Grid, March 2016, Early Access.

   - Link: ieeexplore.ieee.org/xpl/articleDetails.jsp?arnumber=7433462

6. **Sarker, M. R.**; Dvorkin, Y.; Ortega-Vazquez, M.A., "Optimal Participation of an Electric Vehicle Aggregator in Day-Ahead Energy and Reserve Markets," IEEE Transactions on Power Systems, November 2015, Early Access.

   - Link: ieeexplore.ieee.org/xpl/articleDetails.jsp?arnumber=7328775

7. **Sarker, M. R.**; Ortega-Vazquez, M.A.; Kirschen, D.S., "Optimal Coordination and Scheduling of Demand Response via Monetary Incentives," IEEE Transactions on Smart Grid, vol. 6, no. 3, pp. 1341-1352, May 2015

   - Link: ieeexplore.ieee.org/xpl/articleDetails.jsp?arnumber=6980133

8. **Sarker, M. R.**; Pandzic, H.; Ortega-Vazquez, M.A., "Optimal Operation and Services Scheduling for an Electric Vehicle Battery Swapping Station," IEEE Transactions on Power Systems, vol. 30, no. 2, pp. 901-910, March 2015

   - Link: ieeexplore.ieee.org/xpl/articleDetails.jsp?arnumber=6857439

Conference Publications

1. **Sarker, M. R.;** Ortega-Vazquez, M.A., "Optimal Investment Strategy in Photovoltaics and Energy Storage for Commercial Buildings," in 2015 IEEE Power & Energy Society General Meeting, pp. 1-5, 26-30 July 2015.

   - Link: ieeexplore.ieee.org/xpl/articleDetails.jsp?arnumber=7285594

2. Sun, K.; **Sarker, M. R.;** Ortega-Vazquez, M.A., "Statistical Characterization of Electric Vehicle Charging in Different Locations of the Grid," in 2015 IEEE Power & Energy Society General Meeting, pp. 1-5, 26-30 July 2015

- Link: ieeexplore.ieee.org/xpl/articleDetails.jsp?arnumber=7285794

3. **Sarker, M. R.**; Pandzic, H.; Ortega-Vazquez, M. A., "Electric Vehicle Battery Swapping Station: Business Case and Optimization Model," 2013 International Conference on Connected Vehicles & Expo, Las Vegas, NV, USA, 2-6 Dec. 2013.

   - Link: ieeexplore.ieee.org/xpl/articleDetails.jsp?arnumber=6799808

Chapter 1

INTRODUCTION

1.1 Background

The global trend is aiming towards the transition of the transportation sector from internal combustion engine (ICE) vehicles, which use gasoline for motion, to electric vehicles (EVs), which use electricity for motion. Such a push for the electrification of the transport sector is occurring due to the effects of climate change since ICE vehicles emit carbon dioxide emissions into the atmosphere. The Environmental Protection Agency (EPA) estimated of the total emissions in 2013, transportation was responsible for 27% with electricity at 31% and industry at 21% [5]. With electrification, emissions can be reduced since a mix of renewable resources, *e.g.* wind and photovoltaics (PVs), and conventional generation, *e.g.* coal, can be used to supply the energy needs of EVs. For such a scenario to occur, however, the EV penetration must increase.

The global Electric Vehicle Initiative estimated the global EV penetration in 2015 to be 665,000, which is more than a three-fold increase from 2013 [6]. The electrification is led by the United States at 39%, Japan at 16%, and China with 12% of the total EV population in 2015 [6]. This increase is in part due to the benefits EVs provide to consumers, which include lower day-to-day operating costs (see Figure 1.1) and less emissions resulting in being environmentally conscience, along with the social benefits of EVs being a stand-out technology. From the viewpoint of the power grid, the current and increasing population of EVs brings forth both benefits and challenges.

The batteries inside EVs are not only beneficial for transportation purposes but also to provide grid-related services [7, 8, 9, 10]. EVs are poised to effectively provide energy arbitrage [8, 9, 10], voltage regulation [11], frequency regulation [12, 13, 14, 15, 16], and backup
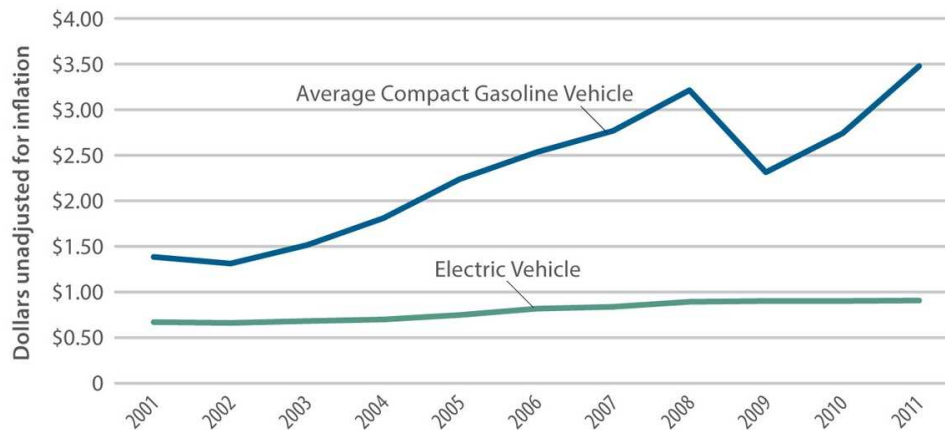
Figure 1.1: Comparison between the cost of travelling 27 miles for an average compact vehicle and an EV. Assumes a 27 miles per gallon gasoline vehicle (average compact fuel efficiency) and an EV efficiency of 0.34 kWh/mile (Nissan Leaf). Data obtained from [1].

power due to the on-demand charging and discharging capabilities, known as grid-to-vehicle (G2V) and vehicle-to-grid (V2G) [17, 18], respectively. These modes can be controlled by an energy management system (EMS) that seeks to meet certain objectives while considering the characteristics and behavior of the EVs. While EVs are seen as power grid resources, they also introduce challenges because of the additional electricity consumption required to meet transportation needs. This entails, in some cases, revamping of the power grid assets [8, 19], *e.g.* lines and transformers, or even additional generation in order to accommodate the power needs. However, by managing the charging schedule of EVs, the current grid can accommodate a large penetration of EVs [7].

The benefits EVs provide to society far outweigh the challenges, if properly managed. However, their are several issues hindering the widespread adoption of EVs by consumers. The objective of the following subsection is to present and discuss the issues related to EVs.

1.2 Issues pertaining to EV adoption

Even though the adoption of EVs is increasing year-over-year [6], the rate is still small compared to the immense vehicle population in the world. This is the case because of issues

	Type	All Electric Range	All Gasoline Range	Total
Nissan Leaf	EV	75	-	75
BMW i3	EV	81	-	81
Tesla Model S	EV	265	-	265
Toyota Prius	PHEV	11	600	611
Chevrolet Volt	PHEV	38	344	382

Table 1.1: Efficiency data of common PHEV and EVs [3]

pertaining to range anxiety, slow charging times, lack of infrastructure, and upfront costs.

Range Anxiety

The notorious range anxiety has troubled current and potential EV owners [9, 20, 21]. Range anxiety is when the driver of an EV worries the battery will run out of energy before the destination or a charging station is reached. Majority of EVs are equipped with Lithium-ion (Li-ion) chemistry-based batteries due to their high energy density [22, 23]. However, these batteries have a shorter comparable all electric range to their equivalent ICE vehicles. EVs can be characterized into two subgroups, which are plug-in electric vehicles (PEVs) and plug-in hybrid electric vehicles (PHEVs) [4]. The PHEVs use a combination of an electric battery and combustion engine for motion, whereas the PEVs are based on a pure electric battery [4]. In general, PEVs have a larger capacity electric battery than PHEVs.

Table 1.1 shows efficiency data of common PHEV and PEVs [3]. As shown, the Tesla Model S has the largest all electric range at 265 miles as compared to the Nissan Leaf, at 75 miles. On the other hand, plug-in hybrid electric vehicles such as the Toyota Prius and Chevrolet Volt use a combination of an electric battery along with a combustion vehicle for transportation and thus the total range is much higher. In addition, the issue of range anxiety is non-evident in PHEVs because at any given time, the consumers can approach a gasoline station to replenish their reservoir.

Range anxiety can be mitigated by either improving battery technology so the all electric range is increased, and/or by installing adequate EV infrastructures. While research is

	Requirements	Rating	Typical Time	Typical Cost
AC Level I	120 volts/12 amps	1.6 kW	< 17 hrs	-
AC Level II	240 volts/16 amps	3.3kW	< 7 hrs	$1,354 [27]
DC Fast Charging	480 volts/125 amps	60 kW	< 30 mins	$10,000 [28]

Table 1.2: Available EV charging levels [4]

ongoing on the former, the latter is a must for widespread EV adoption.

Lack of Public Infrastructure

In most countries, the infrastructure for ICE vehicles, *i.e.* gasoline stations, is well-developed. However, such cannot be said for EVs. In the United States alone, their are 121,000 gasoline stations [24] as compared to the 12,922 EV charging stations (see [25] for a detailed map of EV stations) as of 2015. Innovative companies such as ChargePoint [26] are developing networks of public charging stations and is based on a pay-as-you-go and subscription model. From an investor's point-of-view, however, they may not invest in EV infrastructure because the current population of EVs may not be sufficient to generate revenue to offset the installation costs. At the same time, there is a lack in EV penetration because owners do not see sufficient public infrastructures to justify the purchase.

Furthermore, charging stations may still employ slow charging equipment which does not benefit EV owners. Thus, more innovative approaches of public charging need to be deployed in order to decrease wait-time for EV charging.

Slow Charging Times

Unlike ICE vehicles which only require a few minutes to fill up their gasoline reservoir, EVs must plug-in to an electric source to be charged [7]. Such charging can take approximately minutes to many hours depending on the vehicle and type of infrastructure, *e.g.* residential charging can take upwards of 7 hours[1]. Currently, for direct charging there are

---

[1] Calculations are based on characteristics of a Nissan Leaf EV with a 24 kWh battery [29].

three levels available, Level I, Level II, and Level III (DC Fast Charging) which are summarized in Table 1.2 [4]. In Table 1.2, Level I is when the vehicle plugs directly into a standard power outlet. The majority of EVs in the market come pre-packaged with Level I cordset which on one side contains the standard SAE J1772 plug [4, 30] and on the other side is a standard household plug. These household outlets are readily available in all locations (*i.e.* residential, workplace, and commercial), however, the tradeoff is the large time requirements. On the other hand, Level II requires installation of specialized chargers, *e.g.* [31], along with potential infrastructure upgrades.

Lastly, DC fast charging, *i.e.* Level III, is a specialized installation usually in public areas, *e.g.* Tesla supercharging stations [32], and they result in the fastest charging in less than 30 minutes[2][1]. However, they require specialized cordsets to attach to EVs [4] and large investments in the equipment.

Upfront Costs

Most EVs, *e.g.* Nissan Leaf, Tesla Motors, among others, use Lithium-ion (Li-ion) battery chemistry. From 2012 to 2015, the price of Li-ion batteries has decreased from approximately 500 to 300 \$/kWh showing the benefit of economies of scale and innovation in the field [33]. However, for a typical EV (*e.g.* Nissan Leaf) that houses a 24 kWh battery the cost of the battery was \$12000 in 2012 to \$7200 in 2015. Therefore, for a Nissan Leaf [29] priced at \$29,000 retail, the cost of the battery ranged from approximately 41% to 25% of the total retail price from 2012 to 2015, respectively.

This is a significant reason as to why EVs are priced much higher than their traditional ICE counterparts as of 2015. However, the price per kWh battery is rapidly decreasing with time [34]. For example, the best-in-class players, *e.g.* Panasonic, are expected to have Li-ion prices at approximately 170 \$/kWh by 2025 [35]. This is a positive sign for the advent of EVs. In addition to such cost decreases, the upfront cost of EVs can be further offset by exploiting the flexibility of EVs as grid resources and in return generate revenue or minimize the total cost of energy consumption.

The objective of the next section is to present a general overview of the solutions developed to tackle these issues related to EVs from a power system point-of-view.

1.3   Literature Survey

In the early 1980s, it was first discovered load management strategies must be in place to handle the advent of EVs [36]. Over the years, the concept of EVs being used as a variable energy storage device that can charge, *i.e.* G2V mode, and discharge, *i.e.* V2G mode [37, 38, 39], on-demand was introduced and developed. Such concepts opened up research and industry sectors to the capabilities of the EV batteries. However, these capabilities can only be harnessed if EVs are equipped with bidirectional chargers and such research has been summarized in [39, 40]. From the point of view of the power system, intensive research has been undertaken to study the benefits of these EV modes of operation, *e.g.* see [41], to provide distribution grid services, *e.g.* maintaining grid limits, by performing in G2V and V2G mode, or globally providing services in the wholesale electricity markets, *i.e.* regulation and energy markets. The focus of this survey is on the works related to the use of EV batteries as grid resources.

Previous works have attempted to extract grid services from EVs in centralized verses decentralized strategies. Because wholesale electricity markets are not designed to manage large numbers of small consumers, profit-seeking entities, *e.g.* aggregators, are expected to emerge and serve as coordinators between these consumers and the wholesale markets [7]. On the other hand, at the distribution level, consumers may opt to perform under an aggregator where the entity takes control of the EV operations, or in a decentralized manner where the consumers manage the operations of their EV with the use of an EMS. The participation in any services or a combination thereof in a decentralized or centralized manner can provide a recurring income which may make the vehicles an affordable alternative.

The following subsections will focus on the current works studying EVs at the different levels of the power grid, *i.e.* distribution and transmission, providing various types of grid services.
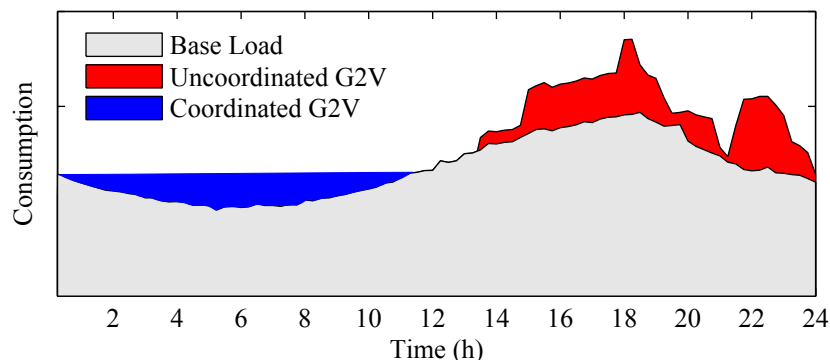
Figure 1.2: Theoretical example of the increase of EV demand on the base load with coordinated verse uncoordinated G2V charging

1.3.1 EVs performing in grid-to-vehicle mode

Demand Response (DR) is a G2V service that both EV owners and the power grid can reap benefits from, if and only if properly implemented. EVs can perform DR by shifting their charging in G2V mode to another period in time to meet certain objectives, *e.g.* to lower costs or to meet grid objectives, or by modulating their charging power. In general, research has shown majority of EVs tend to arrive at their final destination, *i.e.* home, at some point in the afternoon (*e.g.* 1700 hrs), and thus will begin charging immediately if coordination techniques are not in place [42]. An example of G2V is shown in Figure 1.2 where if EVs are uncoordinated then the the base load will increase during the peak-hours of the day, as opposed to the coordinated case where charging occurs in the nighttime hours, i.e valley-filling. Such uncoordinated operations may cause stress to the local distribution grid by overloading assets, *e.g.* transformers and lines, and increases the total system costs since peaking power plants must come online to meet the increased power needs [7]. Several works have proposed methods to manage EV charging in order to meet certain outcomes and these are summarized below:

- EVs can mitigate renewable energy uncertainty, *e.g.* wind [43, 44, 45, 46] and PVs [47, 48].

- EVs can maintain a constant consumption profile, *i.e.* valley-filling [49, 50, 51], in order to reduce peaks and increase asset utilization.
- EVs can manage distribution system limits [11, 52, 53, 54, 55, 56] to ensure they are not violated.

The subsequent discussions will explore the works for each of the situations where an EV can provide DR.

1.3.1.1 *EVs and renewable energy resources*

Renewable energy resources (RESs), *e.g.* wind, exhibit uncertainties and variability in time and power output. If these issues are not compensated, then at any given time their may be an excess or deficit of power on the system. The effect of these uncertainties and variabilities can be minimized with the use of EVs and solutions have been developed in works [43, 44, 45, 46]. Specifically in [43, 44, 45], optimal algorithms are developed for managing the EVs while considering the wind as an input. However, these approaches ignore the system-wide operating costs of integrating wind and EV resources, which the approach in [46] considers. In the realm of RESs, PVs are also an uncertain resource that can cause significant issues at the distribution level, such as voltage deviations [47]. For example, cloud coverage can cause PVs to decrease from a high output of power to close to zero output in a small amount of time. Such issues can also be managed with EVs and optimal frameworks were developed in works [47, 48].

1.3.1.2 *EVs performing demand response and management of grid limits*

Another technique to manage EV charging is to maintain a constant demand profile, or also known as valley-filling shown in Figure 1.2. The work in [49] developed a control algorithm using non-cooperative games to shift EV consumption to nighttime hours in an attempt to keep the charging constant over many hours. The algorithm in [49] can perform in a decentralized manner where minimal communications is required to reach the global

optimum. Similar to [49], the work in [50] develops an optimization model and considers explicitly the EV owners' convenience. Another work [51] bridges the communication barrier between the power utility and EVs using a control signal to reach the same valley-filling outcome. Other techniques attempt to use EVs to ensure proper grid limit maintenance such as power losses [52], nodal voltage deviations [11, 53], and transformer capacity limits [54, 56, 57, 58, 55]. As for power losses, the work in [52] developed an optimization algorithm to shift charging to minimize distribution system power losses in a centralized manner. On the other hand, voltage deviations are more evident in distribution grids because of the lateral design of the system as compared the networked transmission grid [59, 60]. In [11, 53], optimal algorithms were developed to schedule EVs in a centralized way that maintains voltages within defined bounds. As for transformer capacity violations, it is expected that EVs will typically be connected to chargers located in residential homes, which are connected to local pole-top distribution transformers. With the increased EV load, such transformers will be more likely to experience capacity overloads resulting in accelerated aging (or also known as loss-of-life) as assesed in [61, 62]. To mitigate such adverse effect of overloads, operating models are developed that cater EV charging behavior in [54, 56, 57] and appliance behavior in [58] to the dynamics of the transformer.

All of these algorithms that use EV load management to benefit the power grid, *i.e.* [11, 43, 44, 45, 46, 47, 48, 49, 50, 51, 52, 53, 54, 55, 56, 57, 58], do not consider the impact of their approaches to the economics of EV owners. Essentially, the electricity tariff consumers are subject to from their power utility company is ignored and thus the algorithms force charging behaviors that may not be in the best interest for the consumers. On the other hand, the power industry is slowly transitioning consumers, albeit mostly the commercial ones (see Duke Power [63] and Southern California Edison [2]), to time-varying electricity tariffs since it motivates demand response (DR) naturally. However, pilot projects such as the Pacific Northwest Smart Grid Demonstration Projects [64] have discovered that even residential consumers find benefits in such tarriffs, *e.g.* real-time pricing (RTP) and time-of-use (ToU). Examples of these tariffs along with the conventional flat tariff is shown in Figure
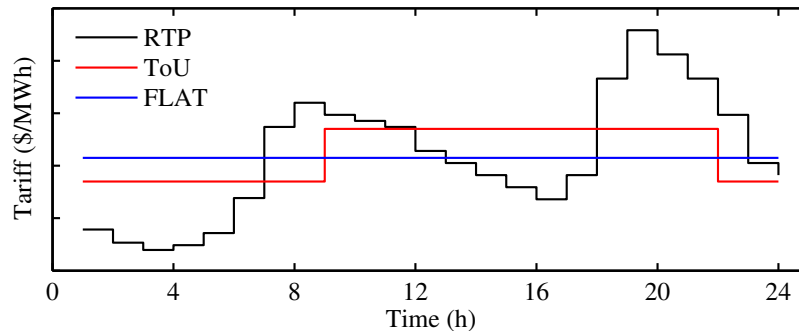
Figure 1.3: Price tariff structures

1.3. If EV owners are under RTP (or even other less time-varying structure such as ToU) in the near future and such algorithms are implemented, they will be worse off economically and will opt to perform their own decentralized management to reduce electricity bills, thus leading to potential damage to the grid. This is the case because each of the algorithms attempt to meet some system need by exploiting the EV batteries. However, if EV batteries are used as grid resources then they must be compensated for their services economically. As a solution, incentive mechanisms must be in place to compensate consumers for assisting the system's well-being. The work in [65] attempts to develop a mechanism of giving coupon incentives on top of flat price tariffs, however, by using flat tariffs EVs cannot provide services economically due to the lack of change in prices.

1.3.2   EVs performing in vehicle-to-grid mode

Time varying-tariff structures enable V2G to be economic for EV owners, if proper techniques are implemented. Energy arbitrage with EV batteries is a technique that exploits the difference in prices during the day to obtain further revenue for the owners. For example, an EV can charge in the nighttime periods of the day in G2V mode when electricity prices are low and then discharge in V2G mode in the evening hours of the day when prices are high. Several works developed operating models of arbitrage in the local distribution grid under time-varying tariffs [10, 18, 66, 67, 68]. The underlying goal of these models was to

use V2G to increase revenue for consumers, as opposed to sole G2V operations. However, because V2G requires additional charging to store energy in the batteries to be discharged later, the EV batteries will undergo life cycle degradation (see [10, 69]) in addition to the expected degradation for transportation energy needs. Thus, models for V2G applications must consider the cost of degrading the battery verses the revenue collected from performing arbitrage or other such services that require discharging actions [10]. Unlike [18, 66, 67, 68], the work in [10] developed an optimal framework considering such degradation trade-offs for arbitrage. From [10], it was concluded the potential cost savings to consumers is decreased as a function of the EV battery costs. Thus, additional streams of revenue must be introduced in order to assist the widespread adoption of EVs and one such approach is to combine the management of EVs with household appliances, which do not experience degradation similar to batteries.

1.3.3 EVs and household appliance management

Consumers can, as an ensemble, manage EV arbitrage with scheduling of household appliances such as electric water heaters (EWH) [70], heating, ventilation, and air conditioning (HVAC) [71], refrigerators (REF) [72], among others. Table 1.3 shows typical appliances found in residential home organized into three categories: fully-deferrable, deferrable but non-interruptable, and non-deferrable. Loads such as EWHs, HVACs, and REFs are thermostatically-controlled and thus have inertia which can be stored for a period of time. For example, a smart EMS can pre-schedule the EWH to turn ON during the nighttime hours when prices are low in order to pre-heat water for the consumers when they wake up. This way appliances can be predictive in order to lower the electricity bill of consumers. This type of "smart home" control has been the focus of much research and industry products.

The research works in [73, 74, 70, 75, 76, 71, 72] developed frameworks to schedule household appliances. Specifically in [73, 74], optimal scheduling models are developed for arbitrary appliances that have pre-determined energy requirements but accuracy is reduced because thermal inertia is not considered. The approach in [75] developed an optimal control

	Deferrable		Non-Deferrable
	Fully	Non-Interruptable	
EV	✓		
EWH	✓		
HVAC	✓		
REF	✓		
Washing machine		✓	
Dishwasher		✓	
Dryer		✓	
Lights			✓
TV			✓

Table 1.3: Typical household loads categorized into fully deferrable, deferrable but non-interruptable, and non-defferable.

algorithm and [76] developed a heuristic algorithm, however, both considered pre-determined temperature thresholds of appliances, *i.e.* if the threshold is reached, appliance must turn ON or OFF. Accurate models of thermal inertial response of appliances were considered in [70, 71, 72] for certain appliances and then embedded into control algorithms. A common shortcoming in all of these works [73, 74, 70, 75, 76, 71, 72] is in the development of a complete household EMS that considers the optimal scheduling of all appliances (*e.g.* thermostatically-controlled loads, loads such as washing machines, and especially EVs) as an ensemble with the goal to minimize electricity costs for consumers.

At the industry-level, companies are researching and developing innovative technologies for appliance management. At the forefront is the Nest Thermostat which is capable of scheduling HVAC's by learning the consumers' day-to-day behavior [77]. This is seen as a retrofit to the current thermostat in the household. On the other hand, smart appliances are being developed, *e.g.* EWHs [78], which include learning algorithms and bi-directional

communication. Others are developing digital platforms, *e.g.* [79, 80], where consumers can visualize and control their energy consumption in real-time.

Even though the benefits of reduced electricity bills, insight into appliance consumption, and real-time control are viable with a complete "smart home", practically it may be expensive [81]. For example, in the case of an EWH, the smart appliance counterpart has a 50% increase in its price as compared to the conventional appliance [78]. However, the innovative players in this industry are reducing costs quickly to make it affordable for the average consumer. As an alternative, however, further revenue can be collected from just the EVs if consumers participate in more services.

1.3.4 Aggregated participation of EVs in power markets

While managing appliances is one option to offset the cost of EVs, another option is to extract additional services from EVs instead of solely relying on G2V and/or V2G at the distribution level. Due to the fast response of EV batteries [17], they are poised to provide energy and/or ancillary services at the transmission level, through the wholesale power markets. Specifically, EVs do not have startup or shutdown costs compared to conventional generation and thus the provision of ancillary services (*i.e.* in the regulation market) from EVs leads to lower system costs [13]. However, due to the capacity restrictions set forth by wholesale power markets, *e.g.* 1 MW minimum capacity in Pennsylvania-Jersey-Maryland (PJM) [82] and 0.1 MW in California Independent System Operator (CAISO) market [83], hierarchical agents must aggregate a large fleet of EVs. An EV owner may be motivated to participate under an aggregator because they receive additional compensation, and do not need to manage the day-to-day operations. The later motivation is only viable if the aggregator provides guarantees each vehicle will receive their energy needs for transportation. Research has been conducted on the business and operating models of aggregators for market participation [84, 13, 16, 85, 86, 87, 14, 88]. The approaches can be characterized into two strategies, where the first includes separate participation in the energy market [84] and regulation market [13, 16], or the second considering a combined participation strategy in both markets

[85, 86, 87, 14, 88].

The separate participation in markets poses concerns. The first priority of EV owners is to receive their energy needs for transportation. However, the ancillary markets have limited capacity requirements pre-defined by the power system operator (SO) and thus bids/offers by aggregators can be rejected if not competitive. Therefore, relying on such markets for transportation needs may result in a lack of energy for EV owners. While the energy market is also competitive in nature in terms of bidding/offering, any participant may purchase electricity at the market clearing price in any given period (*i.e.* a price-taker) [89]. On the other hand, approaches that only consider the energy market participation are foregoing potential revenue from the regulation market, as was done in [84]. As a solution, approaches in [85, 86, 87, 14, 88] co-optimize the participating in both markets simultaneously to determine offering/bidding strategies.

In [85] and [87], the core assumption is that the aggregator participates in ancillary markets on privileged terms, *i.e.* aggregator's offers into the market are always accepted and its revenue is fixed at a certain percentage of its capacity being deployed in the real-time, *e.g.* 10%. However, in practice the aggregator's revenue depends on the outcome of a competitive market process [90]. Furthermore, in [86], the aggregator is assumed to submit quantity-only zero-price bids (*e.g.* 10 MW at 0 $/MW representing price-taker bids) into both markets, thus assuming the ancillary service offers will be accepted. This assumption, however, may reduce the revenue if the actual acceptance is not as anticipated by the aggregator. A common shortcoming in [84, 13, 16, 85, 86, 87, 14, 88] is the use of simplified market clearing procedures of the SO, which has an impact on the potential revenues obtained by the aggregator in a real-life deployment. Additionally, the approaches do not consider the effect and compensation of EV battery cycling degradation, which if considered would alter the participation strategy in each market for the aggregator. A complete model must study the economic trade-offs of both markets in a realistic market environment while considering degradation.

1.3.5 Required infrastructure for the roll-out of EVs

In summary, the aforementioned approaches provide revenue streams for residential consumers that can offset the large upfront cost of owning an EV. The consumers will essentially have a choice of either participating in services via an aggregator, or individually, which has limited options (*i.e.* energy arbitrage) because individual market participation is not viable. As a profit-seeking business entity, the aggregator may need to provide additional compensation or products (*e.g.* installation of a free EMS in homes) to entice a large enough fleet of consumers loads, *e.g.* EVs and potentially other loads such as EWHs, for a viable business. While EVs will spend most of their time parked at their residential homes and can provide services as discussed, other times will be spent at the workplace or commercial locations [42, 91]. It has been shown that with public (*i.e.* workplace and/or commercial) EVCS infrastructure in place, 1 in 73 people would drive an EV, as opposed to the national average of 1 in 1400 in the US [92]. Therefore, adequate EV charging infrastructure is needed to ease range anxiety. Such charging infrastructure may be in the form of parking lots equipped with chargers [93] or charging stations strategically placed in a city [94, 95]. To properly allocate infrastructure, the traffic routes of EVs along with power grid limitations must be considered as was done in [93]. In [95], the allocation optimization considered the distance between each charging station installation in order to ensure the daily journey needs of EVs are met. However, once allocation of infrastracture is performed, operating procedures must be developed.

1.3.5.1 EV charging stations (EVCS)

The public infrastructure that is poised to provide such needs are public AC and/or DC, *i.e.* fast charging, electric vehicle charging stations (EVCS) installed at commercial and workplace locations [96]. A typical charging station can provide EVs power ranging from 1.6 to 7.2 kW (Level 1-2 protocols) and up to 120 kW of power using DC Level 3 protocol [96]. Several works have developed operating operating procedures for these stations to interact

with each individual EV customer, such as done in [97, 98, 99], or with the power grid, such as in [93, 100, 101, 102, 103, 104].

Specifically, [93] developed a two-stage framework, where in the first-stage the profits from an ensemble of charging stations participating in energy and reserve markets is considered. On the other hand, [100] considered in the real-time, the scheduling of both the charging stations and commercial buildings. Such an approach ensured the coordinated charging is economically justified for both EVs and buildings that host the stations. The approaches in [93, 100] scheduled EVs solely considering the impact to the power grid, however, the work in [101] explored the viewpoint of EV owners as well. Furthermore, [101] showed alternative approaches, *e.g.* [93, 100], that manage EV charging to maintain the grid may contradict EV owners' requirements. Optimal sizing and operation of an ESS for charging stations is studied in [102] such that energy procurement and ESS operational costs are minimized. A rule-based control algorithm was developed in [103] that routes power between the station, grid, ESS, and photovoltaics. In [104], a scheme is developed that allocates power from the grid plus ESS to a network of charging stations and also routes EV customers.

In addition, the EVCSs have not only been considered in theory. Commercial businesses have developed around this concept to take advantage of the growing EV penetration. This sector includes entities that install, *e.g.* General Electric [105], among others, and those that both install and manage EVCSs, *e.g.* ChargePoint [26], Tesla Motors [32], among others. For entities that manage EVCSs, their revenue streams are based on the money collected from each EVs charging needs, and for the case of Tesla Motors, their charging network is free to use for their EV models. In general, EVCS are seen as large investments because of the required equipment, potential grid retrofits, and licensing permit costs. These costs can be offset if stations operated similar to an aggregator and thus managed the charging and discharging as ensembles to participate in wholesale markets, or simply exploit retail tariffs provided from their power utility (*e.g.* RTP or ToU).

1.3.5.2 Alternative to EV charging stations

While adequate infrastructure will aid in the widespread adoption of EVs, it is also crucial to deploy the type of infrastructure that will ease the tensions of owning an EV. The issue of slow charging will still be evident with public EVCSs since they will tend to use Level II charging, see Table 1.2. A solution to this is fast charging stations using Level III technology, however, then the issue of fast degradation of the battery comes into play. An alternative solution presented by the industry and research community is battery swapping stations (BSSs). These stations resemble traditional gasoline stations, where a consumer arrives at the station and a swap is performed of their depleted battery with a fully charged one that the BSS keeps in stock [106, 107, 108]. Real-life applications have shown this operation can be performed even quicker than filling a gasoline tank [109]. Several pioneering research works have developed operating (*e.g.* [110, 111, 112]) and business models (*e.g.* [106, 107, 108]) for BSSs.

In [110], the optimal locations where BSS can be installed and operated in distribution systems are determined. In this model, the type of load, the required reinforcements to the distribution system, and reliability of the system are explicitly considered. However, the EV model uses a heuristic approach to determine charging/discharging schedules. An economic dispatch model that uses BSS to manage wind power intermittency is developed in [112]. In [111], the number of batteries to be purchased along with their charging schedules are determined using a basic dynamic programming framework. However, the number of batteries purchased depends on the scheduling model of the EV batteries which, in such an approach, is simplified to a wide extent. A common shortcoming of all the BSS works is the interaction with the electricity markets which can generate additional revenue, since in essence the BSS can operate similar to an EV aggregator.

The business aspect of the BSS has also been the subject of research. The idea of a subscription pricing structure, along with the required infrastructure cost, is presented in [107]. The associated risks, classification of investments, and potential services that could

be sold by the BSS are investigated in [106]. The detailed cost analysis required for the startup of a BSS is performed in [108]. However, these models are simplified since they do not consider the interactions between the BSS and the power system.

The BSS business and operating models have not only been treated in theory. Commercial businesses have developed around the BSS concept to take advantage of the existing EV populations. For example, the company Better Place in 2012 installed multiple stations that handle specific type of EVs [113]. In 2013, Tesla Motors introduced battery swapping technology for their EVs and in late 2014, deployed their first pilot station in California [109]. Also, several utilities in China installed BSSs for their EV population in 2013 [114]. However, the profits in such actual BSSs are entirely dependent on the fees charged for battery swapping, and ignore the extra revenue that could be collected by participating in the energy and ancillary services markets. Altogether, a complete operating and business model of a BSS must consider the interactions with EV owners and the wholesale electricity markets to maximize its revenue potential.

1.3.6 Degradation of batteries

EVs are equipped with batteries, which in most cases are Li-ion based chemistries. Battery energy storage (ES) systems, such as available in EVs, are highly beneficial if exploited for power grid services. However, by doing such exploitation, they undergo adverse degradation effects that must also be taken into consideration. In most cases, however, research has been segregated into works on chemical properties, *e.g.* [115, 116, 117, 118, 119] of Li-ion batteries to those who develop models for their exploitation, *e.g.* [8, 9, 10, 120].

Some pioneering works exist on bridging the gap between battery chemistry mechanisms and grid economics [10, 121, 122]. In [121], battery ES is explored in the context of a microgrid considering both cycle-life degradation and power losses due to the charging/discharging. Additionally, the tradeoff between charge optimization and battery degradation were explored in [10, 122] for EV Li-ion batteries. The work in [10] developed an operating model considering an economic indice for cycle-life degradation against power grid revenues. Such

an approach enables entitis, *e.g.* aggregators, to reimburse customers for exploitation of their batteries for grid services. Without such mechanisms in place, EV owners are unlike to participate since their batteries are being degraded.

The battery ES systems are treated as assets to stakeholders. Therefore, to economically exploit such systems, the economic cost of degrading the batteries must be taken into consideration in the day-to-day operating frameworks.

1.3.7 Summary

This survey presented the landscape of EV developments in the research community and industry. It can be seen EVs are poised as excellent resources for grid services. They can be managed either solely by the owner or a hierarchical entity, such as an aggregator. They can provide services when charging at home, workplace, or commercial location. For the widespread adoption of EVs, further research is required to extract services from EVs to generate more revenue for owners. In addition, the issues of slow charging times and range anxiety, can be managed by installing proper EV infrastructures that can provide services to the grid and thus generate profits. The next section discusses the proposed frameworks developed in this dissertation to tackle such issues.

1.4 Proposed Frameworks

In this dissertation, six frameworks are developed that overcome issues with EVs: range anxiety, slow charging times, lack of public infrastructure, and EV costs.

In the first proposed framework, the focus is on extracting services from a residential household to aid the power grid in mitigating distribution line overloads. Each consumer is equipped with an EMS that optimizes the operation of appliances, including EVs, in order to minimize the electricity costs. However, if all consumers selfishly optimize their own benefits against an electricity tariff, *e.g.* RTP, then their will be syncing of power consumption. This will lead to overloads in the distribution power grid. Therefore, a hierarchical aggregator can provide monetary incentives to consumers in order to motivate demand response shifting

from overloaded periods to normal periods. The aggregator performs its own optimization to maximize profits while determining the least-cost allocation of consumer demand response. Overall, this framework allows the consumers to obtain additional revenue by using their controllable loads to take advantage of energy arbitrage and the potential incentives from the aggregator. Essentially, these additional revenues can provide a justification for offsetting the costs to own EVs. In addition, it develops a business model of an aggregator to take part in the day-to-day operations of coordinating a large ensemble of consumers.

- **Sarker, M. R.**; Ortega-Vazquez, M.A.; Kirschen, D.S., "Optimal Coordination and Scheduling of Demand Response via Monetary Incentives," IEEE Transactions on Smart Grid, vol. 6, no. 3, pp. 1341-1352, May 2015

In the second proposed framework, the aggregator model is further developed to manage the effect EV charging/discharging on distribution transformers. Majority of EVs are expected to be plugged-in and charging at residential homes. Such residential homes are connected to pole-top distribution transformers, which will overload with the addition of EV loads. As a consequence, transformers will experience accelerated aging and thus loss-of-life will occur. An aggregator framework is developed that co-optimizes EV charging/discharging behavior and transformer aging in order to determine an optimal tradeoff between EV arbitrage revenue and transformer aging costs. This framework can be seen as an extension of the first proposed framework based on monetary incentives, since the aggregator must compensate EVs in order to manage their temporal charging behavior and this results in additional reduction of costs. This framework is based on the following work:

- **Sarker, M. R.**; Olsen, D. J.; Ortega-Vazquez, M. A., "Co-Optimization of Distribution Transformer Aging and Energy Arbitrage Using Electric Vehicles," in IEEE Transactions on Smart Grid, March 2016, Early Access.

In the third proposed framework, the aggregator model is further developed to take advantage of the wholesale markets, including energy and secondary regulation. EV batteries

can be used to extract both energy and regulation services to the grid. However, these services can only be provided if they are economically justified against the cost of degrading the battery by additional charging/discharging beyond transportation needs. Therefore, a model is developed where an aggregator manages a large fleet of EVs to determine its bidding and offering schedule in the power markets, while considering the economics of providing such services. The EV owners obtain additional revenue from allowing an aggregator to use the vehicle to participate in both markets. With this framework along with the incentive framework, the revenue collected by EV owners will help offset EV costs and essentially increase the adoption. This framework is based on the following work:

- **Sarker, M. R.**; Dvorkin, Y.; Ortega-Vazquez, M.A., "Optimal Participation of an Electric Vehicle Aggregator in Day-Ahead Energy and Reserve Markets," IEEE Transactions on Power Systems, November 2015, Early Access.

The previous three frameworks explored aggregator business models for the residential sector, *i.e.* consumers. In the fourth proposed framework, a different business model for an aggregator is explored where it manages electric vehicle charging stations as ensembles. In addition to residential charging, EVs are also expected to obtain energy from charging stations installed in commercial and workplace locations. This will require infrastructure in the form of charging stations. The infrastructures energy needs will be procured through a power utility, which may not have the capacity to provide such volatile and highpower needs on-demand and cannot provide energy at the minimal cost. As a solution, an aggregator can manage an ensemble of charging stations in order to participate in wholesale electricity markets to reduce energy porecurement costs. The benefits of this framework is threefold: 1) the stations can focus on their business model of providing services to EV customers instead of attempting to minimizing energy costs, and 2) the charging stations do not need to change their business procedures to conform to the aggregator's framework. This framework is based on the following work:

- **Sarker, M. R.**; Pandzic, H.; Sun, K., Ortega-Vazquez, M. A., "Optimal Market Participation of Aggregated Electric Vehicle Charging Stations Considering Uncertainty," in IEEE Transactions on Smart Grid, *to be submitted August 2016*

In the fifth proposed framework, the issue of EV infrastructure is tackled. An operating and business model is developed for a BSS. This BSS resembles a traditional gasoline station, where consumers arrive at the station with their depleted batteries and receive a fully charged battery in return. The BSS has a stock of EV batteries which must be scheduled to be ready for incoming customers that require a swap. The outcome of the operating model is a bidding and offering strategy to participate in the wholesale energy market in order to generate revenue. The deployment of BSSs can reduce issues of range anxiety and slow charging times, since consumer's can do a swap with a fully charged battery. Overall, this proposed BSS framework is a viable alternative to charging for EV owners and also introduces a business entity in the power system that extracts services from EV batteries. This framework is based on the following work:

- **Sarker, M. R.**; Pandzic, H.; Ortega-Vazquez, M.A., "Optimal Operation and Services Scheduling for an Electric Vehicle Battery Swapping Station," IEEE Transactions on Power Systems, vol. 30, no. 2, pp. 901-910, March 2015

In all of these frameworks, the common element is battery energy storage systems, either mobile such as equipped in EVs or stationary. Improved operating models of such energy storage systems can lead to additional revenue generation or even extended cycle-life. The research on such systems, however, has typically been segregated into focus on the chemistry and material properties and focus on the grid integration, operation, and economic performance (such as done in the previous frameworks). This gap is notorious in both the research community and in commercial usage of batteries; especially for grid applications where the day-ahead market-based decision-making tools use simplified models that limit the operations of the battery because the batteries' cycle-life degradation and charging/discharging

efficiencies are not properly characterized. The sixth proposed framework proposes a data-driven methodology to characterize energy storage systems embedded into a decision-making optimization model. Such data-driven approaches enable the major battery characteristics along with grid economics to be co-optimized as a mixed integer linear program, which benefits from low computational burden and optimality. This proposed framework improves the operations of energy storage systems for additional revenue generation for both EVs and stationary applications. This framework is based on the following work:

- **Sarker, M. R.**; Murbach, M. D.; Schwartz, D. T., Ortega-Vazquez, M. A., "Optimal Energy Storage Management System: Trade-off between Grid Economics and Health," in IEEE Transactions on Smart Grid, *to be submitted August 2016*

In general, these approaches target several problems, such as offsetting the upfront costs of owning an EV, slow charging times, public infrastructure, and range anxiety. By providing solutions to these issues, it may assist the increased adoption of EVs. In addition, from a business standpoint, the proposed frameworks introduce new players in the market, *e.g.* an aggregator, whose roles are to essentially manage the day-to-day operations of large fleets of controllable loads, *e.g.* EVs. These frameworks are organized and presented as described in the following subsection.

1.5 Outline of the dissertation

Chapter 2: Optimal Coordination and Scheduling of Demand Response of Residential Consumer Loads

In Chapter 2, the first proposed framework is developed and results are shared. The mixed-integer linear program (MILP) is developed for both the consumer and the aggregator. The consumer attempts to minimize costs, while the aggregator attempts to maximize profit. The framework includes two stages, where in the first, the consumers provide their optimal schedule of loads, and if overloads are present, the aggregator initiates the second

stage where incentives are used. Results are shown on the effectiveness of incentives to mitigate overloads on distribution feeder lines.

Chapter 3: Co-optimization of Distribution Transformer Aging and Energy Arbitrage using Electric Vehicles

In Chapter 3, the second proposed framework is developed. An optimization model is developed for an aggregator co-optimizing the tradeoff between EV charging/discharging behavior and distribution transformer aging. Results are presented on the model's effectiveness in managing many EVs connected to a distribution transformer, while in some cases even increasing the potential lifetime.

Chapter 4: Optimal Participation of an Electric Vehicle Aggregator in Day-Ahead Energy and Reserve Markets

In Chapter 4, the third proposed framework is developed. The optimization problem is developed for an aggregator managing a large fleet of EVs. The model considers the power market structures for the energy and regulation market. The model is flexible to be applied to any market. The model considers the trade-off of participating in the energy verses the regulation market, while considering battery degradation. Results are presented on the revenue potential for the aggregator.

Chapter 5: Optimal Market Participation of Aggregated Electric Vehicle Charging Stations Considering Uncertainty

In Chapter 5, a framework is developed for an aggregator to manage an ensemble of electric vehicle charging stations. The framework includes the business case for the aggregator along with the day-to-day bidding/offering model in the wholesale electricity markets. Results are shown on the revenue potential of the aggregator along with the benefits of managing uncertainty in the electricity market prices and the aggregated charging station demand, which are both highly volatile.

Chapter 6: Optimal Operation and Services Scheduling for an Electric Vehicle Battery Swapping Station

In Chapter 6, a framework is developed for the BSS. The framework includes the business case for the BSS along with the day-to-day operating model. The discussions include the benefits of the BSS to consumers and the power system. Results are shown on the revenue potential of the BSS along with the benefits of managing uncertainty in the electricity market prices and consumer swapping demand.

Chapter 7: Optimal Energy Storage Management System: Trade-off between Grid Economics and Health

In Chapter 7, a data-driven methodology and optimization model is developed for exploiting battery-based energy storage systems at high power (high C-rate) outputs while characterizing the effect on degradation and efficiencies. Results are shown on the potential revenue benefits with such a model.

Chapter 8: Conclusion

In Chapter 8, conclusions are provided for this dissertation.

Chapter 2

OPTIMAL COORDINATION AND SCHEDULING OF DEMAND RESPONSE OF RESIDENTIAL CONSUMER LOADS

2.1 Introduction

In this chapter, the motivation is to exploit the flexibility of controllable loads (*e.g.* see Table 1.3) for DR and in reduce electricity bills of consumers [8]. To provide DR, however, consumers must be equipped with an EMS which schedules controllable loads while communicating with grid entities. An EMS's objective is to minimize the electricity bill of consumers by scheduling loads, which include thermal loads such as an EWH, HVAC, REF, and non-thermal loads such as washing machines (WM), dishwashers (DW), and EVs, as an ensemble. However, the savings are highly dependent on the electricity tariff and examples of flat, ToU, and RTP are shown in Figure 1.3. The EMS can exploit electricity tariffs by optimizing the controllable loads to be scheduled to turn ON during the low-price periods of the day. However, if the EMS of each individual consumer were to schedule against RTP tariff then the majority of loads would activate at the lowest priced periods of the day. As a solution, a hierarchical aggregator provides monetary incentives to invoke DR such that overloads are mitigated.

As for the contributions, the developed framework uses a combination of RTP and incentives to minimize the cost of electricity for consumers while mitigating overloads on distribution system lines. A decentralized approach is applied with price-based signals sent downstream to consumers by a hierarchical agent, *e.g.* an aggregator, and demand-based signals from EMS sent upstream to the aggregator. As response to the RTP, consumers are then able to determine their base consumption profiles at the Pre-Scheduling (PS) stage and

adjust their demand at the Re-Scheduling (RS) stage in response to additional signals, *i.e.* incentives, sent by the aggregator. The aggregator must provide these incentives and at the same time participate in the electricity markets to obtain its profits.

In the followings sections, the aggregator's role and operations are discussed followed by the consumers'.

2.2 Aggregator as an intermediary

With the RTP tariff structure, consumers can now schedule loads considering the actions at the wholesale electricity markets. However, because electricity markets are not designed to manage large numbers of small consumers, profit-seeking entities called aggregators are expected to emerge and serve as intermediaries between these small consumers and the wholesale markets [7, 17, 18]. The aggregator's role is to communicate with the EMSs to provide real-time updates of the electricity tariff and in return receive optimized load schedules.

While consumers will save on their electricity bill by allowing their EMS schedule loads under a specific tariff provided by the aggregator, the distribution power grid, *e.g.* distribution feeders, could experience excessive loads that may lead to damage. This is the case because each EMS attempts to minimize the total electricity cost incurred by the consumer on a day-to-day basis. This results in many consumers' loads to be scheduled at the lowest-priced hours of the day (*e.g.* at 0300 hours under RTP in Figure 1.3), resulting in a stacking effect. For example, all EVs under a distribution feeder will tend to schedule charging at the lowest priced period.

2.2.0.1 Aggregator's role

The aggregator supplies its consumers via distribution networks which usually have a radial topology [59]. The functions of an aggregator can be performed by a utility company that owns and operates the distribution network or by a separate commercial entity. If the aggregator is the Distribution System Operator (DSO), it incurs all the costs associated

with the use or abuse of the system. On the other hand, if it trades as a separate commercial entity, it must compensate the DSO for all the costs resulting from its transactions with consumers. These costs include the cost of repairing the damage caused by thermal overloads on system components. However instead of incurring these costs, the aggregator can reward responsive consumers that shift their load away from the overloaded periods with monetary incentives.

2.3 Incentives for demand response (DR)

Incentives provided by the aggregator act as a mechanism to invoke DR in consumers in order to keep the distribution system within its operating limits. To achieve this, the aggregator offers time-dependent economic incentives $\beta_{t,i}$, where t is an index to the set of time periods T and i is an index to the set of incentives I. These incentives are offered to all consumers as an adjustment on top of the electricity prices at time period t. Consumers are free to accept or reject the incentives that they are offered. However, if a consumer responds positively and is chosen by the aggregator, then an agreement between the parties is created. The consumer then modifies its demand and receives the corresponding reward. For fairness, all consumers must be allowed to respond and the incentives must be non-discriminatory.

As an example, consider two consumers where consumer 1 is more flexible than consumer 2. Both consumers will receive the same set of incentive parameters, which are [1, 5] $/MWh. Consumer 1's demand decrease to these incentives is [2, 3] kWh and consumer 2's decrease is [1, 2] kWh. Since the aggregator's objective is to procure DR at the least-cost, it will therefore use consumer 1's service. Such analysis of DR procurement is performed by the aggregator's profit maximization model.

The next subsections discuss the framework in which the consumers minimize their cost of electricity procurement, while the aggregator attempts to maximize its profits and maintain the grid limits.
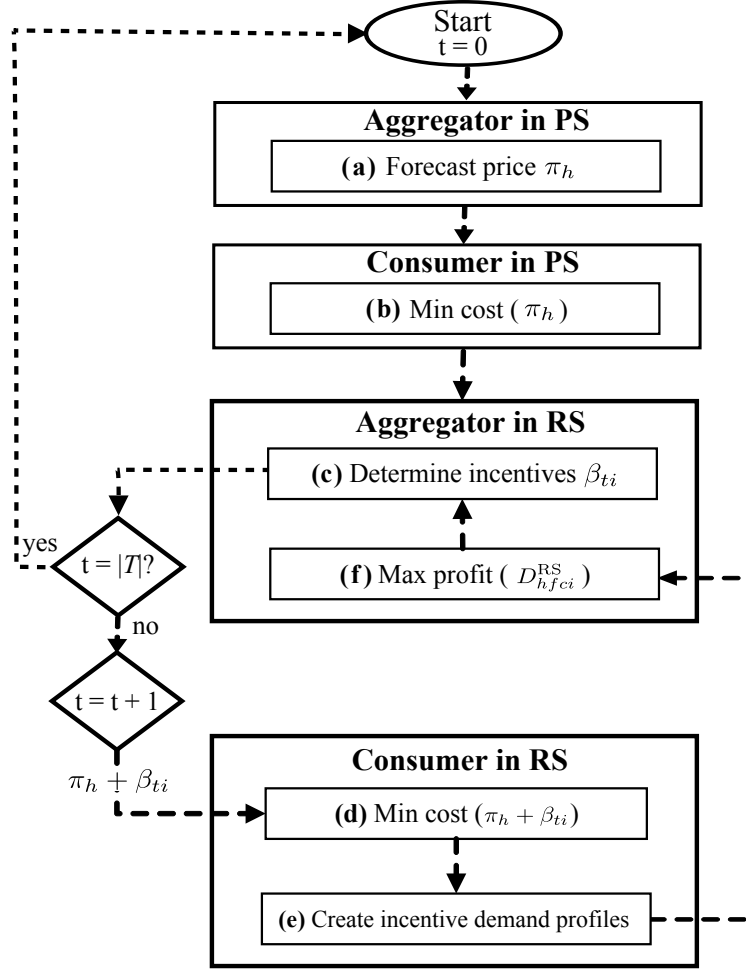
Figure 2.1: Interactions between the aggregator and consumers

2.4 Framework

The framework developed for the optimal coordination and scheduling of DR of residential consumers is shown in Figure 2.1. The figure shows the interactions of the consumer and the aggregator at both, the PS and RS stages.

At the PS stage, the aggregator forecasts the next-day wholesale prices λ_h and determines the base case demand profile of its consumers. This profile takes into account the consumers' response to the time varying prices of electrical energy but not the additional incentives used to deal with the constraints imposed by the distribution network. The PS stage has a time-

Figure 2.2: Rolling window horizon

horizon of 24 hours, divided into 96 15-minute intervals (Δt). In the PS stage, the retail tariff at period sent by the aggregator to all its consumers takes the form of Equation (2.1) below:

$$\pi_h = \lambda_h + \lambda^{\mathrm{u}} + \lambda_h^{\mathrm{p}} \qquad (2.1)$$

Where λ_h is the wholesale energy price, λ^{u} is the distribution system usage price, and λ_h^p is the aggregator's profit margin. In response to these prices, the automated energy managers of the consumers optimize their anticipated load usage and submit their pre-scheduled demand profile to the aggregator. The aggregator combines the profiles $D_{h,f,c}^{\mathrm{PS}}$ of all the consumers c located at distribution node f. Potential overloads in the system are then identified using these aggregated PS profiles. If overloads are expected, then the RS stage is required. The RS stage considers a rolling window from $h = [t, |T|+t-1]$ [73], as illustrated in Figure 2.2. For example, at period $t = 10$ the optimization would occur from $h = [10, 96+101] = [10, 105]$. In each rolling window, incentives are issued only for the current period of the horizon, thus allowing the aggregator and the consumers to be proactive and to maximize their respective benefits. This is the case because the aggregator has the most accurate knowledge of the consumer demand when optimizing at period t as opposed to the future periods where they may change their consumption, *e.g.* late arrival of the EV.

The aggregator sends to the consumers the time-varying prices π_h and the incentive set $\beta_{t,i}$. Consumers calculate what their optimally adjusted demand profile $D_{h,f,c,i}^{\mathrm{RS}}$ would be for each $\beta_{t,i}$. This profile represents each consumer's ability to respond to a given incentive over the rolling window. The consumer performs their optimization for the number of incentives the aggregator chooses to offer, *e.g.* $|I| = 6$ requires 6 independent optimizations from the consumers. Using these individual profiles the aggregator selects within the pre-defined set

the optimal $\beta_{t,i}$ for each consumer that will meet its adjusted demand without violating network limits. The aggregator performs its optimization only once in each time period. The RS stage thus yields an agreement on price and quantities between each consumer and the aggregator. The quantities agreed with each consumer are such that violations of system operating limits are mitigated.

From the aggregator's perspective, the prices include the DR incentives needed to achieve this goal and at the same time, they reflect each consumer's optimal balance between comfort and cost. This approach is a non-iterative decentralized algorithm, which has a guaranteed solution if consumers are participating in DR. By avoiding iterations, the communication between the aggregator and consumers is minimal and potential nonconvergent processes are avoided.

2.4.1   Example: consumer's response to incentives

The consumers' response to an incentive at period t shifts the energy from this period to later periods. This is known as the rebound effect. Figure 2.3 shows a consumer's response to incentives at period $t = 6$, in which the controllable loads shifts to periods $t = 8$ and 9. Figure 2.3 also shows that different incentives, *e.g.* β_1 and β_2, yield a different profile $D_{h,f,c,i}^{\mathrm{RS}}$, which the aggregator considers when mitigating overloads. However, the incentives the aggregator needs to offer at the RS stage in order to motivate consumers to shift their demand and mitigate all the overloads must be based on sound economic principles, *i.e.* supply and demand curves [89].

2.5   Procurement of DR: supply-demand economic principles

The procurement of DR by the aggregator are base on supply-demand principles. Since the aggregator requires DR, it can be seen as the demand-side. Whereas, the consumers provide DR and thus are the supply side. The crossing of the supply and demand curves equates to the equilibrium price at which the DR is priced at. A theoretical diagram of this is depicted in Figure 2.4. Figure 2.4 illustrates how the supply and the demand are balanced on a specific
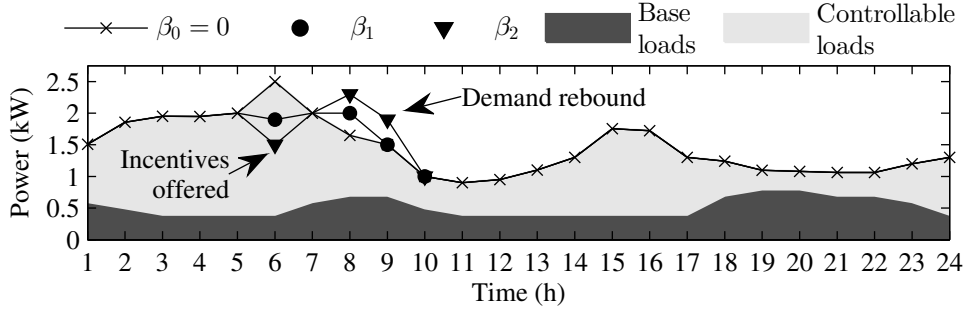
Figure 2.3: Example of a single consumer's response to incentives β_i at $t = 6$.
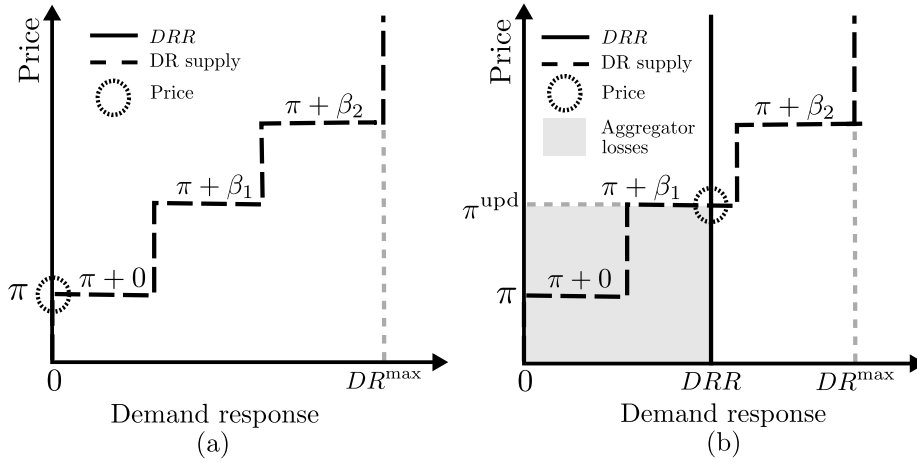
Figure 2.4: Non-overload case in (a) and the overload case in (b).

distribution feeder at a particular period. It also shows the process the aggregator performs in its optimization to determine which consumer's offers are accepted and the amount of DR.

For simplicity in Figure 2.4, the time index has been dropped from the incentives β_i and the real-time prices π_h. The ability of each consumer to supply DR is calculated by taking the difference between $D_{h,f,c}^{\text{PS}}$ and $D_{h,f,c,i}^{\text{RS}}$. These values are then aggregated to obtain the cumulative stepwise curve (dashed line in Figure 2.4) representing the DR supply curve. The stepwise price function in Figure 2.4 is the sum of the retail RTP π, which is fixed from the PS stage, and the incentives β_i for each step.

Each step in this curve represents the total demand response offered by the consumers to a specific incentive, which the aggregator can use to mitigate overloads, if economical. If,

based on the consumer demand profiles at the PS stage, the aggregator determines that the feeder will be overloaded, it calculates its demand response requirement (DRR). The DRR thus represents the reduction in consumer demand required to bring the flow on the feeder within its line capacity (LC) limit.

Figure 2.4a shows a case where the aggregator's $DRR = 0$ because the LC limit is not violated. There is thus no need for the aggregator to offer any incentive, and the profiles agreed upon at the PS stage at price π are used with no gain or loss in revenue. In the case shown in Figure 4b, the consumers' response to retail price π results in the LC limit being violated. The aggregator therefore needs a $DRR > 0$ and consumer demand reduction is required. With the stepwise function, the aggregator may accept offers at different β_i values for each consumer depending on their DR amount and location in the network. The aggregator optimally determines the required incentive β_i needed to obtain this DRR. The accepted consumers then receive $\pi^{\mathrm{upd}} = \pi + \beta_i$ for the demand reduction, where π was already agreed upon in the PS stage and is reimbursed and an additional β_i is given for the reduction. The total amount that the aggregator has to pay to the consumers to avoid an overload is shown in gray in Figure 2.4b.

There may be cases where a large incentive is required to obtain consumer response. In some extreme cases, the DRR of the aggregator and the customers' supply may not intersect. In the former case, the aggregator incurs a very large cost to obtain DR from the consumers while in the latter, it incurs damage costs to the distribution system assets. Regular occurrence of such cases provide a basis for investment in upgrading the distribution network so that it can handle the increased demand.

The following subsections explain the optimization model of the aggregator that incorporates the discussed theories.

2.6 Aggregator Model

2.6.1 Re-scheduling (RS) stage optimization

The aggregator's RS optimization determines which consumers need to be incentivized to re-move overloads stemming from the PS stage schedule. Mathematically, this RS optimization is formulated as follows:

$$\max \quad \Delta t \sum_{h=t}^{|T|+t-1} \sum_{(f\in B)} \sum_{(c\in C)} \sum_{(i\in I)} (\pi_h + \beta_{t,i})(D^{\mathrm{RS}}_{h,f,c,i} - D^{\mathrm{PS}}_{h,f,c}) \cdot \eta_{f,c,i} - \Delta t \sum_{h=t}^{|T|+t-1} \lambda_h \cdot p_h^{\mathrm{market}} \quad (2.2)$$

The first term in the objective function (2.2) represents the amount collected (if positive) or paid (if negative) by the aggregator. If the first term is negative, it indicates that a payment was made to consumers at period t because incentives were needed. On the other hand, if the term is positive the demand is reduced at period t, but a rebound is expected in subsequent periods and will result in revenue for the aggregator (see Figure 2.3). Changes in demand between the RS and the PS are calculated using the binary variable $n_{f,c,i} \in \{0,1\}$. This binary variable determines the optimal incentive demand profile $D^{\mathrm{RS}}_{h,f,c,i}$ to be agreed upon with each consumer. $\beta_{t,i}$ depends on which demand response profile is chosen. However, $\beta_{t,i}$ is only given for the current period t of the horizon. Therefore, $\beta_{h,i} = 0$ for $h > t$. The last term represents the profit or loss resulting from purchasing or selling electricity p_h^{market} in the wholesale electricity market.

The optimization is subject to the energy balance constraint (2.3) which determines the amount of energy to be purchased or sold in the wholesale electricity market and includes the network losses.

$$p_h^{\mathrm{market}} = \sum_{(f\in B)} \sum_{(c\in C)} \sum_{(i\in I)} (D^{\mathrm{RS}}_{h,f,c,i} - D^{\mathrm{PS}}_{h,f,c}) \cdot \eta_{f,c,i} + \sum_{(f,g)\in B} R_{fg}\ell_{h,f,g} \quad \forall h \in [t, |T|+t-1] \quad (2.3)$$

In the power balance constraint, however, the aggregator must choose a single RS profile to be used for each consumer. This is managed in constraint (2.4) as shown below.

$$\sum_{(i\in I)} n_{f,c,i} = 1 \quad \forall f \in B, c \in C \quad (2.4)$$

In the next set of constraints, the power flows in the distribution network are modelled [60]. Constraint (2.5) ensures the distribution lines are operating within their limits. This constraint, however, is non-linear and is linearized via the special-ordered-sets-of-type 2 (SOS2) technique [123], further discussed in Appendix B.1.

$$\ell_{h,f,g} \geq \frac{(p_{h,f,g}^{\text{flow}})^2 + (q_{h,f,g}^{\text{flow}})^2}{e_{h,f}} \quad \forall h \in [t, |T| + t - 1], (f, g) \in B \tag{2.5}$$

The next two constraints (2.6 and 2.7) calculate the real and reactive power flows in each distribution line. The real and reactive power, $p_{h,f,g}^{\text{flow}}$ and $q_{h,f,g}^{\text{flow}}$, have a power factor of κ and are used to calculate the current $\ell_{h,f,g}$ and the voltage $e_{h,f}$, taking the resistance $R_{f,g}$ and reactance $X_{f,g}$ of each line into account.

$$p_{h,f,g}^{\text{flow}} = \sum_{(j \in B)} p_{h,g,j}^{\text{flow}} + R_{f,g}\ell_{h,f,g} + \kappa \sum_{(c \in C)} \sum_{(i \in I)} D_{h,g,c,i}^{\text{RS}} n_{g,c,i} \quad \forall h \in [t, |T| + t - 1], (f, g) \in B \tag{2.6}$$

$$q_{h,f,g}^{\text{flow}} = \sum_{(j \in B)} q_{h,g,j}^{\text{flow}} + X_{f,g}\ell_{h,f,g} + (1 - \kappa) \sum_{(c \in C)} \sum_{(i \in I)} D_{h,g,c,i}^{\text{RS}} n_{g,c,i} \quad \forall h \in [t, |T| + t - 1], (f, g) \in B \tag{2.7}$$

Each distribution node has an associated voltage which depends on the real and reactive power flow. This is calculated by constraint (2.8), as shown below.

$$e_{h,f} - e_{h,g} = 2 \left(R_{f,g} \cdot p_{h,f,g}^{\text{flow}} + X_{f,g} \cdot q_{h,f,g}^{\text{flow}} \right) - \left(R_{f,g}^2 + Q_{f,g}^2 \right) \ell_{h,f,g} \quad \forall h \in [t, |T| + t - 1], (f, g) \in B \tag{2.8}$$

In addition, to ensure the distribution grid is operating within limits, the voltage and current must be bounded. This is done with equation (2.9) for the voltage at each node and with equation (2.10) for the current through each line.

$$\underline{e}_f \leq e_{h,f} \leq \bar{e}_f \quad \forall h \in [t, |T| + t - 1], f \in B \tag{2.9}$$

$$0 \leq \ell_{h,f,g} \leq \frac{LC_{f,g}}{\sqrt{R_{f,g}^2 + Q_{f,g}^2}} \quad \forall h \in [t, |T| + t - 1], (f, g) \in B \tag{2.10}$$

2.7 Consumer Model

Consumers' EMS incorporates a cost-minimization model that incorporates specific needs of each load in the home, *e.g.* comfort requirements, and EV availability. Apart from the controllable loads, the house also has non-controllable, *e.g.* lighting, which are consumer controlled and modelled as fixed demands. Table 1.3 shows the appliance loads considered in this framework. The objective of the consumer is to minimize the total cost and it has two stages, the PS and RS stage.

2.7.1 Consumer pre-scheduling (PS) stage model

The consumer's PS optimization takes place after the forecasted retail prices τ_h from the aggregator are sent to the consumers and is used to determine the appliance schedule for the next day, which runs from $h = 1$ to $h = |T|$. The objective function (2.11) seeks to minimize the total energy costs and shown below:

$$\min \quad \Delta t \sum_{(h \in T)} \pi_h \left[P_h^{\text{base}} + \sum_{(a \in A)} P_a \frac{\delta_{a,h}}{AL_a} + \sum_{(v \in V)} (p_{v,h}^{\text{chg}} - \eta_v^{\text{dsg}} p_{v,h}^{\text{dsg}}) \right] \qquad (2.11)$$

The objective function of the consumer is subject to the following constraints:

$$0 \leq \delta_{a,h} \leq AL_a \quad \forall h \in T, a \in A \qquad (2.12)$$

$$\sum_{(a \in A)} P_a \frac{\delta_{a,h}}{AL_a} + \sum_{(v \in V)} (p_{v,h}^{\text{chg}} + \eta_v^{dsg} p_{v,h}^{\text{dsg}}) \leq P^{\text{mains}} \quad \forall h \in T \qquad (2.13)$$

In equations (2.11) and (2.13), P_a is the maximum power consumption of appliance a in the set of appliances A, $p_{v,h}^{\text{chg}}$ and $p_{v,h}^{\text{dsg}}$ are the charge/discharge powers of EV v in the set of EVs V of each household, and P_h^{base} is the total base load power, *e.g.* lighting. The appliances have an integer number of operating states AL_a, which allow the appliances to be used in a derated manner (*e.g.* at 50% rather than 100% of rating). The integer decision variable $\delta_{a,h}$ for each appliance must remain at or below the number of operating states AL_a as shown in constraint (2.12). Constraint (2.13) ensures that the household power limit

P^{mains} is not violated. This model is subject to the appliance constraints presented in later subsections.

The RS stage model is similar to the PS stage model and is discussed in the following section.

2.7.2 Consumer re-scheduling (RS) stage model

At the RS stage, consumers can make adjustments to their PS profile for $h = [t, |T| + t - 1]$ in response to the incentives provided by the aggregator. Equation (2.14) implements these adjustments, where $p^\uparrow$ and $p^\downarrow$ represent increase and decrease in the power consumed by each load. The increase and decrease adjustment in power depend on the PS stage load profiles U^{PS} and are calculated in constraint (2.16) for the appliances and constraint (2.17) for the EVs. The loads interrupted due to accepted incentives must be enabled in a future period to maintain comfort requirements. This is also considered in constraints (2.16) and (2.17).

$$\min \quad \Delta t \sum_{h=t}^{|T|+t-1} (\pi_h + \beta_{t,i}) \left[\sum_{(a \in A)} (p^\uparrow_{a,h} - p^\downarrow_{a,h}) + \sum_{(v \in V)} (p^\uparrow_{v,h} - p^\downarrow_{v,h}) \right] \tag{2.14}$$

subject to:

$$\text{Constraints (2.12) and (2.13)} \tag{2.15}$$

$$P_a \frac{\delta_{a,h}}{AL_a} - p^\uparrow_{a,h} + p^\downarrow_{a,h} = U^{\text{PS}}_{a,h} \quad \forall a \in A, h \in T \tag{2.16}$$

$$(p^{\text{chg}}_{v,h} - \eta^{\text{dsg}}_v p^{\text{dsg}}_{v,h}) - p^\uparrow_{v,h} + p^\downarrow_{v,h} = U^{\text{PS}}_{v,h} \quad \forall v \in V, h \in T \tag{2.17}$$

This model is also subject to appliance constraints presented in the next subsections.

2.8 Appliance Models

2.8.1 Electric vehicle (EV)

The EVs are modeled as storage devices that can charge their batteries from the grid in G2V mode, inject power to the household in Vehicle-to-Home (V2H) mode, or inject power back

to the grid in V2G mode. In order to know when an EV can perform these functions, its availability $\alpha_{v,h}$ must be declared upfront as well as its trip schedule $S_{v,h}$.

As EVs charge and discharge, the batteries energy-state-of-charge (eSOC) varies. The eSOC indicates the amount of energy present at a given time h in the battery. Equation (2.18) calculates the eSOC in the battery at each time period h which is a function of its state-of-charge in the previous period, the charge/discharge powers $p_{v,h}^{\text{chg}}$ and $p_{v,h}^{\text{dsg}}$, the charging efficiency η_v^{chg}, and the total energy required for motion ξ_v

$$soc_{v,h}^{\text{EV}} = soc_{v,h-1}^{\text{EV}} + p_{v,h}^{\text{chg}}\eta_v^{\text{chg}}\Delta t - p_{v,h}^{\text{dsg}}\Delta t - \xi_v\frac{S_{v,h}}{\sum_h S_{v,h}} \quad \forall h \in T, v \in V \qquad (2.18)$$

The eSOC, $soc_{v,h}^{\text{EV}}$, also must be within its maximum to avoid the risk of setting the battery on fire, and a minimum to avoid rapid degradation, as shown below:

$$\underline{soc}_{v,h}^{\text{EV}} \leq soc_{v,h}^{\text{EV}} \leq \overline{soc}_{v,h}^{\text{EV}} \quad \forall h \in T, v \in V \qquad (2.19)$$

Furthermore, constraints (2.20) and (2.21) limit the power at c_v^{max} for charging/discharging with the EV availability $\alpha_{v,h}$.

$$0 \leq p_{v,h}^{\text{chg}} \leq \alpha_{v,h} \cdot c_v^{\text{max}} \qquad \forall h \in T, v \in V \qquad (2.20)$$

$$0 \leq p_{v,h}^{\text{dsg}} \leq \alpha_{v,h} \cdot c_v^{\text{max}} \qquad \forall h \in T, v \in V \qquad (2.21)$$

2.8.2   Electric water heater (EWH)

Each consumer's EMS predicts the need for hot water H_h (gal) for the next day based on historical average usage. The model considers the heat rate Q, thermal resistance R, and heat capacity C of EWHs.

Constraint (2.22) determines the water temperature ϕ_h^{water} (°C) with the status of the appliance $\delta_{a,h}$. Constraint (2.23) calculates the temperature in the EWH tank, where G (gal) is the tank capacity and ϕ_h^{out} is the outdoor ambient temperature. Constraint (2.24)

ensures the water temperature remains within bounds.

$$\phi_h^{\text{water}} = \phi_h^{\text{tank}} + \frac{\delta_{ewh,h}}{AL_{ewh}}QR - \left(\phi_h^{\text{tank}} + \frac{\delta_{ewh,h}}{AL_{ewh}}QR - \phi_{h-1}^{\text{water}}\right)e^{\frac{-\Delta t}{RC}} \quad \forall h \in T \tag{2.22}$$

$$\phi_h^{\text{tank}} = \frac{\phi_h^{\text{water}}(G - H_h) - \phi_h^{\text{out}}H_h}{G} \quad \forall h \in T \tag{2.23}$$

$$\underline{\phi}^{\text{water}} \leq \phi_h^{\text{water}} \leq \overline{\phi}^{\text{water}} \quad \forall h \in T \tag{2.24}$$

2.8.3 Heating ventilation and air conditioning (HVAC)

The HVAC system uses the thermal mass inside the house to pre-heat or pre-cool during low-price periods, while keeping the temperature within acceptable bounds $\underline{\phi}^{\text{room}}$ and $\overline{\phi}^{\text{room}}$ set by the consumer as shown in (2.25). Constraint (2.26) updates the room temperature where Q, R, and C are the thermal parameters of the house. While the definition of Q, R, and C for the HVAC and EWH is the same, the parameter values are different.

$$\phi_h^{\text{room}} = \phi_h^{\text{out}} + \frac{\delta_{hvac,h}}{AL_{hvac}}QR - \left(\phi_h^{\text{out}} + \frac{\delta_{hvac,h}}{AL_{hvac}}QR - \phi_{h-1}^{\text{room}}\right)e^{\frac{-\Delta t}{RC}} \quad \forall h \in T \tag{2.25}$$

$$\underline{\phi}^{\text{room}} \leq \phi_h^{\text{room}} \leq \overline{\phi}^{\text{room}} \quad \forall h \in T \tag{2.26}$$

2.8.4 Refrigerator (REF)

Shifting refrigeration load in time provides minimal discomfort to consumers if the temperature inside the refrigerator remains within bounds as shown in (2.28). Constraint (2.27) calculates the temperature ϕ_h^{ref}, where $\psi = e^{\frac{-\Delta t \cdot TI}{TM}}$, TI is the thermal insulation, TM is the thermal mass, η^{ref} is the efficiency, and P^{comp} is the compressor power.

$$\phi_h^{\text{ref}} = \psi\left(\phi_{h-1}^{\text{ref}} - \phi_h^{\text{room}}\right) + \phi_h^{\text{room}} - \frac{\delta_{ref,h}}{AL_{ref}}(1 - \psi)\frac{\eta^{\text{ref}}P^{\text{comp}}}{TI} \quad \forall h \in T \tag{2.27}$$

$$\underline{\phi}^{\text{ref}} \leq \phi_h^{\text{ref}} \leq \overline{\phi}^{\text{ref}} \quad \forall h \in T \tag{2.28}$$

2.8.5 Dishwasher, washing machine, and dryer

These types of loads are in the category of non-interruptible and deferrable loads. Constraint (2.29) ensures that their operation is within the time range specified by the consumer $TR_{d,h}$,

where d is the index of the subset of the appliance set A. Constraint (2.30) ensures that operation is not interrupted once it has begun. Constraint (2.31) ensures the operation of the appliance is equal to its cycle time CT_d.

$$\delta_{d,h} \leq TR_{d,h} \quad \forall h \in T, d \in A \tag{2.29}$$

$$\sum_{z=t+1}^{t+H_d} \delta_{d,z} \geq CT_d \cdot (\delta_{d,h+1} - \delta_{d,h}) \quad \forall h \in T, d \in A \tag{2.30}$$

$$\sum_{(h \in T)} \delta_{d,h} = CT_d \quad \forall d \in A \tag{2.31}$$

2.9 Simulation Results

100 consumers with varying EV driving patterns were simulated using the 2009 NHTS data [124]. Each consumer has all the appliances described above and one EV. Typical curves for market prices λ_h and outdoor temperatures are based on PJM data [125], for every Thursday during January-March 2013. Thursday was chosen in order to show the impact on a typical weekday. The retail RTP π_h was calculated using equation (1), where $\lambda^u = 20$ \$/MWh and the profit margin $\lambda_h^p = 0.1 \cdot \lambda_h$. 50 consumers were placed on each of the last two nodes of the IEEE 4-node distribution network [126]. Each consumer is allocated 15 kW as its mains power limit. The line limits of the distribution system were reduced and only one phase of the network was considered. Since all the power flows through the substation feeder to reach the consumers, this line will overload if the EV penetration increases. The feeder line capacity LC was set at 600 kVA.

The nominal eSoC of the EV batteries is 24 kWh. The eSoC, however, can range only between a minimum of 15% and a maximum of 95% of the nominal eSoC [127]. The charging and discharging power is 3.3 kW, the initial eSoC of the EVs are randomized, and the round trip charging/discharging efficiency is assumed to be 90% [85]. The thermal parameters and temperature bounds of the appliances were randomized and each appliance was given two levels of operation (50% and 100%). The EWH, HVAC, and REF power are uniformly randomized between [3.5 4.0], [2.5 4.0], and [0.20 0.40] kW, respectively. Consumers have
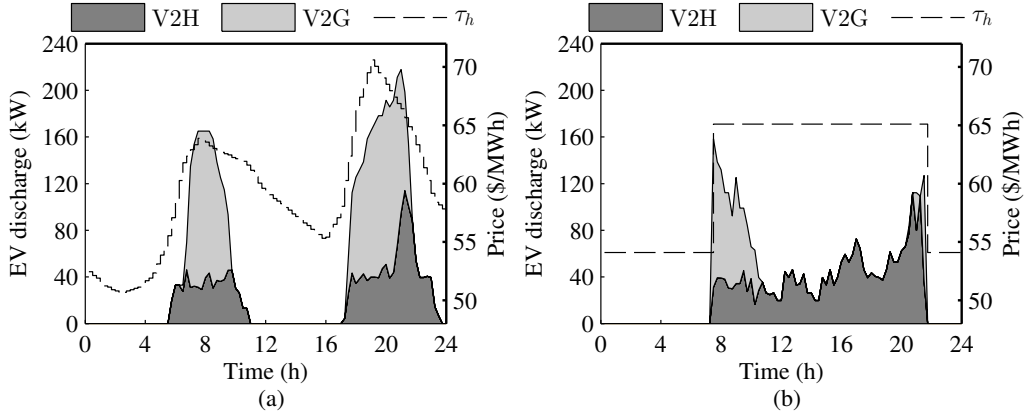
Figure 2.5: EV discharge power in V2H and V2G for (a) RTP and (b) ToU tariff.

randomized dishwasher, washing machine, and dryer schedules each with a rating of 1.0 kW. The base load varies within the range [50 200] W and is randomized for each consumer. The EWH water usage was forecasted as explained in [128] considering the number of members in the household and their age. The power factor is 0.9.

The approach described in [129] is used to calculate the thermal overloads if the line capacity limit is violated, which then is used to obtain the percentage loss of tensile-strength, $W_{t,f,g}$ [130]. In general, lines require repair when their tensile-strength drops below 85% of the nominal [131]. The value of the line maintenance cost $LMC_{f,g}$ is assumed to be \$100,000 [59]. Based on this observation, equation (2.32) defines the potential damage cost $DC_{t,f,g}$ as a percentage of $LMC_{f,g}$ if incentives are not used:

$$DC_{t,f,g} = LMC_{f,g} \cdot W_{t,f,g} \tag{2.32}$$

With these case study parameters, several simulations were performed and their results are discussed below.

2.9.1   Impact of tariffs at the PS stage

Tariffs influence how each consumer's EMS schedules loads. Flat, ToU, and RTP tariffs are considered to investigate the consumers' response to each and to determine which would
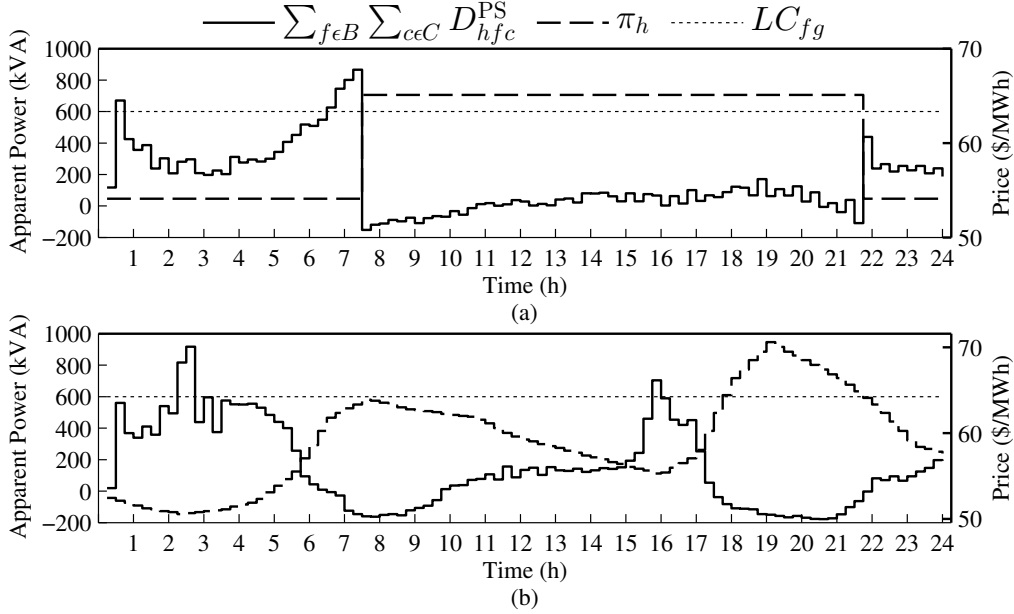
Figure 2.6: Total demand profile in PS with one EV per household on (a) ToU with EMS, and (b) RTP with EMS.

require incentives to avoid overloads. The EV penetration is assumed to be 100%. Figures 2.5a and 2.5b show V2H and V2G power under RTP and ToU, respectively. Buying excess energy to discharge and sell later in V2G/V2H mode does not make sense under a flat tariff because prices are the same during all periods. The EVs enable consumers to sell excess energy in V2G after supplying household loads in V2H. The RTP schedules a larger portion of discharge power in V2G mode as compared to V2H, thus selling energy to the aggregator. With ToU (off-peak: 0000 to 0715, 2145 to 2400 hours at 54.1 $/MWh and peak: 0730 to 2130 hours at 65.1 $/MWh), the majority of the discharge is in V2H mode. The total discharge under RTP and ToU are 1248.8 and 872.9 kWh, respectively. The RTP incorporates multiple low and high price periods where the EMS can exploit EVs, whereas ToU has limited price blocks. The RTP tariff thus provides larger benefits with regards to the EVs.

Figure 2.6 shows the consumers' EMS response to ToU and RTP. Here again, consumers have no incentive to schedule their loads under a flat tariff. This results in a larger demand

during peak-hours. In addition, the consumers' response to a flat tariff is the worst-case scenario. With a flat tariff of 59.6 \$/MWh (average of the retail RTP π_h), the total PS stage energy costs for all consumers is \$271.5 with a line damage cost of \$154.0. With the ToU tariff, the energy cost decreases to \$169.0 with a line damage cost of \$128.20. However, under the RTP tariff, the energy cost is \$150.4 with the smallest line damage cost of \$120.33. The RTP tariff provides the most benefits to consumers and the aggregator, because the former pays the least for energy and the latter incurs the least damage cost for overloads. However, the RTP case in Figure 2.6b exceeds the line limits thus requires the use of incentives in order to avoid the damage costs.

2.9.2 *Mitigating line overloads with incentives at the RS stage*

Figure 2.7 illustrates the benefits of using incentives at the RS stage to remove overloads under RTP for different levels of EV penetration. Consumers are assumed to have an EMS that can receive and act on the basis of RTPs and incentives. The set of incentives offered to consumers consists of $[0, 1, 2, 5, 10, 30]$ \$/MWh.

Figure 2.7 shows the incentives the aggregator offers to the consumers are sufficient to reduce the demand below LC at each period. The rebound effect causes the demand to increase at later periods to ensure the desired level of comfort is maintained. With lower EV penetrations, *e.g.* 30% in Figure 2.7a, enough capacity is available during off-peak periods to handle this rebound without adverse effects. As EV penetration increases, more costly incentives are required to mitigate overloads. For example, in the case of 100% EV penetration in Figure 2.7c, the available capacity is small and the amount of overload is large. When the initial incentives are given, the potential overloads are mitigated but create new overloads during subsequent periods. To correct these new overloads, the aggregator has to offer further incentives. For instance, the incentive given at 0230 in Figure 2.7c eliminates an overload but this shifts the demand to a later period causing a new overload and the need for more costly incentives.

Figure 2.8a shows the potential damage cost under the RTP tariff if incentives are not
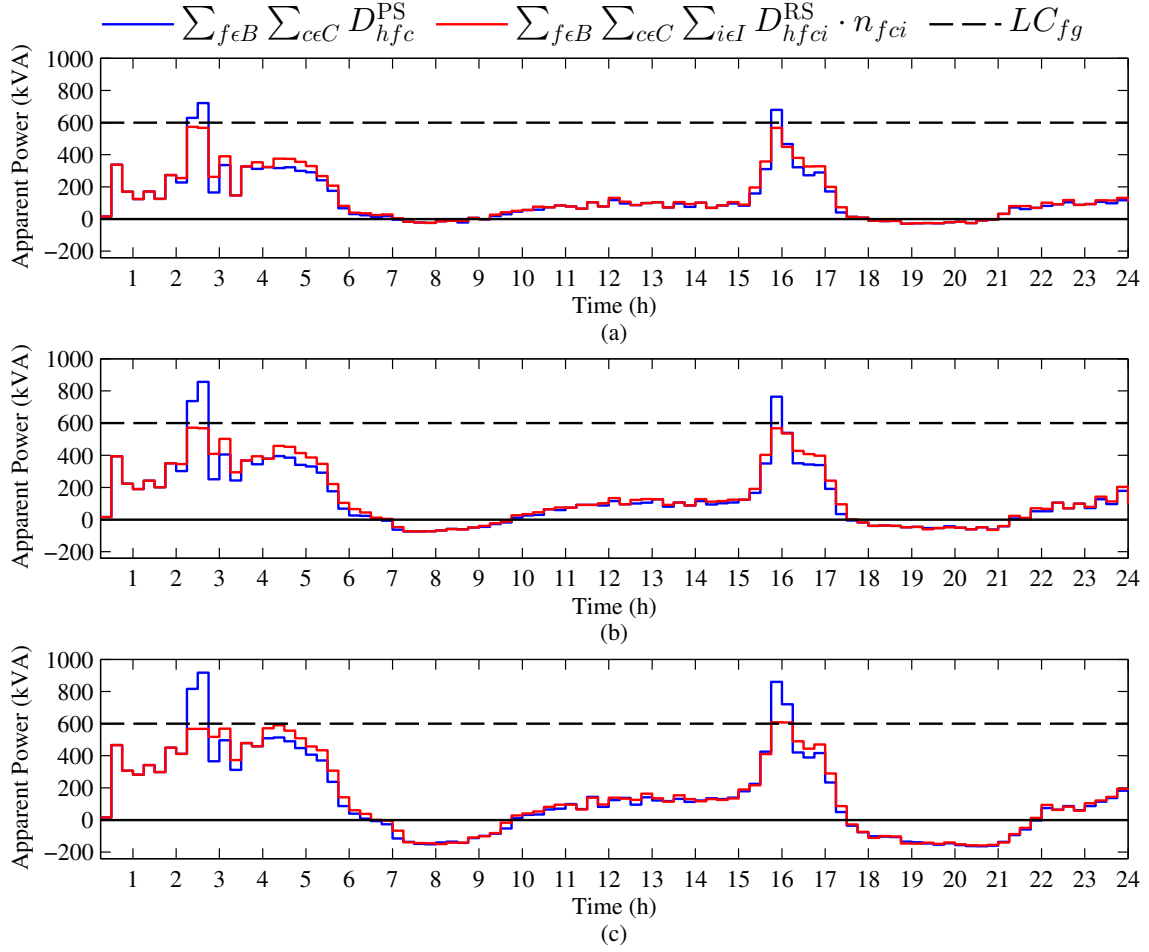
Figure 2.7: (a) 30%, (b) 60%, (c) 100% penetration showing demand in PS (black), and after incentives are used in RS (red).

offered. In Fig 2.8a, at 100% EV penetration, the line overloads are high resulting in high potential damage costs compared to the 30% and 60% penetration levels. If there are no overloads, then the damage cost is zero as is the case for hour 16:00 with penetrations of 30% and 60% EVs. As an alternative to paying the damage costs, the aggregator can reward consumers with incentives. The total incentive cost at 30%, 60%, and 100% EV penetration from Figure 2.7 are $0.39, $0.71, and $0.85, respectively. If the aggregator does not use incentives to motivate consumers to shift their energy consumption, then the incurred
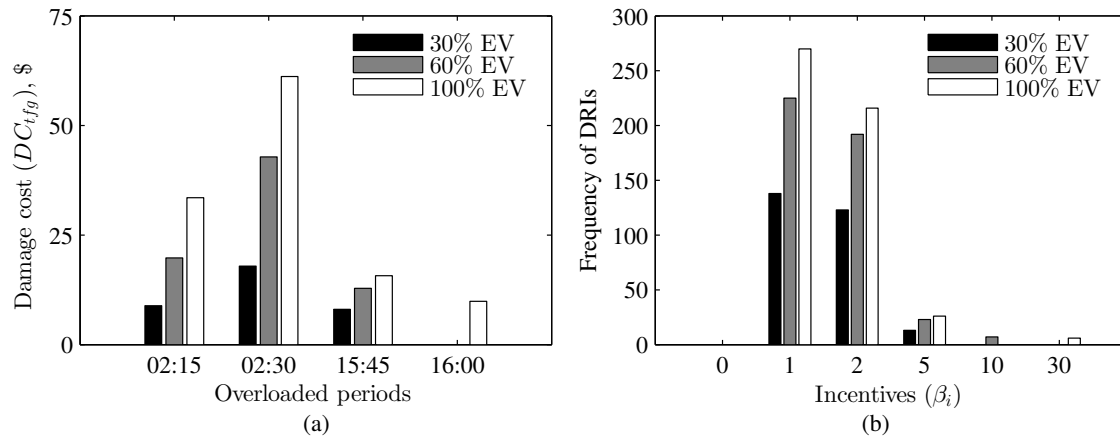
Figure 2.8: (a) Damage cost for overloaded periods under RTP and (b) frequency of incentives paid.

potential damage costs are much higher than the total rewards given to consumers. However, in the long run since incentives decrease aggregator profits and increase operating costs, the retail price of energy will increase for consumers.

The aggregator must also analyze whether the set of incentives that it offers to the consumers are effective in motivating DR. Figure 2.8b shows that, at larger EV penetration levels (*e.g.* 100%), incentives are not only more frequent but also larger (*e.g.* 30 $/MWh). Dealing with larger overloads requires the participation of less flexible consumers, who demand larger incentives. From Figure 2.8b, it can be seen that large incentives are infrequently given to consumers. However, if given frequently, it indicates inflexible consumers which either have limited interest in participating in DR or have strict comfort requirements. If this case persists over time, the distribution system may require reinforcement due to a lack of DR at an economic value to the aggregator. On the other hand, the high frequency of smaller incentives, *e.g.* 1 $/MWh, shown in Figure 7b shows that consumers are participating at an economic value to the aggregator. Over time as the aggregator learns about its consumer-base, it will determine a tighter range of incentives that yields enough response to remove the overloads at each period.

The proposed approach can also be implemented for infrequent situations, *e.g.* sporting events, when a large fleet of EVs may require energy for transportation. The only requirement will be a management entity, *e.g.* stadium, capable of providing their consumption and DR schedule to the aggregator to use in mitigating overloads. In addition, another extreme case includes when the number of EVs increases for a temporary period of time, *e.g.* visitors from neighboring areas. Even though the current area, for example, may have a low EV penetration (30%), the visiting EVs resemble the impact on the demand at 60% or even potentially higher levels, which as shown in Figure 2.8 can be managed effectively.

2.9.3 *Distribution system avoided costs*

Consumers' participation in DR requires investments in smart-grid technologies. This section examines how much investment is justified and determines the point where the rate of DR participation becomes too high and causes overloads during periods of low prices. It is assumed DR participants have an EMS capable of receiving RTPs and incentives. The tensile-strength loss $W_{t,f,g}$ of the feeder is determined for the worst-case demand scenario where all consumers respond to a flat tariff on a daily basis. The number of days needed to reduce the tensile strength to the minimum of 85% is then calculated. If demand is shifted from peak price hours to off-peak hours using DR, there will be fewer overloads and the number of days before the line must be replaced will increase.

Present-Value (PV) analysis is performed to determine the current investments in order to delay or avoid repair costs. In the analysis, one p.u. cost is accrued by the aggregator at a future day when the strength of the line reaches 85% due to overloads. An interest rate of 5% compounded monthly is used in the PV analysis [131]. Figures 2.9a, 2.9c and 2.9e show the effect of 30%, 60%, and 100% EV penetrations on the number of days during which the feeder line can withstand increased loading until it must be replaced. The present values of investments are shown in Figures 2.9b, 2.9d and 2.9f for these same EV penetrations. For example, at 0% consumer participation in DR and 30% EV penetration (Figure 2.9a), overloads could be withstood for 600 days. This line will therefore have to be replaced after
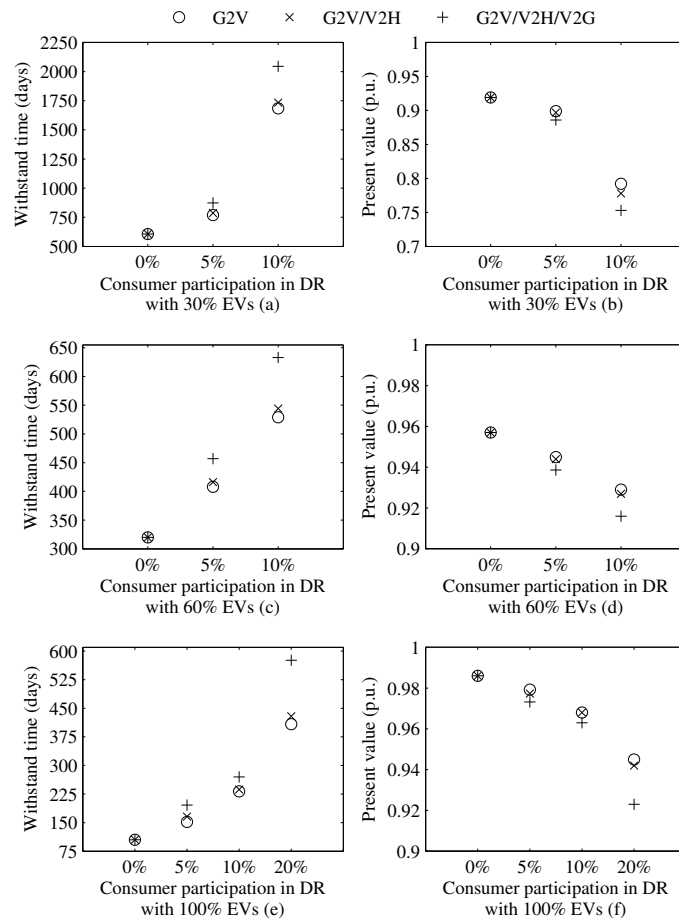
Figure 2.9: Withstand time for 30%, 60%, and 100% EV penetration in (a), (c), and (e), respectively. PV investment for 30%, 60%, and 100% EV penetration in (b), (d), and (f), respectively.

600 days at a cost of 1 p.u. However, 1 p.u. in 600 days is equivalent to a PV of 0.93 as shown in Figure 2.9b. This amount can be invested in consumer participation to avoid the lump-sum cost of replacing the line.

The worst-case situation includes consumers charging their EVs as soon as they arrive in their homes, which is represented by 0% consumer participation in DR. As the EV penetration increases at this DR participation level, the withstand time of the feeder decreases due to non-optimal charging, as shown in Figures 2.9a, 2.9c, and 2.9e. Lower withstand
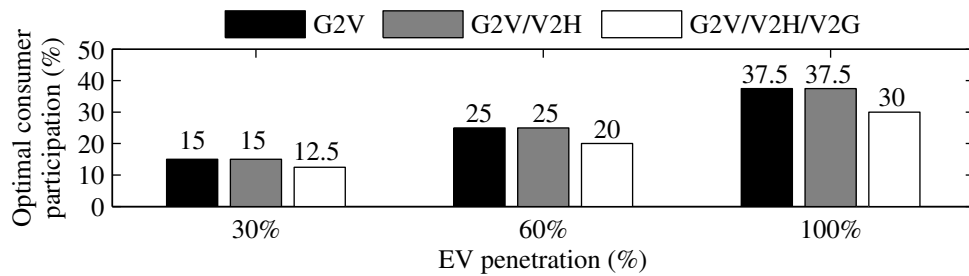
Figure 2.10: Optimal consumer participation in DR until incentives are required.

times justify larger investments in DR. As the participation in DR increases (*e.g.* from 0% to 10%), the withstand time of the feeder increases and the justifiable present value of investments decreases. This occurs because more consumers are shifting their consumption from high-price to low-price hours, thus mitigating the overloads.

Figure 2.9 also shows how limiting the EV modes of operation affects the amount of investments that can be justified. In G2V, EVs are limited to charging only. In G2V/V2H, EVs can discharge and supply loads in the home. In G2V/V2H/V2G, any excess energy after supplying loads can be sold back to the system. V2H and V2G aid the system by decreasing the amount of power flowing through the feeder. Comparing G2V and G2V/V2H modes in Figure 2.9 shows V2H results in only a slight increase in withstand time and decrease in justifiable investments. This is the case because V2H occurs during high-price periods. However, RTP tariff decreases consumption during these high-price periods and limits the power that could be injected in V2H. On the other hand, G2V/V2H/V2G modes create larger benefits. With V2G, EVs discharge during high-price periods and the power is used to supply other consumers in the system, including those that are not participating in DR. The G2V/V2H/V2G mode thus result in the largest withstand times and the least justifiable investments for all EV penetration levels.

Figure 2.10 shows that all EV penetration levels have an optimal DR participation level. Lower values of optimal DR participation are beneficial because they require smaller investments. The G2V/V2H/V2G mode requires the least consumer participation because of the

benefit of V2G. Since the demand is shifted to lower price hours, an increase in consumer participation in DR above the optimal level may cause overloads and require incentives.

2.10 Conclusion

This chapter presents a methodology to exploit flexibility of household appliances and EVs to manage the operation of the distribution grid. In the approach, an aggregating entity seeks to maximize profits, while consumers seek to minimize costs of purchasing electricity under time-varying tariffs. In addition to day-ahead tariffs, the aggregating entity offers incentives to relieve overloads in the system. Enabling the demand-side to participate in daily operations has several advantages, not only in avoiding overloads in the operating time frame, but also in the long run by avoiding or deferring investments in the grid.

The use of incentives in this framework is not purely limited to maintaining distribution line limits. Other applications are:

- Voltage stability - EVs can moderate their charging/discharging to maintain the voltage at a node.
- Frequency regulation - similar to voltage stability, EVs can receive frequency signals and modulate charging accordingly.
- Wholesale Power Markets - an aggregator can control the charging/discharge of EVs to obtain revenue from wholesale markets and a portion of this revenue can be passed on to consumers.
- Damage mitigation - EVs can moderate their charging/discharging to minimize damage to assets, *e.g.* distribution transformers.

In the next chapter, a framework is developed in which an aggregator manages charging/discharging of EVs connected to distribution transformers to ensure the loss-of-life of the transformer is minimized, while at the same time, the EVs arbitrage revenue is maximized. The next chapter's framework, where EVs should be rewarded for their participation, is an ideal application for the incentive mechanism developed in this chapter.

Chapter 3

CO-OPTIMIZATION OF DISTRIBUTION TRANSFORMER AGING AND ENERGY ARBITRAGE USING ELECTRIC VEHICLES

3.1 Introduction

In Chapter 2, a framework was developed on how an aggregator can incentivize consumers to shift their power consumption in time to maintain the power grid. Such a framework can also be applied to controlling EV charging and discharging to maintain grid assets, *e.g.* pole-top distribution transformers.

The advent of EVs will bring forth increases in power transmitted over the distribution power grid. Since it is expected for consumers to mostly charge EVs at their homes [42], the major impact will be on the local pole-top distribution transformers. This impact would translate into accelerated aging of the transformers [132] and earlier replacement to accommodate the additional power peaks required by the EVs' load.

This chapter proposes a centralized strategy of co-optimizing transformer loss-of-life with EV charging and discharging in order to minimize the total cost of operations. The consumers allow a management entity, *e.g.* an aggregator, to perform the scheduling of their EVs. The management entity seeks to minimize the energy procurement costs of its consumers by taking advantage of their price tariff to schedule charging (G2V) and energy arbitrage (V2G or V2H), and to minimize the transformer damage due to EV charging, while ensuring that EVs receive their required energy for transportation. With this, the aggregator obtains revenue from the transformer owner for maintaining lifetime, and some portion of this revenue must be given to consumers for their services. Through compensation, all parties can benefit financially. Furthermore, a transformer life expectancy analysis is performed for strategies

in which consumers independently manage their EVs (*i.e.* decentralized) and in which a management aggregator takes control (*i.e.* centralized).

The major contributions of this work are as follows:

- Centralized co-optimization model of transformer aging and energy arbitrage of EVs.

- Analysis of the use of EVs in G2V, V2H, and V2G to maximize the lifetime of the transformer under various levels of EV penetration.

- Methodology to analyze the costs/benefits of a transition from decentralized to centralized operational strategy for EV charging.

3.2 Transformer Model

The aging of transformers is dependent upon thermal effects from loading. The IEEE standard C57.91[1] [132] proposes a model for estimating the various transformer temperatures, which are correlated with its aging factor and *LoL*.

In order to estimate the transformer windings' hottest-spot temperature (HST), the following equation is used:

$$\theta_t^{\mathrm{HST}} = \theta_t^{\mathrm{A}} + \Delta\theta_t^{\mathrm{TO}} + \Delta\theta_t^{\mathrm{HST}} \quad \forall t \in T \tag{3.1}$$

where θ_t^{HST} is the windings' hottest-spot temperature, θ_t^{A} is the ambient temperature, $\Delta\theta_t^{\mathrm{TO}}$ is the top-oil rise over the ambient temperature, and $\Delta\theta_t^{\mathrm{HST}}$ is the winding HST rise over the top oil temperature, all for time period t in the set of all time periods T. From (3.1), the value $\Delta\theta_t^{\mathrm{TO}}$ is calculated by:

$$\Delta\theta_t^{\mathrm{TO}} = (\Delta\theta_t^{\mathrm{TO,U}} - \Delta\theta_{t-1}^{\mathrm{TO}})(1 - e^{\frac{-\Delta t}{\tau^{\mathrm{TO}}}}) + \Delta\theta_{t-1}^{\mathrm{TO}} \quad \forall t \in T \tag{3.2}$$

---

[1]Alternative approaches such as genetic algorithms [133] and methods based on experimental tests [57] can also be used to estimate the transformer life.

where $\Delta\theta_t^{\mathrm{TO,U}}$ is the ultimate top-oil rise over the ambient temperature, Δt is the time interval, and τ^{TO} is the top-oil time constant. In (3.2), the $\Delta\theta_t^{\mathrm{TO}}$ is dependent on the state in the previous period.

The term $\Delta\theta_t^{\mathrm{HST}}$ in (3.1) is calculated with Equation (3.3), where $\Delta\theta_t^{\mathrm{HST,U}}$ is the ultimate top-oil rise over the ambient temperature, and τ^{w} is the windings time constant. Note that as in equation (3.2), the term $\Delta\theta_t^{\mathrm{HST}}$ is also dependent on its previous state.

$$\Delta\theta_t^{\mathrm{HST}} = (\Delta\theta_t^{\mathrm{HST,U}} - \Delta\theta_{t-1}^{\mathrm{HST}})(1 - e^{\frac{-\Delta t}{\tau^{\mathrm{w}}}}) + \Delta\theta_{t-1}^{\mathrm{HST}} \quad \forall t \in T \tag{3.3}$$

The equations that calculate $\Delta\theta_t^{\mathrm{TO,U}}$ and $\Delta\theta_t^{\mathrm{HST,U}}$ are shown in (3.4) and (3.5), respectively.

$$\Delta\theta_t^{\mathrm{TO,U}} = \Delta\theta^{\mathrm{TO,R}} \cdot \left(\frac{k_t^2 \cdot R + 1}{R + 1} \right)^n \quad \forall t \in T \tag{3.4}$$

$$\Delta\theta_t^{\mathrm{HST,U}} = \Delta\theta^{\mathrm{HST,R}} \cdot k_t^{2 \cdot \mathrm{m}} \quad \forall t \in T \tag{3.5}$$

where $\Delta\theta^{\mathrm{TO,R}}$ is the top-oil rise over ambient at the rated load, $\Delta\theta^{\mathrm{HST,R}}$ is the hottest-spot rise over top-oil at the rated load, k_t is the ratio of the load on the transformer to its nameplate rating, R is the ratio between the losses at rated load and at no load, and m and n are the cooling parameters of the transformer. The ratio k_t is defined as:

$$k_t = \frac{TX_t^{\mathrm{load}}}{TX^{\mathrm{rating}}} \quad \forall t \in T \tag{3.6}$$

where TX_t^{load} is the load on the transformer in a certain period and TX^{rating} is the nameplate rating. It can be seen that as the load ratio k_t increases, the transformer temperatures vary based on Equations (3.1) to (3.5). Equation (3.7) relates the accelerated aging factor, F_t^{AA}, to the winding hottest-spot temperature, θ_t^{HST}.

$$F_t^{\mathrm{AA}} = exp\left(\frac{15000}{383} - \frac{15000}{\theta_t^{\mathrm{HST}} + 273} \right) \quad \forall t \in T \tag{3.7}$$

The term F_t^{AA} is the accelerated aging factor at a given temperature θ_t^{HST}. If $F_t^{\mathrm{AA}} > 1$ then the transformer is experiencing accelerated aging. With this factor, the *LoL* of the
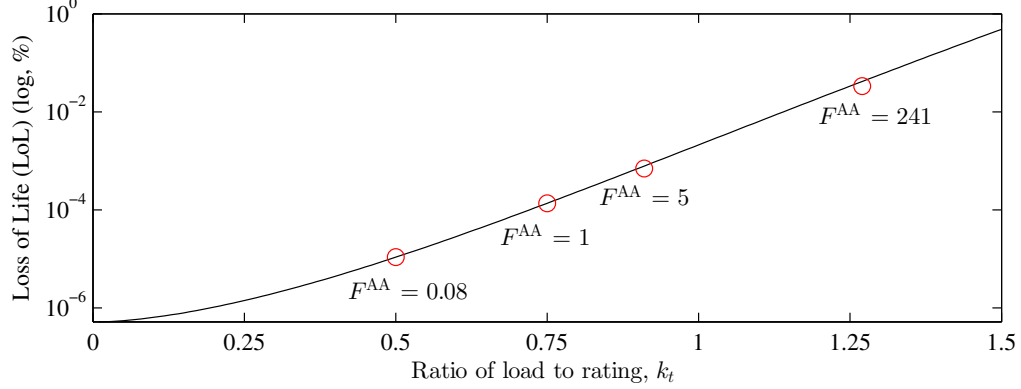
Figure 3.1: Loss-of-life as a function of the loading on the transformer for $\Delta t = 15$ min. Note that the y-axis is logarithmic.

transformer can be determined as shown in Equation (3.8) below:

$$LoL_t = \frac{F_t^{\text{AA}} \cdot \Delta t}{\beta} \quad \forall t \in T \tag{3.8}$$

where β is the normal insulation life of the transformer. Note that according to IEEE standard, a typical transformer must have a minimum normal insulation life (β) of 180,000 hours (20.5 years) [132].

With equations (3.1)-(3.8), the aging of the transformer can be estimated taking into consideration loading, temperature, and characteristic parameters. For example, if a transformer with parameters: $m = 0.8$, $n = 0.9$, $R = 6$, $\Delta\theta^{\text{TO,R}} = 56°C$, $\Delta\theta^{\text{HST,R}} = 80°C$, $\tau^{\text{TO}} = 90$ min, $\tau^{\text{w}} = 7$ min; is loaded at 90%, where $\theta_t^{\text{A}} = 24°C$, $\Delta\theta_{t-1}^{\text{TO}} = 25°C$, and $\Delta\theta_{t-1}^{\text{HST}} = 20°C$, for a Δt of 15 minutes, the transformer would lose 75.5 minutes of its insulation life. As shown, high loadings lead to accelerated aging of the transformer.

The effect of k_t on the LoL is shown in Fig. 3.1. In addition, the aging factor F_t^{AA} is shown for certain k_t ratios. The loading on the transformer increases exponentially the aging factor and thus the LoL at high loadings. This thermal-based transformer model can be embedded into an optimization framework.

3.3 Consumer Perspective

Consumers are assumed to reside in a household connected to the distribution system and to purchase their electricity under a variable electricity tariff π_t. Therefore it is expected that the consumers will strive to minimize their electricity costs, by optimizing their consumption under tariff π_t. In general, consumers are not responsible for day-to-day wear and tear of distribution system assets, especially local pole-top transformers. In some instances, consumers pay a fixed cost per month for the usage of the distribution system [134]. The distribution system operator (DSO), which in many cases is the same entity as the power utility company, has the responsibility of installing and maintaining distribution assets in order to provide electricity to its consumer-base.

Since the consumers are not responsible for the day-to-day damage of the transformer they are connected to, their optimization problem only considers the management of their assets (*i.e.* EVs). The consumers can manage their own EV charging and discharging by installing an energy management system or smart charger in their home [7, 10]. Such a management system can consider the electricity tariff, travel schedule of the EV, and other factors to procure energy at the least cost on behalf of the consumer. In addition, the management system may be able to take advantage of the EV battery to perform energy arbitrage (*e.g.* V2G or V2H) if it provides further cost savings. In general, this method is independent from the perspective of the power utility and does not require the use of a management entity.

3.3.1 Decentralized strategy: consumer optimization model

The consumer's goal is to minimize its electricity costs, therefore the objective function can be written as:

$$\min \quad \Delta t \cdot \sum_{t \in T} \sum_{v \in V} \pi_t \cdot \left(p_{t,v}^{\mathrm{chg}} - \eta_v^{\mathrm{dsg}} \cdot p_{t,v}^{\mathrm{dsg}} \right) \tag{3.9}$$

Where π_t is the electricity tariff, η_v^{dsg} is the discharging efficiency for EV v in the set of

EVs V, and $p_{t,v}^{\text{chg}}$ and $p_{t,v}^{\text{dsg}}$ are the charging and discharging powers, respectively.

The objective function (3.9) is subject to several constraints. In constraint (3.10), the energy state-of-charge is a function of its previous state, charging efficiency η_v^{chg}, power obtained from the grid $p_{t,v}^{\text{chg}}$ and injected to the grid $p_{t,v}^{\text{dsg}}$, total energy required for transportation ξ_v, and the motion schedule $S_{t,v} \in \{0, 1\}$. The parameter ξ_v is calculated based on the expected total miles that the EV v will travel and then multiplied by a conversion factor (kWh/miles) to obtain the total energy needs. The parameter $S_{t,v} = 1$ if the EV is in motion in period t, otherwise $S_{t,v} = 0$. Furthermore in (3.10), the energy for motion at period t is calculated as $\xi_v \frac{S_{t,v}}{\sum_{(t \in T)} S_{t,v}}$. For example, if an EV consumes 5 kWh for its trip and travels for a total of 5 time periods, then the EV consumes 1 kWh every time period t.

The actions of charging and discharging the EV, however, needs to be within the maximum power P_v^{max}. Also, the EV can only charge or discharge if it is available and connected to the household circuits. This availability is determined by the parameter $\alpha_{t,v} \in \{0, 1\}$, as shown in constraints (3.11) and (3.12). Note that $\alpha_{t,v} = 1$ before departure from the home and also after arrival from a trip back to the home, otherwise $\alpha_{t,v} = 0$. Also, in all time periods, the state-of-charge must be within the minimum and maximum bounds as shown in constraint (3.13). Constraint (3.14) ensures the total energy content of the battery at the end of the optimization horizon is the same as it was at the beginning of the day. Lastly, constraint (3.15) ensures the total load including the base consumption P_t^{base} is bounded by the household's power limit P^{limit}.

$$soc_{t,v} = soc_{t-1,v} + \eta_v^{\text{chg}} p_{t,v}^{\text{chg}} \Delta t - p_{t,v}^{\text{dsg}} \Delta t - \xi_v \frac{S_{t,v}}{\sum_{(t \in T)} S_{t,v}} \quad \forall t \in T, v \in V \tag{3.10}$$

$$0 \le p_{t,v}^{\text{chg}} \le \alpha_{t,v} \cdot P_v^{\text{max}} \quad \forall t \in T, v \in V \tag{3.11}$$

$$0 \le p_{t,v}^{\text{dsg}} \le \alpha_{t,v} \cdot P_v^{\text{max}} \quad \forall t \in T, v \in V \tag{3.12}$$

$$soc_v^{\text{min}} \le soc_{t,v} \le soc_v^{\text{max}} \quad \forall t \in T, v \in V \tag{3.13}$$

$$soc_{t=|T|,v} = soc_v^{\text{init}} \quad \forall v \in V \tag{3.14}$$

$$-P^{\text{limit}} \le P_t^{\text{base}} + p_{t,v}^{\text{chg}} - p_{t,v}^{\text{dsg}} \le P^{\text{limit}} \tag{3.15}$$

3.4 Aggregator's Perspective

Consumers' EV self-optimizations could result in increased damage to the distribution pole-top transformer to which they are connected. The owner of the transformer, *i.e.* utility or DSO, will incur these costs in two parts: 1) a loss of the currently installed transformer, and 2) required investment of a transformer of larger capacity transformer in order to accommodate increased EV loading. To reduce these costs, the owner of the transformer (*e.g.* DSO), or separate management entity (*e.g.* aggregator), can control the charging/discharging of EVs in a centralized fashion. The transfer of money between the DSO, aggregator, consumers, and the utility can be seen in Fig. 3.2. If the aggregator is separate from the transformer owner, the owner should pay the aggregator a portion r^{manage} of the savings r^{save} it obtains from not needing to frequently replace transformers. On the other hand, if the transformer owner is acting as the aggregator, then the savings are directly captured. In addition, the consumers pay their energy bill r^{energy} to the utility company.

In this work, a model is developed for the aggregator which focuses only on the consumers, their EVs, and the transformer. In this centralized strategy, the consumers allow the aggregator to control their EVs. The aggregator co-optimizes the transformer damage cost and cost of energy (including any arbitrage profits) to determine the charging/discharging profiles with the lowest total cost of operations. In return, the consumers receive compensation c^{pay} from the aggregator to offset their increased energy cost (compared to the decentralized case), $\Delta r^{\mathrm{energy}}$. All parties benefit if $r^{\mathrm{save}} > r^{\mathrm{manage}} > c^{\mathrm{pay}} > \Delta r^{\mathrm{energy}}$.

3.4.1 Centralized strategy: aggregator co-optimization model

The aggregator objective function is defined as:

$$\min \quad TX^{\mathrm{cost}} \sum_{t \in T} LOL_t + \Delta t \sum_{t \in T} \sum_{v \in V} \pi_t \left(p_{t,v}^{\mathrm{chg}} - \eta_v^{\mathrm{dsg}} \cdot p_{t,v}^{\mathrm{dsg}} \right) \tag{3.16}$$
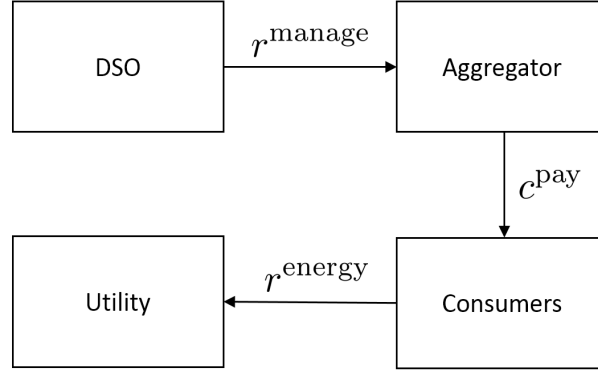
Figure 3.2: Revenue/payments by the aggregator from/to the consumer and DSO

subject to:

$$\text{Constraints } (3.1) - (3.5), (3.7), (3.8), \text{ and } (3.10) - (3.15) \tag{3.17}$$

$$k_t^+ - k_t^- = \frac{TX_t^{\text{base}} + \sum_{(v \in V)} \left(p_{t,v}^{\text{chg}} - p_{t,v}^{\text{dsg}} \right)}{TX^{\text{rating}}} \quad \forall t \in T \tag{3.18}$$

$$\theta_t^{\text{HST}} \leq \overline{\theta_t^{\text{HST}}} \quad \forall t \in T \tag{3.19}$$

In (3.16), the LoL_t is multiplied by the total transformer cost TX^{cost} to obtain the damage cost to the transformer. The transformer cost is defined as $TX^{\text{cost}} = TX^{\text{rating}} \cdot TX^{\text{price}}$, where TX^{rating} is the nameplate rating and the TX^{price} is the price per kVA. For instance, for a transformer that costs \$4152.5 (*i.e.* a transformer with a rating of 25 kVA priced at 166.1 \$/kVA [135]) that is loaded at 90%, with the parameters as specified in Section 3.2, the damage cost is then \$0.03.

Note that the second term in (3.16) is identical to the consumers' decentralized objective function (3.9), because now the aggregator is responsible for managing EV energy procurement costs. The consumers are hands-off in the management of their EVs with the guarantee they will receive their energy needs for transportation and revenue for assisting the grid.

The operator's objective function is subject to the transformer model equations (3.1)-(3.5), (3.7), (3.8), and the EV constraints (3.10)-(3.15). An additional constraint determines the absolute loading of the transformer while considering the base consumer load TX_t^{base} and
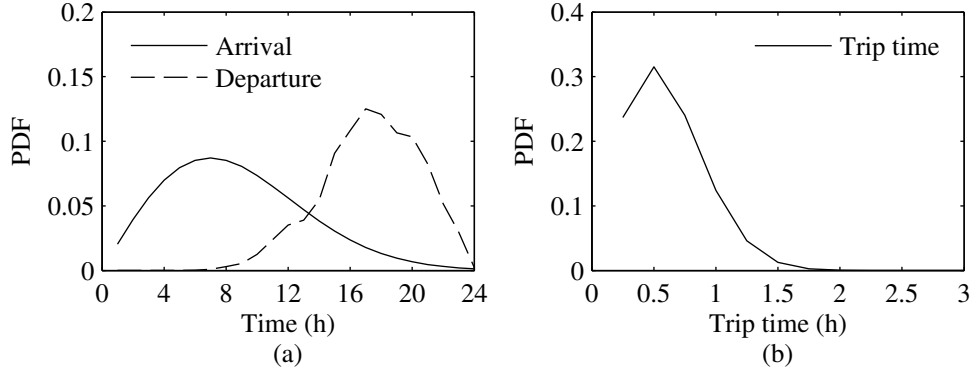
Figure 3.3: PDFs of the arrival time to the home and departure time from the home (a), and trip travel time (b).

the net EV power consumption, which is (3.18). Note that TX_t^{base} is the sum of the base load of all consumers in each period t, $i.e.$ $\sum P^{\text{base}} = TX^{\text{base}}$. Also, in (3.18) the total load could be negative and this makes the loading ratio k_t, negative. To avoid this, two non-negative variables, k_t^+ and k_t^- are introduced in (3.18) and $k_t = k_t^+ + k_t^-$. Such a formulation models the absolute value of the loading ratio. Furthermore, in (3.19) the hot-spot temperature θ_t^{HST} is bounded by the maximum temperature $\overline{\theta_t^{\text{HST}}}$ to avoid gassing in the solid insulation and the oil [132].

With the transformer equations in the optimization, the model becomes non-linear. Transformer equations (3.4), (3.5), and (3.7) are linearized using SOS2 [123], as discussed in Appendix B.1.

3.5   Simulation Results

The proposed strategies are applied to a pole-top transformer with a rating of 25 kVA, servicing 6 residential consumers with an individual household limit of 15 kW [136, 8]. Each consumers' consumption profile was obtained from a database of empirical data from the region of Austin, Texas and San Diego, California [137], and scaled so that the peak loading (without EVs) is similar to loadings in a typical suburban feeder, as described in [138].
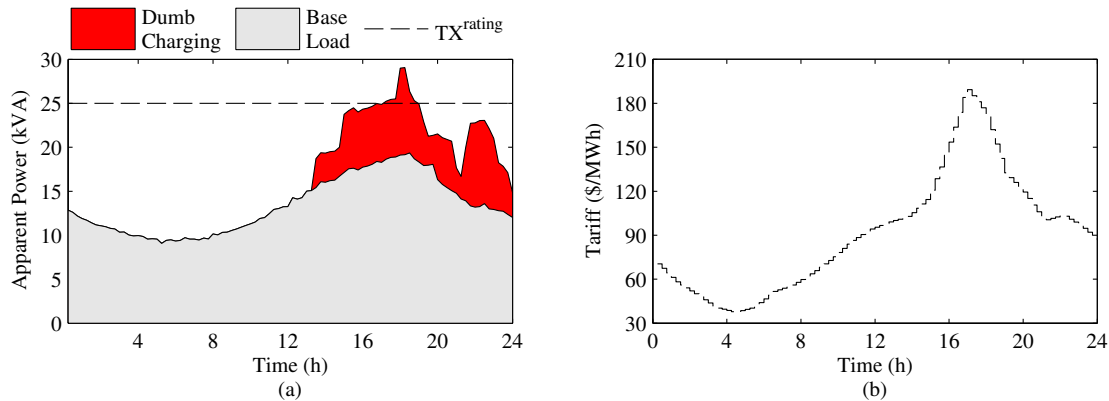
Figure 3.4: Dumb charging at 100% (6) EV penetration, base load, and transformer rating shown in (a), and the real-time electricity tariff shown in (b).

The 2009 National Household Travel Survey (NHTS) data [124] is used to determine the characteristics of EVs and generate dumb-charging profiles.

With such data, representative profiles were created by using K-means clustering [139]. Fig. 3.4a shows the base load and dumb charging load for 100% EV penetration, and Fig. 3.4b shows the real-time price tariff, (*i.e.* average price of 92.1 \$/MWh with a range from 37.6 to 189.3 \$/MWh and the median price of 92 \$/MWh), obtained from [2].

Using the NHTS dataset [124], probability distribution functions (PDF) were created for the departure time from the home, arrival time to the home, and trip travel time. The PDFs are shown in Fig. 3.3 and were used to generate the characteristics of the EVs. The EVs are available for charging and discharging during the period before they depart and the period after they arrive home again.

For the EV characteristics, the charging/discharging power rate is set at 3.3 kW and the energy capacity of EV batteries is 24 kWh, as in [8]. The state-of-charge, however, can only range from a minimum of 15% and a maximum of 95% of the total capacity because of safety and electrochemical constraints on the battery [127]. The round-trip efficiency is set to 90% [8] and the initial energy state-of-charge is uniformly randomized between 15% and 60% of $soc_v^{\max}$. A conversion factor of 0.33 kWh/mile [42] was used to convert the total
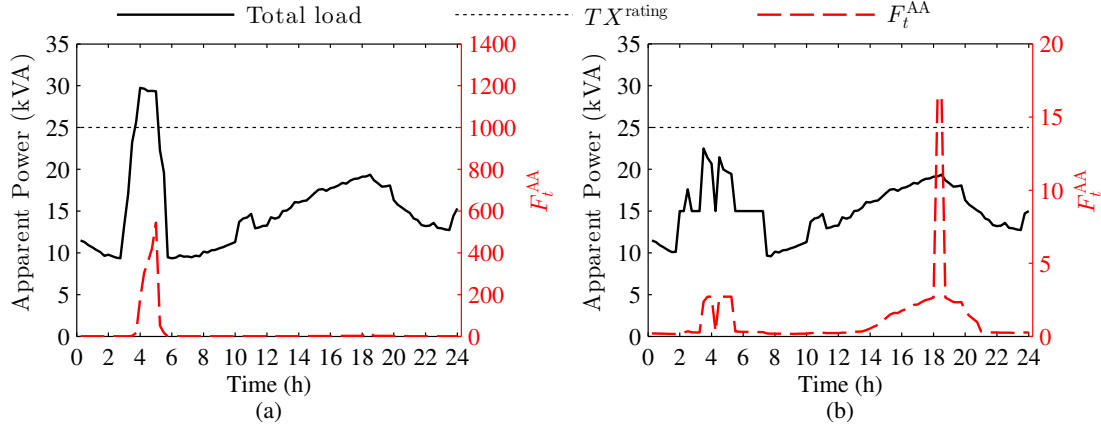
Figure 3.5: Loading on the transformer and aging factor for the decentralized case in (a) and centralized case in (b) with only G2V enabled.

miles travelled, obtained from NHTS [124], to the total energy required for motion ξ_v.

Historical data of ambient temperatures from July 2014 was obtained from San Diego, California [140]. The ambient temperatures were in the range [18.9, 25.6] °C with an average temperature of 21.7 °C. The initial transformer temperatures are set by performing the optimization and using the end-of-day temperature results. The maximum hot-spot temperature is 140 °C as discussed in [132]. The transformer parameters are as described in Section 3.2 and in [141]. The cost of the transformer replacement is 166.1 $/kVA, which considers the fixed and variable costs in a consolidated per-unit of kVA term, as discussed in [135].

The outcome of the centralized optimization is the optimized EVs charging/discharging profiles and associated transformer impacts (e.g. aging, LoL, and damage cost) and arbitrage benefits. By contrast, the decentralized optimization ignores the transformer damage. Therefore, a post-process calculation of the transformer damage is performed using the total load profile obtained from the optimization in order to be able to compare against the centralized optimization.
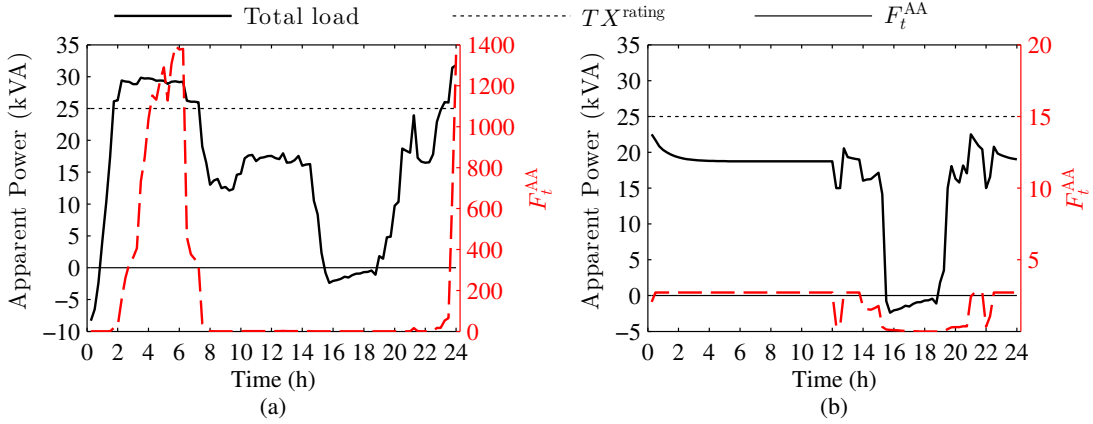
Figure 3.6: Loading on the transformer and aging factor for the decentralized case in (a) and centralized case in (b) with V2G enabled.

3.5.1 Decentralized versus centralized strategy

In the decentralized case, the consumers optimize the charging/discharging of their EVs and in the centralized case, the aggregator optimizes all EVs as an ensemble. Both models were simulated for 100% EV penetration to show the total load and the aging effect on the transformer (F_t^{AA}).

The total load through the transformer including EVs, the transformer rating, and the associated aging acceleration factor F_t^{AA} are shown in Fig. 3.5(a) for the decentralized case and in Fig. 3.5(b) for the centralized case, both while allowing only G2V (*i.e.* EVs only charge to meet their energy needs for transportation). By comparing Fig. 3.5(a) and Fig. 3.5(b), it can be seen that the loading on the transformer has higher peaks in the decentralized case because each consumer attempts to minimize only their cost of operation independently. Such actions result in the syncing of power consumption during the low-priced periods of the day (*e.g.* 0400 hours). On the other hand, in the centralized case the aggregator optimizes the EVs while also considering the transformer *LoL*. Therefore, the charging of the EVs is spread out during the low-price periods. This minimizes the peak power consumption during the nighttime and consequently reduces the total F_t^{AA}. However, the cost of energy
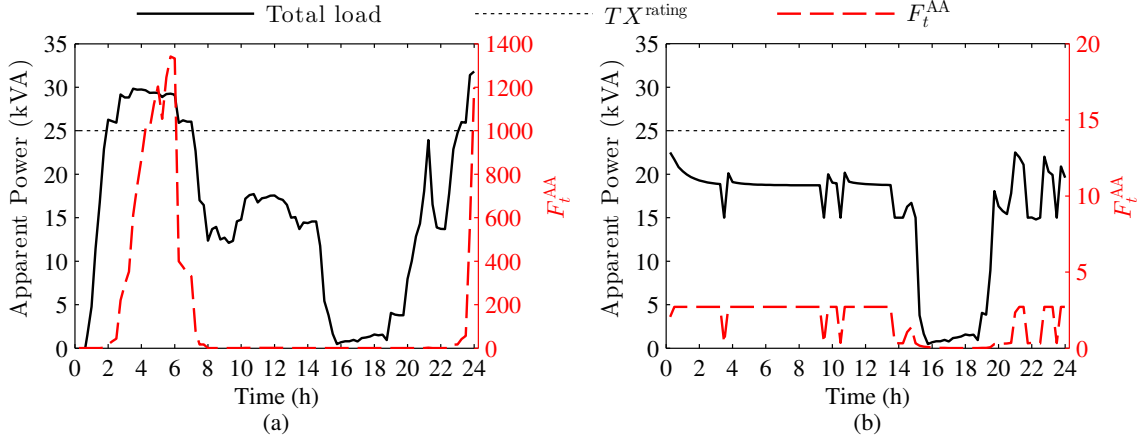
Figure 3.7: Loading on the transformer and aging factor for the decentralized case in (a) and centralized case in (b) with V2H enabled.

is increased as a tradeoff for improving the transformer lifetime. The aggregator will need to compensate the consumer for such a tradeoff.

Some EVs have the capability to discharge their batteries to supply energy directly to the grid in V2G mode. Similar to Fig. 3.5, Fig. 3.6 shows the decentralized case in (a) and the centralized case in (b) with V2G enabled. In the decentralized case in Fig. 3.6(a), the EVs charge in excess of transportation needs during the low-price periods (*e.g.* 0200 to 0800) in order to discharge during the high-price periods. The discharge leads to the total load on the transformer to be negative during 1500 to 1800 hours because all EVs are offsetting the base loads and then supplying energy back to the grid. To perform V2G, however, excessive charging occurs resulting in a large increase in the total aging factor F^{AA}, ultimately reducing the lifetime of the transformer. On the other hand, with centralized management as shown in Fig. 3.6(b), the aggregator keeps the loading on the transformer relatively constant during the nighttime periods. This results in a lower total aging factor F^{AA}. Again, to achieve the low aging factor the aggregator must reduce energy arbitrage and consumers must be compensated.

The last mode in which an EV can perform is in V2H. That is, EVs can discharge their

batteries to offset the base loads of the consumer, but cannot export power to the grid. Fig. 3.7 shows the total load and aging factor for the decentralized and centralized case in (a) and (b), respectively. The V2H operation is similar to V2G, except that the total F^{AA} is lower in both the decentralized and centralized operations. This is the case because in V2H, EVs are constrained to discharge only up to the magnitude needed to offset base loads, while in V2G mode the EVs have more freedom to take advantage of arbitrage. Essentially, V2G does not reduce transformer damage as much as V2H because the high-price periods (in which the consumer would prefer to discharge) may not correlate with the high base load periods (in which the total F^{AA} can be most effectively reduced). Regardless of the strategy, V2H provides slightly lower aging effect to the transformers as compared to V2G, but does not capture the maximum benefits from energy arbitrage.

The centralized strategy is superior in keeping the total F^{AA} low, whereas the decentralized strategy maximizes the benefits from charging/discharging of the EVs under real-time pricing. Most consumers would prefer to perform under the decentralized strategy unless the aggregator can provide the necessary incentives for a hand-over of control of the EVs.

3.5.2 Effect on the transformer life expectancy

The centralized and decentralized strategies are run for EV penetrations from 0 to 6 (*i.e.* 0% to 100% EV penetration) for a 24-hour period in order to see the effect on the transformer life and the associated transformer damage cost. The damage to the transformer is assumed to occur on a daily basis and by using the following equation an approximate value for the transformer life expectancy in years is obtained:

$$TX^{\mathrm{life}} = \frac{1}{365 \cdot \sum_{(t \in T)} LoL_t} \tag{3.20}$$

Fig. 3.8 shows the life expectancy for the dumb (*i.e.* unoptimized), centralized, and decentralized charging cases for G2V in (a), V2G in (b), and V2H in (c). Note that the G2V case with dumb charging is shown in Fig. 3.4(a), where the EVs charge immediately when they arrive home without any sort of management. With zero EV penetration (*i.e.*
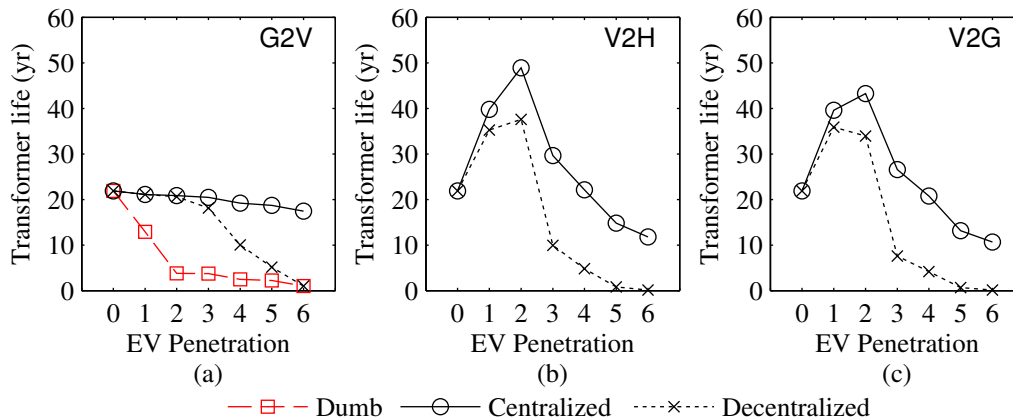
Figure 3.8: Transformer life expectancy in the dumb, centralized, and decentralized strategies under G2V (a), V2H (b), and V2G (c) operations.

base load shown in Fig. 3.4(a)), the typical life expectancy as stated in the IEEE standard C57.91 of 20.5 years is sustained [132]. This can be seen in all subplots in Fig. 3.8 at 0 EV penetration.

From Fig. 3.8a it can be seen that as the EV penetration increases, the life expectancy under the dumb charging strategy decreases significantly. This is expected since the EVs are adding their charging power onto the peak base load as shown in Fig. 3.4(a) in red. In the decentralized case considering only G2V, the expectancy is closely maintained at the typical 20.5 years up to 50% EV penetration (3 EVs). However, with further increase in EV penetration, the transformer life decreases drastically. This is the case because each consumer is self-optimizing their benefits and thus a large peak is created in the low-price periods (see Fig. 3.5(a)). In the centralized case with G2V (Fig. 3.8(a)), the life expectancy remains near the typical value, even under high EV penetration. For example, at a penetration of 6 EVs, the life only decreases to 17.45 years.

The life expectancy with V2H enabled is shown in Fig. 3.8(b). Since V2H discharging offsets the base loads, the transformer life expectancy is increased from the typical life for low EV penetrations under both strategies. This is beneficial because the transformer owner

obtains increased lifetime of their sunk-cost asset. However, with higher EV penetration in the decentralized case (*e.g.* greater than 3 EVs), the life is significantly decreased because of the excessive charging during the low-price periods (see Fig. 3.7(a)). With centralized charging at 100% EV penetration, the life is 11.8 years. This shows that by enabling V2H, the transformer owner experiences a decrease of 5.65 years of transformer lifetime, because EVs will increase their charging in order to offset house loads during peak price hours. Under V2H, the aggregator receives additional transformer life and consumers receive arbitrage benefits.

With V2G enabled, as shown in Fig. 3.8(c), neither strategy experiences an increase in lifetime as high as that in V2H. This effect occurs because V2G takes full advantage of the price difference in the electricity tariff and therefore obtains larger amounts of energy during the nighttime period as compared to V2H. In the centralized case under 100% EV penetration, the lifetime is 10.64 years. Therefore, V2G is not beneficial in terms of minimizing the damage cost of the transformer as compared to V2H. However, it does provide the largest arbitrage benefits to the consumers, and has the lowest overall operational cost.

In Fig. 3.8(b) and Fig. 3.8(c) it can be seen that for some penetration levels, the lifetime of the transformer is more than doubled. This is technically feasible in terms of the electrical and thermal characteristics of the transformer. However, other external factors, *e.g.* storms, corrosion, etc., may be a limiting factor on this extended lifetime. An analysis of these factors is outside the scope of this work.

With the initial introduction of EVs, the most probable operating mode is G2V, then V2H, and finally V2G. This is the case because V2H/V2G require bidirectional chargers in the EVs and V2G requires bidirectional power flow in the grids as well [40]. At high penetrations of EVs, the transformer will experience a relatively small decrease in lifetime if and only if the system is centrally managed under all modes of operations. The transformer owner, however, must provide the proper incentives to a management aggregator for performing this centralized strategy. At the same time, the aggregator must provide the proper incentives to consumers for participation in such a strategy. If the transformer owner opts to forgo cen-
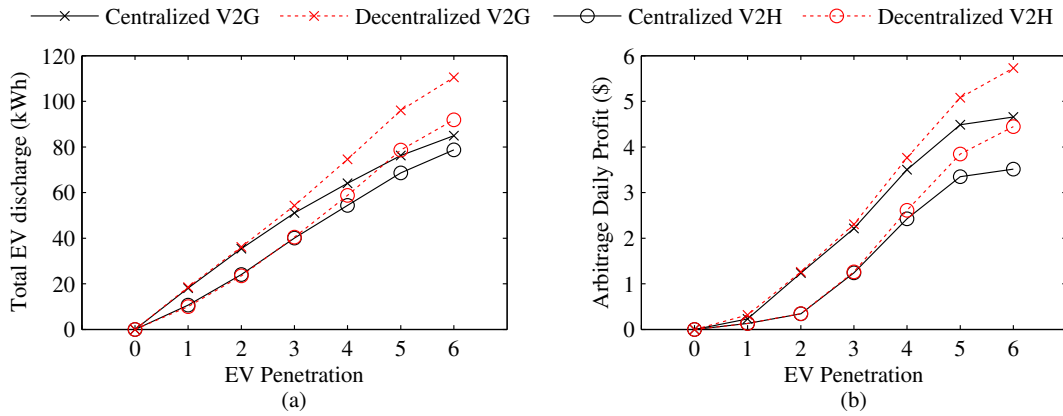
Figure 3.9: Total EV discharge in (a) and arbitrage daily profit/loss in (b) for different strategies and modes of operation (V2G, V2H).

3.5.3 Tradeoff between arbitrage and transformer damage

The notion that there is a tradeoff between obtaining the maximum benefits of arbitrage and the minimum transformer damage cost is evident in the centralized strategy. On the other hand, the decentralized strategy favors maximum arbitrage benefits and ignores the transformer. It is of importance to analyze these aspects. Fig. 3.9 shows the total discharge energy that is supplied by the EVs and the overall profit/loss for V2G and V2H modes. Note that overall profit is defined as the total discharge revenue minus total cost of charging energy (including transportation needs) for the EV. In addition, Fig. 3.10 shows the daily transformer damage cost for both strategies with varying EV penetration.

The total energy discharged by EV batteries is always higher in the decentralized case as compared to the centralized case, as is shown in Fig. 3.9a. Consequently, the arbitrage profits are also higher in the decentralized case, as shown in Fig. 3.9b. This is expected because in this strategy, consumers take advantage of arbitrage to its fullest potential ignoring the transformer's damage. With low EV penetrations (*i.e.* less than 4 EVs), the centralized and
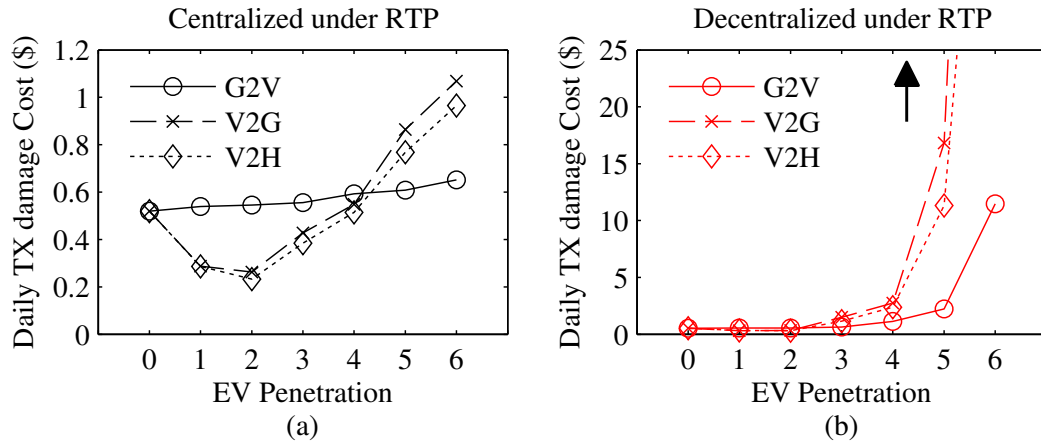
Figure 3.10: Daily transformer damage cost for the centralized (a) and decentralized strategy (b) with varying EV penetration.

decentralized strategies have negligible difference in the total EV discharge and arbitrage profits. This is the case because the aggregator can use the few EVs connected to the transformer to cater a charging/discharge profile that both reaps arbitrage benefits and reduces the damage cost as shown in Fig. 3.10(a) for V2G and V2H. In addition, the EVs' ability to discharge during the peak hours actually reduces the overall damage cost compared to G2V mode (see Fig. 3.10(a)). However, as the EV penetration grows in the centralized strategy, the additional charging of the EVs starts to increase the transformer damage and therefore the centralized strategy begins to limit arbitrage activities, as shown in Fig. 3.10)(a). This discharge limiting ultimately reduces the total arbitrage profits as a tradeoff for maintaining the transformer life.

Under 100% EV penetration, the total daily arbitrage profits in V2G mode in the decentralized and centralized case are \$5.73 and \$3.94, respectively. In addition, the life expectancies of the transformer for the decentralized and centralized strategies are 0.10 years and 10.6 years, respectively. For a loss of \$1.79 of arbitrage profit, the centralized case can provide an increase of two orders of magnitude in the transformer life expectancy. The transformer owner and the aggregator can perform such analyses to effectively determine the tradeoffs
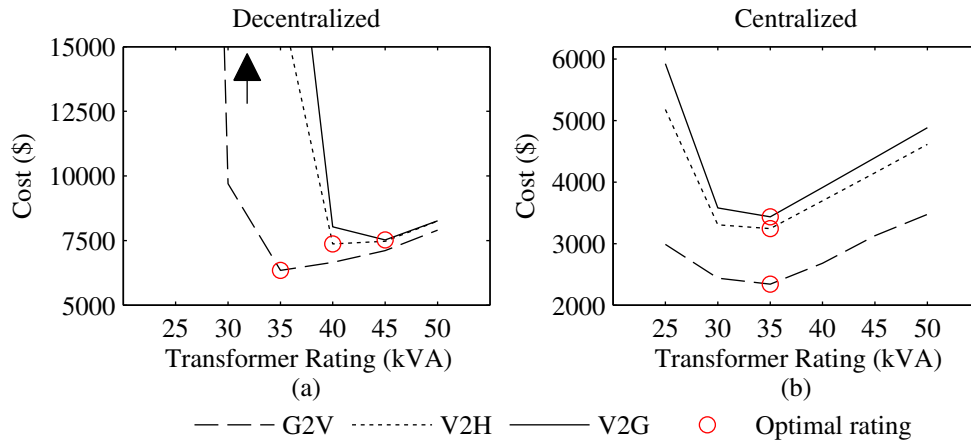
Figure 3.11: Perpetual replacement cost of transformers in decentralized in (a) and centralized in (b) for G2V, V2G, and V2H operations. Note that results are shown for the 100% (6) EV penetration case and the y-axis cost scales

and benefits of both strategies.

3.5.4 Determining the optimal replacement transformer rating

Once the 25 kVA transformer reaches its end-of-life, the transformer owner must decide the capacity rating of the replacement transformer. To do so, an optimization is performed over a set of replacement transformer ratings $S = \{25, 30, 35, 40, 45, 50\}$ kVA. The present cost of perpetual replacements [142] is calculated using a 5% annual interest rate [143]. This approach balances the replacement transformer cost and the replacement frequency. The results are shown in Fig. 3.11. Fig. 3.11(a) shows the decentralized strategy and Fig. 3.11(b) shows the centralized strategy under G2V, V2G, and V2H operations for the 6 EV case. By considering the already-established loadings on the transformer (shown in Fig. 3.5-3.7) and by varying the transformer rating, it can be seen that the present cost of perpetual replacements in the decentralized strategy is much higher than in the centralized strategy, due to the lack of coordination between consumers. In addition, the optimal transformer rating that minimizes this cost is 35 kVA in the centralized strategy regardless of the mode

	# of EVs	Investment deferral benefit ($)	Consumer arbitrage benefit ($)	Max. potential profit ($)
G2V	1	0.13	−0.07	0.06
	4	267	−20.7	246
	6	6,369	−64	6,305
V2H	1	10.2	−3.7	6.5
	4	795	−110	685
	6	53,589	−614	52,975
V2G	1	8.2	−5.5	2.7
	4	1,100	−139	961
	6	73,074	−652	72,422

Table 3.1: Decentralized to Centralized Annualized Benefits

of operations, whereas in the decentralized strategy, the optimal rating varies from 35 to 45 kVA, with V2G requiring the largest capacity.

3.5.5 Maximum potential revenue of the aggregator

For the aggregator to develop a business case, it must quantify its potential profit from a decentralized to centralized transition. It is shown in Fig. 9b that the consumers obtain greater arbitrage benefit in the decentralized strategy compared to the centralized strategy. On the other hand, the transformer owner obtains the benefit of increased transformer lifetime under a centralized strategy compared to a decentralized one. The aggregator can negotiate to obtain a share of the transformer lifetime benefit, and a portion of that must be provided to consumers to compensate for their lower arbitrage revenue.

The cost of the optimally-sized transformer replacement (as described in Section 3.5.4) is discounted based on the lifetime of the 25 kVA transformer (see Fig. 3.8) and a 5% interest rate. For example, if the 25 kVA transformer reaches its end-of-life in 10 years,

then a replacement transformer must be installed and its present cost is 61% of the future cost. The present cost in the centralized strategy is subtracted from the cost in decentralized strategy to obtain the investment deferral benefit for transitioning to a centralized strategy. This represents the transformer owner's benefit, of which the aggregator can negotiate its share.

On the other hand, the aggregator must quantify the benefit (in actuality, the cost) for consumers of a transition to a centralized strategy. This is calculated by taking the difference between the annual arbitrage revenue in the centralized and decentralized strategies.

Table 3.1 shows these benefits in the first and second column for the different modes of operation (*i.e.* G2V, V2H, and V2G) and EV penetrations. The last column is the maximum profit the aggregator can obtain, which is the sum of the investment deferral benefit and the consumer arbitrage benefit (loss). The investment deferral benefits are annualized by representing the one-time transformer replacement cost with the equivalent-annual-annuity approach, as described in [142].

From Table 3.1, the benefit seen by the transformer owner is highest in V2G mode under 100% EV penetration. This is because in the decentralized strategy, the consumers have the maximum flexibility to use their EVs for arbitrage, which is extremely damaging to the transformer. In contrast, a centralized strategy avoids much of this damage. Therefore, the aggregator has a strong case to negotiate a contract with the transformer owner. However, with low EV penetrations (*e.g.* 1-4), the annualized deferral benefit is much smaller. In this case, the aggregator may not have a strong business case when considering the cost to equip and control these EVs.

The consumer arbitrage benefit (shown in the second column) is negative in all cases. This is expected because in the decentralized strategy consumers are able to generate more revenue from energy arbitrage (see Fig. 3.9(b)). Thus, consumers must be compensated for their loss in revenue by the aggregator, otherwise they would not be willing to hand over control of their EVs. The maximum potential revenue (last column) shows the amount of money available for the aggregator's business case. A portion of this money should be

given to consumers for allowing the control of their EVs for the aggregator's benefit, and the transformer owner will likely want to retain some of the investment deferral benefit. Using an analysis such as the one shown in Table 3.1, an aggregator can negotiate contracts with both the transformer asset owner and consumers in which all the entities profit.

3.6 *Conclusion*

A centralized model is developed in this chapter which co-optimizes the transformer loss-of-life (LoL) with electric vehicle (EV) charging and discharging for arbitrage, while ensuring the EVs obtain their energy needs for transportation. Such a model can be implemented by the transformer asset owner, *e.g.* distribution system operator, or a separate hierarchical entity. The model considers the transformer's thermal temperatures, accelerated aging factor, and LoL. For comparison, a decentralized model is also presented which could be implemented by consumers' energy management systems or smart chargers in their homes. In the decentralized approach, the consumers are not responsible for transformer damage and thus optimize their EV charging/discharging only for arbitrage.

Results show that in the centralized strategy the transformer life decreases under high penetrations of EVs when charging only. In the decentralized strategy, the transformer must be fully replaced under similarly high penetrations after fractions of its expected lifetime. Furthermore, when the EV penetration is moderate, the transformer life is increased beyond its expected lifetime when performing in vehicle-to-home (V2H) and vehicle-to-grid (V2G) modes under both strategies. This is the case because the EVs discharge their battery and decrease the net load experienced by the transformer during peak hours, when transformer damage is greatest.

In the decentralized strategy, the EV consumers receive additional revenue for performing energy arbitrage, as compared to the centralized strategy (V2G mode at a high EV penetration). The centralized aggregator essentially limits energy arbitrage in order to maintain or even increase the lifetime of the transformer. However, the decrease in arbitrage benefit is more than offset by the transformer investment deferral benefit, creating a situation where

a management aggregator can reduce the costs of the consumers and the transformer owner simultaneously, and still have a viable business case.

Although the benefits of centralized EV charging management have been demonstrated in this chapter, the DSO would have to invest in communications and control infrastructure in order to implement such a strategy, and thus would have to weigh their potential costs and benefits to ensure such a venture is profitable.

The proposed model and results that can be obtained with it will:

- inform DSOs of the potential impact EVs may have on their distribution transformer assets
- quantify the market potential for new businesses, *i.e.* aggregators, to emerge and manage EVs

In the next chapter, a framework is developed considering an aggregator's participation in the wholesale power markets. Such a framework allows for further revenue generation by the aggregator which can then be used to reward EV owners for their participation.

Chapter 4

OPTIMAL PARTICIPATION OF AN ELECTRIC VEHICLE AGGREGATOR IN DAY-AHEAD ENERGY AND RESERVE MARKETS

4.1 Introducton

EVs are poised as effective participants in both the energy and reserve markets. In the energy markets, they can shift consumption in time to exploit the low and high prices of the day. On the other hand in the reserve markets where capacity must be on stand-by in the DA and then deployed in the RT based on the need of the system, EV batteries can react quickly to provide such services. The combined participation in these markets increases the revenue potential of EV owners. However, the aggregator exploiting EVs must consider the tradeoff between the cost of degrading the batteries verses revenue potential from the markets and thus make an optimal economic decision.

In this chapter, a framework is proposed to assess the aggregator's capabilities to provide energy and different reserve services in a realistic market environment [120]. The aggregator participates in the energy market as a price-taker, and its offers to the ancillary services market are optimized taking into account both i) the probability of acceptance and ii) the probability of deployment in the market environment. The former represents the expected probability of the aggregator's offers being accepted in the DA ancillary market, thus receiving the revenues at the market capacity price for its bid, and the latter is the probability the accepted offer to be deployed in the RT, thus receiving the revenues for the deployed energy at the RT energy price.

The contributions of this framework are as follows:

- An optimal strategy for both energy and reserve markets considering their tradeoffs

and effect on EV battery degradation.

- Realistic approach to participating in the voluntary reserve markets with price-quantity offers that are justified.

- Assessing the expected profit the EV aggregator can collect by participating in the energy and regulation market.

4.2 Power system entities

4.2.1 Electric vehicle's perspective

EV owners can allow the aggregator to manage their EVs' scheduling by charging energy in G2V mode and discharging energy in V2G mode, as long as these priorities are fulfilled:

1. Energy requirements for transportation are not comprised,
2. Monetary benefits are provided for participation, and
3. Compensation is provided for the aggregator's additional usage of EV batteries.

For the aggregator to properly schedule EVs, each EV must inform their availability $\alpha_{t,v} \in \{1, 0\}$ (1 if available to charge/discharge, and 0 otherwise) at each time period t for each vehicle v. During the availability periods ($\alpha_{t,v} = 1$), the EVs must obtain their energy for motion ξ_v and charge any additional energy that the aggregator schedules to provide services to the power grid. In essence, the process from the EVs perspective should be well-integrated and automated with minimal owner participation.

4.2.2 Aggregator's perspective

The goal of the the aggregator is to exploit its EV fleet to maximize profits. The profits are the difference between the revenues for providing services to the system and the costs of services provision. The costs of providing these services are a function of the incurred battery degradation that must be reimbursed to EV owners. In order for the services from

EVs to be economically viable, the revenues must outweigh the cost compensation for the degradation of EV batteries. If this is not the case, then using EV batteries beyond supplying their motion needs does not make economic sense.

The aggregator participates in two markets: day-ahead energy and day-ahead regulation. However, in the regulation market it submits separate up and down offers. The aggregator can submit competitive offers in order to provide a share of the regulation services, because the SO fulfills its regulation requirement by selecting the least priced offers.

The markets it participates in and the revenue structure is described below:

- **Day-ahead Energy Market**: aggregator is a price-taker in this market and thus cannot influence its outcome. It forecasts market prices and schedules EVs accordingly to maximize profit.

- **Day-ahead Up Regulation Market**: aggregator can influence the price, *i.e.* price-maker, in this market. The revenues are obtained in the DA in the form of a capacity payment for being on-stand by and an additional deployment payment in RT if called to deploy the energy.

- **Day-ahead Down Regulation Market**: similar to the up regulation market, the DA capacity payment is obtained for stand-by, however, no deployment payment is given since otherwise the EVs receive a double benefit of free energy and revenue.

Considering these opportunities, the aggregator can make optimal decisions on the participation in each individual market.

4.2.2.1 *Probability of acceptance and deployment*

In order to structure a competitive bid pair (*i.e.* price and quantity) in the regulation market, the aggregator must use the probability of acceptance (π^{a}) and probability of deployment (π^{d}). π^{a} represents the aggregator's assumption on the likelihood of its capacity offers p^{cap} to be accepted p^{accept} in the DA regulation market, *i.e.* $\mathrm{Prob}(p^{\mathrm{cap}} \geq 0) \geq \pi^{\mathrm{a}}$. Similarly,
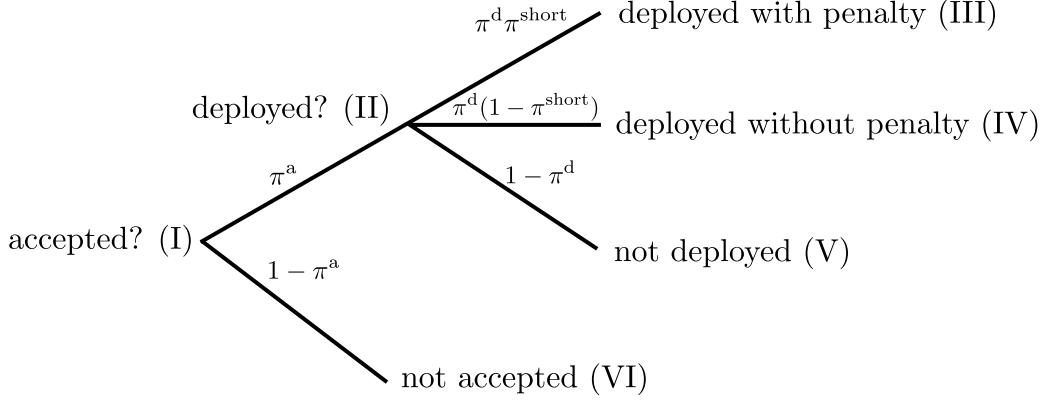
Figure 4.1: Decision tree for regulation market interactions

π^{d} represents the assumed likelihood of the accepted offers p^{accept} to be deployed in real-time, *i.e.* $\mathrm{Prob}(0 \leq p^{\mathrm{depl}} \leq p^{\mathrm{accept}}) \geq \pi^{\mathrm{d}}$, where p^{depl} is the expected power deployment. The system operator cannot call upon the aggregator to deploy more than the DA accepted capacity. Since the aggregator is not aware what fraction of p^{accept} the SO can call upon in the RT, it needs to schedule the purchase of the shortage p^{short} in the RT energy market, where $p^{\mathrm{short}} = p^{\mathrm{accept}} - p^{\mathrm{depl}}$. This shortage power has an associated probability $\mathrm{Prob}(p^{\mathrm{short}} = p^{\mathrm{accept}} - p^{\mathrm{depl}} \geq 0) = 1 - \pi^{\mathrm{d}} = \pi^{\mathrm{short}}$ and thus allows a risk-averse decision to be made by the aggregator.

Figure 4.1 shows the probability-based decision tree considered by the aggregator in its DA model. In branch (I), the DA capacity offer is accepted with a probability π^{a}. After the offer is accepted, it may be deployed by the SO up to p^{accept}, *i.e.* $0 \leq p^{\mathrm{depl}} \leq p^{\mathrm{accept}}$. This occurs with probability π^{d} as shown in branch (II). The aggregator also needs to consider if the actual deployment required by the SO is larger than expected p^{depl}, and thus it considers the cost of the shortage p^{short}. An ideal case without penalties is shown in Figure 4.2a where the aggregator obtains the DA capacity price λ^{cap} for the accepted capacity p^{accept} and the expected RT energy price λ^{RT} for the deployment p^{depl}.

In branch (V), the aggregator expects its DA offer to be accepted with probability π^{a} but

not deployed by the SO in the RT. In this case, it cannot take advantage of the additional revenue for deployment, however, it does not have the risk of being unable to deploy if called upon by the SO. It receives only the DA accepted offer times the capacity price λ^{cap}. In branch (IV), the offer is accepted and the full accepted capacity is expected to be deployed. This occurs without the aggregator assuming any expected energy shortage in the DA because it is able to use its available EV fleet. The aggregator obtains benefits from both the DA capacity and RT market revenue streams. This is summarized in Figure 4.2a when $p^{\text{depl}} = p^{\text{accept}}$.

Figure 4.2b summarizes branch (III) which includes penalties. In branch (III), the aggregator considers some portion its full capacity offer to be accepted and some fraction that to be deployed beyond the expected p^{depl}. This occurs because the aggregator's decisions in the DA are based on estimates of its EV fleet availability in the RT. Therefore, it has the risk of over-offering in the ancillary market, which if accepted, it may not be able to deploy due to a lack of capacity. Thus, it needs to consider the possibility the actual deployment requirement in RT p^{act} to be larger than its expectation p^{depl}. In Figure 4.2b, the aggregator receives the DA capacity revenue. As for RT revenue, the SO requested p^{act} which the aggregator is unable to provide. Therefore, it receives the RT price for p^{depl} and must purchase the actual shortage, $p^{\text{act}} - p^{\text{depl}}$, at λ^{RT}. However, in the DA, the aggregator already considers the possibility of shortage (p^{short}) and thus the decisions are hedged against.

These cases are incorporated into the DA optimization to determine the optimal offering schedule for regulation services. The different cases shown in Figure 4.1 are constructed by determining their corresponding probability of acceptance for regulation up π^{a} and down ϕ^{a}, as well as the probability of deployment for regulation up π^{d} and down ϕ^{d}.

4.2.2.2 Determining market prices for energy and regulation

The aggregator obtains the prices for the reserve and energy markets when these markets clear. In the reserve market, the clearing process requires a quantity-price offer from the aggregator, which must be competitive due to a limited capacity requirement in these markets.
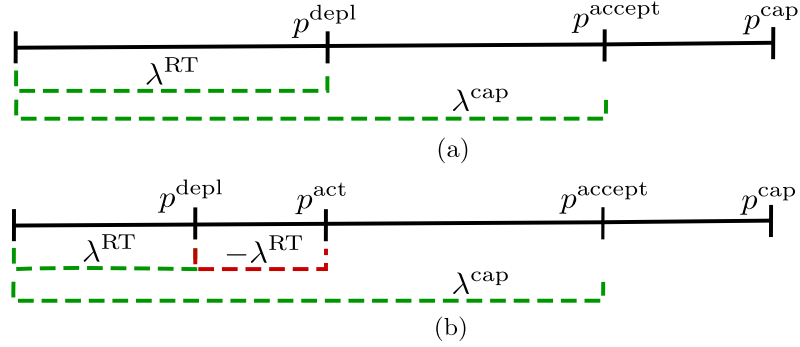
Figure 4.2: Actual revenues and costs when participating in ancillary markets, where (a) is the case with no penalties and (b) includes penalties.

Therefore, the aggregator needs a method to estimate these prices in order to optimally bid into these markets. By using historical data, price-quantity-probability (PQP) curves, as shown in Figure 4.3, can be incorporated into the model. Figure 4.3a represents the complementary CDF of prices, Figure 4.3b represents the complentary cumulative distribution function (CDF) of quantity, and Figure 4.3c shows the PQP curve which is derived from the curves in Figure 4.3a and Figure 4.3b. In order to create these functions, historical data must be obtained from markets for regulation prices, energy prices, and capacity accepted and deployed.

The process to obtain the PQP curve shown in Figure 4.3c is constructed following these steps: i) First, the complementary CDF, *i.e.* 1-CDF, is calculated for prices (see Figure 4.3a) and quantity (see Figure 4.3b), individually. ii) Next, these separate curves are then combined as shown in Figure 3c, where the x-axis is the quantity and the y-axis maps the prices. Each corresponding step in the PQP curve represents a probability π, which has a corresponding market price to be used in the aggregator's optimization model. This process is applied to the reserve prices against the total accepted quantities for regulation up and down with their respected probability of acceptances (*i.e.* π^{a}, ϕ^{a}), and also to the real-time energy price against the regulation deployed in the RT with the probability of deployments (*i.e.* π^{d}, ϕ^{d}). The probabilities are sorted in descending order: $\pi_1 > \pi_2 > \cdots > \pi_{|B|}$ where
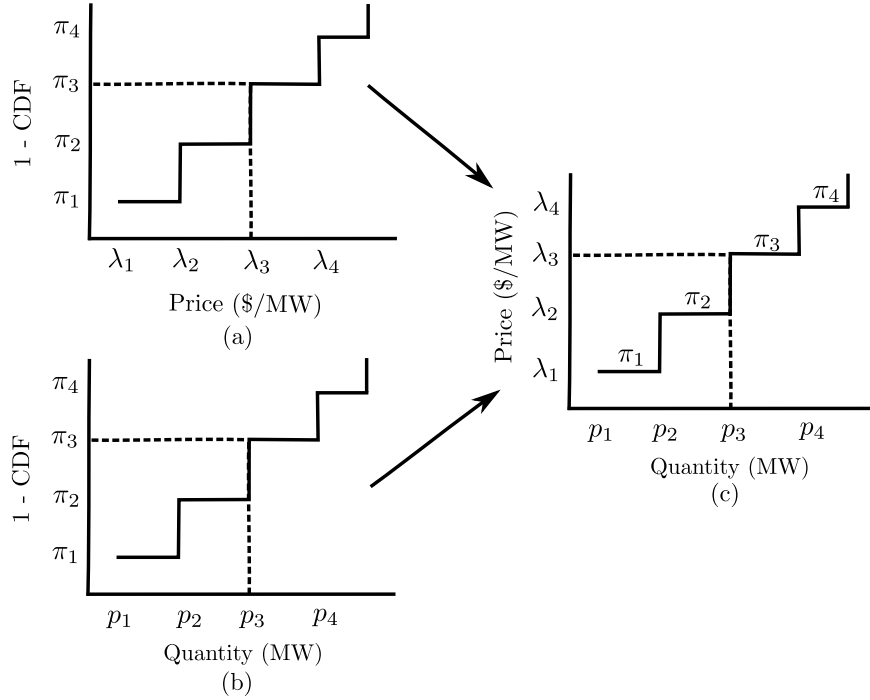
Figure 4.3: Capacity price and total accepted capacity quantity complementary CDF's shown in (a) and (b), respectively. In (c), the price-quantity-probability (PQP) curve is shown which is derived from the curves in (a) and (b).

B is the set of segments with index b. For example, the first two corresponding steps in Figure 4.3c labeled π_1 and π_2 can take on the values of 100% and 90%, respectively. As the price-quantity pair increases, the likelihood decreases.

4.2.3 System operator's perspective

In the presented model, it is assumed the system operator clears a simultaneous energy and reserve pool-based market with unit commitment (UC) in order to determine the schedule and power output of generators. A generic two-stage market structure of a DA and RT planning is implemented in this work. These market structures are common in United States electricity markets, *e.g.* PJM [82] and ERCOT [144]. However, the market design used in this work is generic to be compatible with other market-based power systems [89]. Such

co-optimization of energy and reserve [1] markets yields substantial cost savings for the SO [147, 148], and incentivizes the SO to enable participation of all eligible energy and reserve providers, including EV aggregators. The energy price is a by-product of the clearing process, as well as the least-cost allocation of regulation up/down, resulting in regulation prices [149].

When an imbalance materializes as a lack of generation to meet the demand, then regulation up is required to accommodate such imbalance. On the other hand, if the imbalance materializes as an excess of generation to meet the demand, then regulation down is required. In the DA, the system operator enforces a pre-established requirement of regulation up and down for each hourly period of the optimization horizon, which in this work is determined by the '3+5' rule [150]. This criterion ensures the hourly reserve requirements are set to 3% of the hourly load and 5% of the hourly available renewable energy capacity. Therefore, this rule accounts for all sub-hourly balancing needs of the SO to mitigate the impact of wind power and load forecast errors [151]. The SO then optimally determines in a least-cost manner which market participant's offers to accept to meet the requirement. If a participant's offer is accepted, it receives the market clearing price for the specific service it provides (*i.e.* capacity price for being on standby). If a participant's accepted capacity is called upon for deployment in RT, then they must provide the energy and then receive the RT price for energy deployed. If they are unable to provide the energy, they may purchase it in the RT energy market. In this work, the UC model is implemented as explained in [149].

4.3 Aggregator Optimization Model

4.3.1 Market participation

The aggregator participates in the DA energy and regulation market. In the energy market, the aggregator is a price-taker, thus submitting quantity-only zero-price bids. On the other hand, the regulation market has pre-defined requirements.

---

[1]Throughout this chapter, regulation is assumed to be a joint reserve product, *i.e.* it combines the secondary and tertiary regulation interval, as explained in [145] and [146].

From the aggregator's perspective, their are several actions that can be exploited from EVs. These include:

- **Energy Market Charge (EMCHG)**: Schedule EVs to charge energy from the DA energy market thus receiving the DA energy revenue.
- **Energy Market Discharge (EMDSG)**: Schedule EVs to discharge energy to the DA energy market thus receiving the DA energy revenue.
- **Regulation Up (REGUP)**: Schedule EVs to discharge energy to the grid and receive the capacity revenue for being on-standby and the RT energy revenue for deploying the capacity if required.
- **Regulation Down (REGN)**: Schedule EVs to charge energy to the grid and receive the capacity revenue for being on-standby. No RT deployment compensation collected because EVs will then obtain two benefits of free energy.
- **Stop Charging (STOPCHG)**: Part of the REGUP product which can only occur if a subset of the EV fleet is already scheduled to charge energy from the energy market and are interrupted voluntarily.
- **Stop Discharge (STOPDSG)**: Similar to STOPCHG but bundled with the REGDN product. Also can be only scheduled if the EV fleet is already scheduled to discharge in the energy market.

The scheduling of charging and discharging in the energy, regulation up, and regulation down market are considered by the optimization model as described in the following subsection.

4.3.2 Optimization model

The aggregator seeks to maximize its profits. The objective function of the aggregator is:

$$\max \quad r^{\text{em}} + r^{\text{cap}} + r^{\text{depl}} - c^{\text{regup}} - c^{\text{regdn}} - c^{\text{deg}} \tag{4.1}$$

where r^{em} is DA energy market revenue, r^{cap} is the DA regulation market revenue for capacity, r^{depl} is the expected revenue for deployment in real-time, and in terms of costs, c^{regup} is the cost for regulation up service, c^{regdn} is the cost for regulation down service, and c^{deg} are the battery degradation costs that must be compensated to consumers.

The DA energy market revenue r^{em} is given as:

$$r^{\mathrm{em}} = \Delta t \sum_{(t \in T)} \sum_{(v \in V)} \lambda_t^{\mathrm{DA}} \left(\eta_v^{\mathrm{dsg}} \cdot p_{t,v}^{\mathrm{emdsg}} - p_{t,v}^{\mathrm{emchg}} \right) \tag{4.2}$$

where λ_t^{DA} is the DA energy market price, η_v^{dsg} is the battery discharge efficiency, and $p_{t,v}^{\mathrm{emdsg}}$ and $p_{t,v}^{\mathrm{emchg}}$ are the discharge and charging powers specifically targeted for the energy market, respectively. The revenue r^{cap} is obtained from the DA regulation market as:

$$r^{\mathrm{cap}} = \sum_{(t \in T)} \sum_{(b \in B)} \left[\left(w_{t,b}^{\mathrm{up}} \cdot \lambda_{t,b}^{\mathrm{up}} \right) \cdot \pi^{\mathrm{a}} \cdot p_t^{\mathrm{up}} + \left(w_{t,b}^{\mathrm{dn}} \cdot \lambda_{t,b}^{\mathrm{dn}} \right) \cdot \phi^{\mathrm{a}} \cdot p_t^{\mathrm{dn}} \right] \tag{4.3}$$

where $\lambda_{t,b}^{\mathrm{up}}$ and $\lambda_{t,b}^{\mathrm{dn}}$ are the DA regulation up and down capacity prices, respectively, obtained from the CDF curves. The binary variable $w_{t,b}^{\mathrm{up}} \in \{1, 0\}$ activates only one segment of the capacity price CDF curves as a function of the probability π^{a}. Similar rationale applies for $w_{t,b}^{\mathrm{dn}}$ as a function of probability ϕ^{a}. The revenue term, takes into account the likelihood of capacity offers to be accepted and is represented by branch (I) in Figure 4.1. The power p_t^{up} and p_t^{dn} are the regulation up and down capacity offers to the market. This revenue stream only considers the capacity revenue, however, if the capacity is deployed by the SO, additional revenue for deployment r^{depl} should be accounted at RT prices:

$$r^{\mathrm{depl}} = \pi^{\mathrm{a}} \cdot \pi^{\mathrm{d}} \cdot \eta^{\mathrm{dsg}} \sum_{(t \in T)} \sum_{(v \in V)} \sum_{(b \in B)} \left(v_{t,b}^{\mathrm{up}} \cdot \lambda_{t,b}^{\mathrm{RT}} \right) \left(e_{t,v}^{\mathrm{regup}} + e_{t,v}^{\mathrm{stopdsg}} \right) \tag{4.4}$$

where $\lambda_{t,b}^{\mathrm{RT}}$ is the RT energy price obtained from the CDF curve, $e_{t,v}^{\mathrm{regup}}$ is the expected energy deployment for regulation up service, and $e_{t,v}^{\mathrm{stopdsg}}$ is the energy in regulation up service that is only potentially scheduled in the same period t in which energy market discharging (EMDSG) is scheduled. Each segment of the real-time energy price CDF curve has a binary variable $v_{t,b}^{\mathrm{up}} \in \{1, 0\}$. This variable determines which particular segment b is active, and

it is a function of the probability π^{d}. Therefore, r^{depl} represents the revenue that may be obtained from deployment in the RT market and represents the case in branch III (Figure 4.1). This, however, assumes the aggregator would deploy a fraction of its capacity offer and ignores the risk of being deployed more than it anticipated. In order to account for this outcome, equation (4.5) is the cost c^{regup} for regulation up service:

$$c^{\mathrm{regup}} = \pi^{\mathrm{a}} \cdot \pi^{\mathrm{d}} \cdot (1 - \pi^{\mathrm{d}}) \sum_{(t \in T)} \sum_{(b \in B)} \left(v_{t,b}^{\mathrm{up}} \cdot \lambda_{t,b}^{\mathrm{RT}} \right) \left(p_t^{\mathrm{up}} - \pi^{\mathrm{a}} \cdot \pi^{\mathrm{d}} \cdot p_t^{\mathrm{up}} \right) \tag{4.5}$$

where the difference between the capacity offers p_t^{up} and the expected deployment $\pi^{\mathrm{a}}\pi^{\mathrm{b}}p_t^{\mathrm{up}}$ determines the amount of shortage that may need to be purchased in the RT energy market. This situation can occur with a conditional probability product of $\pi^{\mathrm{a}}\pi^{\mathrm{d}}(1 - \pi^{\mathrm{d}})$, where $1 - \pi^{\mathrm{d}} = \pi^{\mathrm{short}}$, which is represented by branch (IV) (Figure 4.1). This case covers the penalty for being unable to deploy in the RT. Similar rationale applies for regulation down service as shown below:

$$c^{\mathrm{regdn}} = \phi^{\mathrm{a}} \cdot \phi^{\mathrm{d}} \cdot (1 - \phi^{\mathrm{d}}) \sum_{(t \in T)} \sum_{(b \in B)} \left(v_{t,b}^{\mathrm{dn}} \cdot \lambda_{t,b}^{\mathrm{RT}} \right) \left(p_t^{\mathrm{dn}} - \phi^{\mathrm{a}} \cdot \phi^{\mathrm{d}} \cdot p_t^{\mathrm{dn}} \right) \tag{4.6}$$

Since the aggregator is not the owner of the EV batteries, it must compensate EV owners for degrading their batteries. In this work, it is assumed the degradation characteristic is sensitive to the number of cycles and insensitive to the depth-of-discharge, as explained in [10]. The degradation cost is:

$$c^{\mathrm{deg}} = \sum_{(v \in V)} C_v^{\mathrm{bat}} \left| \frac{m_v}{100} \right| \left[\frac{\Delta t \sum_{(t \in T)} \left(p_{t,v}^{\mathrm{emdsg}} + p_{t,v}^{\mathrm{emchg}} \right) - \xi_v}{BC_v} + \frac{\sum_{(t \in T)} \left(\pi^{\mathrm{a}} e_{t,v}^{\mathrm{regup}} + \phi^{\mathrm{a}} e_{t,v}^{\mathrm{regdn}} \right)}{BC_v} \right] \tag{4.7}$$

In (4.7), BC_{v} is the battery energy capacity, C_v^{bat} is the battery cost, ξ_v is the total energy for motion, and m_v is the linear approximated slope of the battery life as a function of the number of cycles [10]. The value of m_v is estimated from manufacturer datasheets [10]. In (4.7), the aggregator must compensate EVs for discharging in V2G mode for energy market arbitrage as determined by the term $p_{t,v}^{\mathrm{emdsg}}$. On the other hand, for energy obtained

for charging from the energy market, it only needs to compensate additional energy on top of the motion needs as determined by subtracting ξ_v. For the regulation services, only the components of the service that degrade the battery are included, *i.e.* $e_{t,v}^{\text{regup}}$ and $e_{t,v}^{\text{regdn}}$. This is the case because stop charge and stop discharge actions do not degrade the battery, instead they only interrupt the actions of the EVs in the period.

The objective function in (4.1) is subject to several constraints. The first set of constraints (4.8) and (4.9) calculate the capacity offer for regulation up and down, respectively. In these constraints, the sum of the energy for each service calculated from each EV must equal the total regulation offer. Furthermore, these constraints relate the offered capacity in the DA regulation market to the expected deployment in the RT. The capacity offer is multiplied by the probability π^{d} for regulation up in (4.8) and ϕ^{d} for regulation down in (4.9), to get RT deployment.

$$p_t^{\text{up}}\pi^{\text{d}}\Delta t = \sum_{(v\in V)} \left(e_{t,v}^{\text{regup}} + e_{t,v}^{\text{stopchg}}\right) \quad \forall t \in T \tag{4.8}$$

$$p_t^{\text{dn}}\phi^{\text{d}}\Delta t = \sum_{(v\in V)} \left(e_{t,v}^{\text{regdn}} + e_{t,v}^{\text{stopdsg}}\right) \quad \forall t \in T \tag{4.9}$$

Constraints (4.10) to (4.15) determine the energy state-of-charge (eSOC) $soc_{t,v}$ of each EV and the energy of each product offered in the market. In (4.10), the eSOC is dependent on the previous state, power obtained from the energy market $p_{t,v}^{\text{emchg}}$ and injected to the energy market $p_{t,v}^{\text{emdsg}}$, motion needs, and motion schedule $S_{t,v}$. Note that this same constraint allows arbitrage in the energy market. However, before arbitrage can be scheduled, the motion needs must be fulfilled which are obtained from the energy market, because unlike the regulation market, this market is open to all participants without any preset SO requirements. This is managed in constraint (4.11). If additional capacity is available in the batteries, they can be scheduled to provide regulation down/up service as shown in constraints (4.12)-(4.13). At all time periods, the eSoC must be within the defined minimum and maximum bounds as shown in constraint (4.14). Constraint (4.15) ensures the total energy at the end of the optimization horizon is the same as it was at the beginning of the day. This ensures the

aggregator returns the EV batteries to their initial state.

$$soc_{t,v} = soc_{t-1,v} + \eta_v^{\text{chg}} p_{t,v}^{\text{emchg}} \Delta t - p_{t,v}^{\text{emdsg}} \Delta t - \xi_v \frac{S_{t,v}}{\sum_{(t \in T)} S_{t,v}} \quad \forall t \in T, v \in V \tag{4.10}$$

$$soc_{t,v} \geq \xi_v \frac{S_{t,v}}{\sum_{(t \in T)} S_{t,v}} \quad \forall t \in T, v \in V \tag{4.11}$$

$$0 \leq e_{t,v}^{\text{regdn}} + e_{t,v}^{\text{stopdsg}} \leq SoC_v^{\text{max}} + soc_{t,v} \quad \forall t \in T, v \in V \tag{4.12}$$

$$0 \leq e_{t,v}^{\text{regup}} + e_{t,v}^{\text{stopchg}} \leq soc_{t,v} - SoC_v^{\text{min}} \quad \forall t \in T, v \in V \tag{4.13}$$

$$SoC_v^{\text{min}} \leq soc_{t,v} \leq SoC_v^{\text{max}} \quad \forall t \in T, v \in V \tag{4.14}$$

$$soc_{t=|T|,v} = SoC_v^{\text{init}} \quad \forall v \in V \tag{4.15}$$

Constraints (4.16) to (4.20) determine how much energy and at which periods regulation and energy market services can be provided. In (4.16) and (4.17), an individual EV can perform charging or discharging if it is available, such that $\alpha_{t,v} = 1$. An EV at a specific period t can either charge for the energy or the regulation down market as shown in constraint (4.16), or it can discharge for the energy or regulation up market as shown in constraint (4.17). This is managed in such constraints by the auxiliary binary variable $z_{t,v}$ and the maximum power P_v^{max} that an EV can provide. If an EV is scheduled to discharge in the energy market, the aggregator may decide to interrupt this discharging by scheduling regulation as shown in constraint (4.18). The same rationale applies for constraint (4.19) to interrupt energy market charging. Since the aggregator must meet each EV's motion requirements, it can only interrupt charging that is in addition to energy obtained for motion as shown in constraint (4.20).

$$0 \leq p_{t,v}^{\text{emchg}} \Delta t + e_{t,v}^{\text{regdn}} \leq \alpha_{t,v} \left(P_v^{\text{max}} \Delta t \right) \left(1 - z_{t,v} \right) \quad \forall t \in T, v \in V \tag{4.16}$$

$$0 \leq p_{t,v}^{\text{emdsg}} \Delta t + e_{t,v}^{\text{regup}} \leq \alpha_{t,v} \left(P_v^{\text{max}} \Delta t \right) z_{t,v} \quad \forall t \in T, v \in V \tag{4.17}$$

$$0 \leq e_{t,v}^{\text{stopdsg}} \leq p_{t,v}^{\text{emdsg}} \Delta t \quad \forall t \in T, v \in V \tag{4.18}$$

$$0 \leq e_{t,v}^{\text{stopchg}} \leq p_{t,v}^{\text{emchg}} \Delta t \quad \forall t \in T, v \in V \tag{4.19}$$

$$\sum_{(t \in T)} e_{t,v}^{\text{stopchg}} \leq \Delta t \sum_{(t \in T)} \left(p_{t,v}^{\text{emchg}} \right) - \xi_v \quad \forall v \in V \tag{4.20}$$

The last set of constraints for the aggregator are related to the regulation and energy market PQP curves as shown in Figure 4.3. In constraint (4.21), binary variable $w_{t,b}^{\text{up}}$ will be active at one specific segment b when parameter PQP_b^{up} equals π^{a}. This rationale applies to constraints (4.21) to (4.24). By deciding which segment of the CDF curves is active, a corresponding market price can be used in equation (4.1).

$$\sum_{(b \in B)} w_{t,b}^{\text{up}} \cdot PQP_b^{\text{up}} = \pi^{\text{a}} \quad \forall t \in T \tag{4.21}$$

$$\sum_{(b \in B)} v_{t,b}^{\text{up}} \cdot PQP_b^{\text{RT}} = \pi^{\text{d}} \quad \forall t \in T \tag{4.22}$$

$$\sum_{(b \in B)} w_{t,b}^{\text{dn}} \cdot PQP_b^{\text{dn}} = \phi^{\text{a}} \quad \forall t \in T \tag{4.23}$$

$$\sum_{(b \in B)} v_{t,b}^{\text{dn}} \cdot PQP_b^{\text{RT}} = \phi^{\text{d}} \quad \forall t \in T \tag{4.24}$$

Note that constraints (4.3)-(4.6) include multiplication of binary and continuous variables, which are linearized as discussed in [123]. The linearization is further explained in Appendix B.1. A discussion on the software and techniques used to solve this model is presented in Appendix A.

4.4   Simulation Results

The proposed approach is applied to a fleet of 1000 EVs managed by an aggregator. The driving patterns are obtained from the 2009 NHTS [124]. The capacity of the EV batteries is 24 kWh [9], however the eSoC can only range between a minimum of 15% and a maximum of 95% of the capacity due to electrochemical constraints on the battery [127]. Both the charging and discharging power rate was 3.3 kW, the initial eSoC was randomized, and the round trip charging/discharging efficiency was set to 90% [85]. The degradation cost was accounted for using equation (4.7) with the cost per EV battery set to [550 450 350 250] \$/kWh and with corresponding slopes $m_v = -[0.015\ 0.012\ 0.008\ 0.0013]$ [9]. The lower

slope is the approximation of 2012 technology and the higher slope represents technological improvement in the battery cycle-life to three times the current value [9, 34].

Historical data was obtained from the ERCOT market for capacity and energy prices along with their corresponding market clearing power quantities from [152]. The data was used to create the price-quantity-probability curves as shown in Figure 4.3 for regulation up and down, and the RT markets. Each curve has 10 steps with descending probability from 100% to 0% with uniform increments and the curves were created for each hour of the operating day, *i.e.* 24 hours. For simplicity, it is assumed the probabilities of acceptance for regulation up/down follow $\pi^{\mathrm{a}} = \phi^{\mathrm{a}}$ and for deployment $\pi^{\mathrm{d}} = \phi^{\mathrm{d}}$. The day-ahead energy market prices were obtained to create a typical representative curve using k-means clustering [139]. In order to model the SO, UC was performed on a modified IEEE RTS-96 with 96 generators, an aggregator, and wind resources [149]. For simplicity, the regulation up/down offers of the generators are 10% of their energy offers. The softwares and techniques used to solve the model are discussed in Appendix A.

4.4.1 *Estimation of the probability of acceptance/deployment*

The aggregator estimates the probability of acceptance and deployment to maximize its revenue for offer acceptance in the DA and capacity deployment in the RT, while compensating EV owners for degradation. In order to determine the best estimation of such probabilities, Monte Carlo (MC) simulations are performed. The process is as follows. First, the aggregator performs its optimization and the offers/bids for the DA energy and regulation market are submitted to the SO. Next, the operator performs UC in the DA to determine the energy price and which offers are accepted for the provision of down and up regulation, resulting in capacity prices. After that, the aggregator is notified whether its offers were accepted, however, it remains unaware if it will be requested to deploy its capacity in the RT. Finally, to validate if the aggregator is able to deploy in the RT with maximum profits, MC simulations are performed. Each trial of the MC consists of a randomly generated wind and demand realization using the sampling process discussed in [153]. The number of MC trials
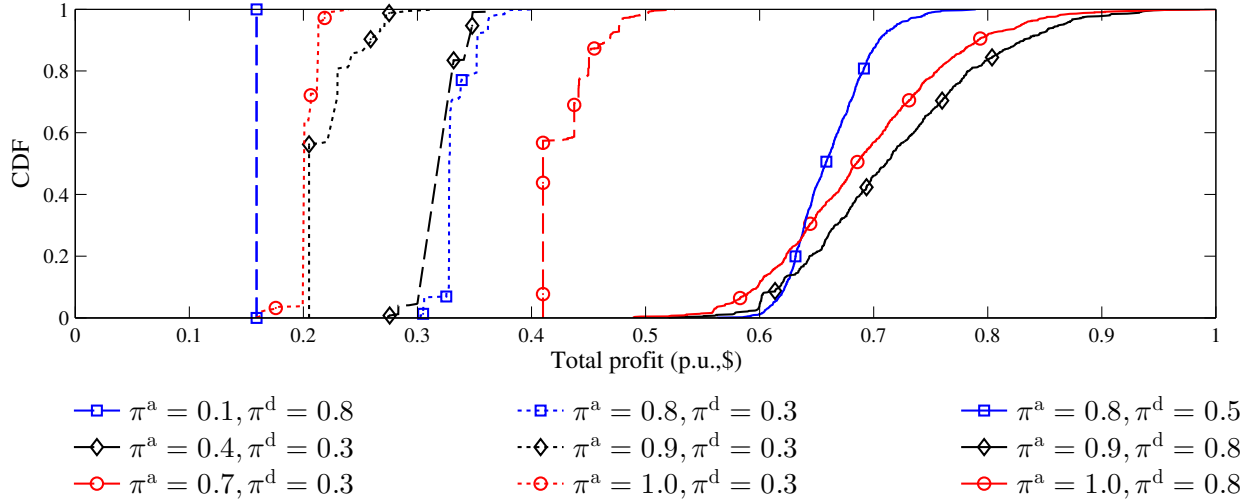
Figure 4.4: CDF of the total profit obtained by the aggregator with varying probabilities. The battery cost is 250 \$/kWh for all trials.

is set to max $(1000, N^{\mathrm{MC}})$, where N^{MC} is the number of MC trials required to ensure a 95% confidence interval of an error less than 1% [154]. The total profits of the aggregator from all trials are used to create a CDF curve for each combination of probability of deployment and acceptance. The results are shown in Figure 4.4. Note that all potential combinations of the probabilities in the range of [0,1] with step-size of 0.1 were solved but only a subset is shown for clarity.

Figure 4.4 shows the CDF where the right-most curves indicate larger profits obtained by the aggregator. When π^{a} is low and π^{d} is relatively high, *e.g.* $\pi^{\mathrm{a}} = 0.1$ and $\pi^{\mathrm{d}} = 0.8$, the majority of the profits are obtained from energy arbitrage, thus all trials result in the same profits (*i.e.* straight line). This occurs because the probability of acceptance π^{a} is too low to yield any accepted offers in the regulation market and results in no deployments. On the other hand, if $\pi^{\mathrm{d}} = 0.3$ and π^{a} is varied (dotted cases in Figure 4.4), the total profits decrease because these combinations result in higher penalty costs, calculated in (4.5)-(4.6), if the aggregator is unable to deploy its capacity offers. As a result, less overall capacity is offered to the regulation market to minimize such costs.

Further shown in Figure 4.4, if π^{d} is increased from 0.5 to 0.8, *e.g.* solid line cases, the total profits are substantially increased, because the aggregator will now be deployed in the RT with a higher probability and so it increases its DA capacity offers. However, less energy is scheduled to be supplied into the energy market so that it may be instead offered to the regulation market. Such a tradeoff materializes because the potential revenue obtained in the regulation market is greater than the energy market.

Moreover in Figure 4.4, the profits decrease when $\pi^{\mathrm{a}} > 0.9$ and $\pi^{\mathrm{d}} > 0.8$, because at this point the aggregator is over-offering into the regulation market and thus when asked to deploy in the RT, it fails to fulfill the requirements due to a lack of energy capacity. This results in additional costs since it must compensate the imbalance through the RT market. The combination of $\pi^{\mathrm{a}} = 0.9$ and $\pi^{\mathrm{d}} = 0.8$ yields the largest profits for the aggregator and is used in subsequent analysis.

4.4.2   Cost/Benefit analysis with varying battery price

Using the best combination of probabilities ($\pi^{\mathrm{a}} = 0.9$ and $\pi^{\mathrm{d}} = 0.8$), the itemized costs and revenues are analyzed with varying battery costs. The aggregator must compensate EVs for the charging and discharging of their batteries for its own monetary benefit. The aggregator, however, must determine how to cycle its fleet of EVs to decide the quantity to provide in energy, and up/down regulation markets to maximize profit.

By varying the battery costs from 550 to 250 \$/kWh, accounting for the expected advancement of battery technologies [34], the itemized expected revenue and costs are shown in Figure 4.5a and Figure 4.5b, respectively, and the expected total profits in Figure 4.5c. At higher battery costs (*e.g.* 550 and 450 \$/kWh), the energy market provides the largest revenue opportunities (Figure 4.5a). On the other hand, the participation of the aggregator in the regulation market is kept to a minimum due to the effect of the degradation costs and the potential inability to deploy in the RT. As the battery cost decreases to 350 \$/kWh, the participation in the regulation market leads to larger revenues (Figure 4.5a), but at the same time the aggregator is unable to deploy some of that capacity in the RT resulting in
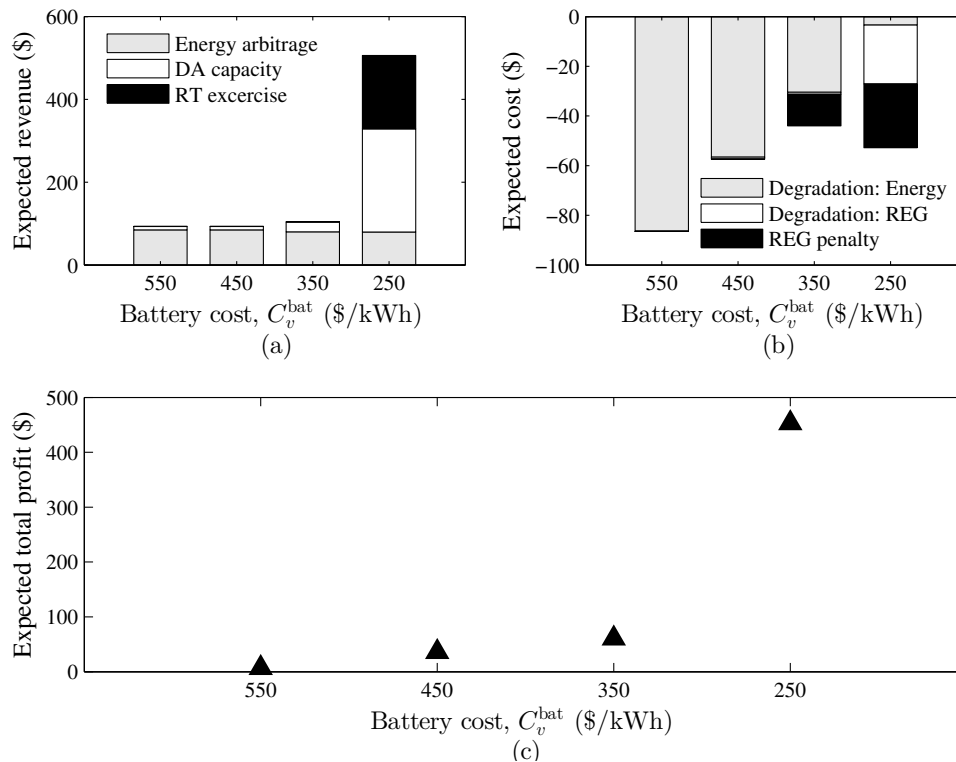
Figure 4.5: Itemized breakdown of the expected revenue in (a) and costs in (b) with varying battery cost. The expected total profits are shown in (c).

penalty costs, as shown in Figure 4.5b.

If the battery cost decreases to 250 $/kWh, the aggregator now decreases its participation in the energy market to increase participation in the regulation market. This shift is explained by lower degradation cost which results in increased revenues from both DA capacity and RT exercise payments as shown in Figure 4.5a. Also shown in Figure 4.5a is the RT exercise revenue which is only obtained because the SO requested the aggregator to deploy a portion of its capacity in the RT.

The aggregator incurs costs which are in the form degradation, because of deployment in the RT, and penalties because of the inability to supply the requirements by the SO. The latter occurs because the aggregator estimates its expected capacity offer and deployment using the probabilities π^a and π^d. For example, in a certain period, the aggregator may offer

into the market a quantity of 2 MW, however, due to its expectation of this full quantity to be accepted in the competitive market, it schedules the EV fleet's charging/discharging for a quantity less than 2 MW depending on the values of π^a and π^d. Therefore, the difference between the offered quantity, which the SO can either accept fully or a portion thereof, and the actual scheduled quantity demonstrates the aggressiveness of the aggregator's market participation. The aggregator runs the risk of over-offering into the market, which it may be unable to deploy and thus must purchase the imbalance in the RT.

Figure 4.5c shows the total expected profits which indicates that for higher costs, the profits are much lower than with lower cost batteries. Overall, when the cost is more than 350 $/kWh, energy market arbitrage is advantageous and as technology improves resulting in lower costs, *e.g.* 250 $/kWh, providing regulation services becomes more profitable. However, note that the aggregator is profitable at all levels of battery costs, which shows potential as a commercial business participating in both markets simultaneously.

4.4.3 Offering strategy of the aggregator in the DA

Using the best combination of probabilities ($\pi^a = 0.9$ and $\pi^d = 0.8$), Figure 4.6 shows the aggregator's DA offering strategy to obtain the revenue/costs, shown in Figure 4.5, when the battery cost is 250 $/kWh. Figure 4.6a shows the DA and RT energy price. The RT price is obtained from the PQP curves from the process in Figure 4.3. Figure 4.6b shows the down/up capacity prices and Figure 4.6c shows the itemized quantities of all services and the total system eSoC. From Figure 4.6b, the down reserve prices are higher during the early hours of the day as compared to the latter hours. This is beneficial to the aggregator because EVs are more likely to be plugged-in during the nighttime hours and thus can provide such services. On the other hand, up reserve prices have two distinct peaks at 0800 and 1900 hours and the aggregator can provide such services around these peaks.

Figure 4.6c shows the itemized breakdown of all potential services the aggregator can provide to the DA energy and reserve markets. The aggregator charges its fleet from the energy market (EMCHG) to meet transportation needs of EV owners. Although the down
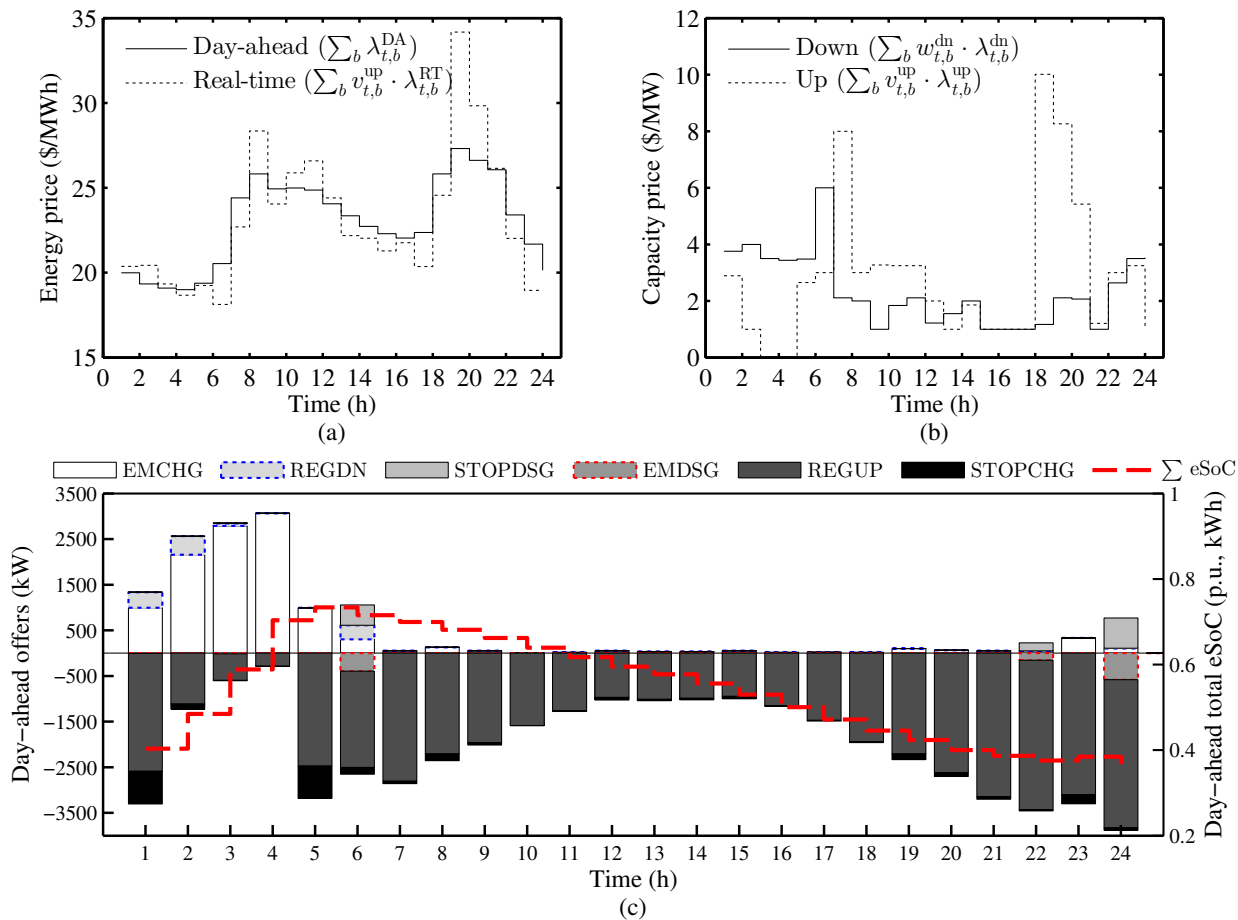
Figure 4.6: (a) DA and RT energy price, (b) REGDN and REGUP capacity prices, and (c) itemized breakdown of capacity, energy, and eSoC in the DA.

reserve prices are cheaper than the DA energy prices, the aggregator schedules a majority of the regulation down (REGDN) between hours 0100 to 0800 so it may use that to provide arbitrage services later during the course of the day. Therefore, procuring transportation needs from the energy market (EMCHG) decreases the risks because if the SO does not accept the down regulation offers, it is still able to meet the EV needs. In addition, down regulation services are not entitled to the exercise revenue because otherwise the aggregator would receive double benefit of energy that can be used for transportation and at the same time being paid for it. As a tradeoff, by scheduling down regulation, the aggregator is decreasing
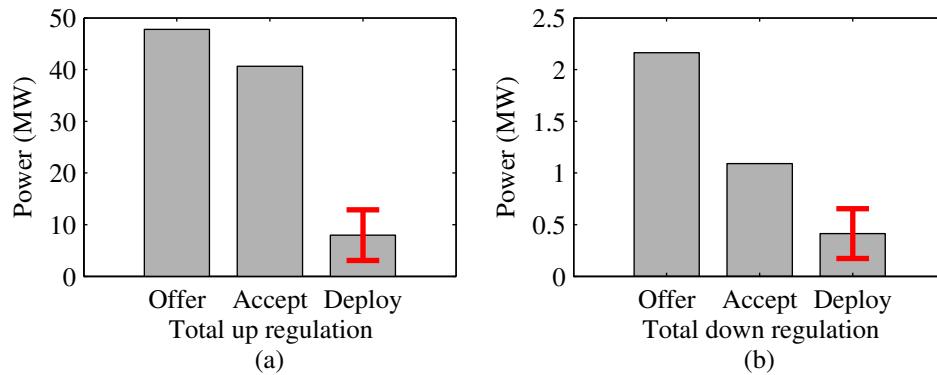
Figure 4.7: Offered, accepted, and actually deployed quantity for (a) up reserves and (b) down reserves.

the potential charging from the energy market (EMCHG), which could be scheduled to discharge back into the grid when profitable. On the other hand, with regulation up, the aggregator may potentially obtain two sources of revenue, DA capacity and RT exercise. Therefore, regulation up provision is scheduled in every period of the operating day and the aggregator is essentially performing arbitrage between two markets. It charges its EV fleet with energy (EMCHG) and a large portion of it is supplied as regulation up (REGUP and STOPCHG) and a smaller portion discharged back into the energy market (EMDSG). As a benefit, if the up regulation offers are accepted but only a portion is requested to be deployed, the aggregator essentially acquires two benefits:

1. the energy stored in the fleet of EVs can be used in future exploitations, and
2. no discharging compensation is required since no deployment materialized.

Degradation has a major effect on the benefits that the aggregator may attain from providing energy arbitrage and regulation. However, for regulation, the aggregator can essentially schedule for up/down regulation in the DA to obtain the capacity revenue for being on-standby and have a chance that it will not be deployed in the RT. This is the best case for the aggregator, since it is virtually using its EVs without causing any degradation, hence no compensation to the EV owners. This effect can be seen in Figure 6c with the large

amount of up regulation offers, because the aggregator is aware only a portion of these will be accepted and even smaller portion will be actually deployed in the RT.

The total offered, accepted, and deployed quantities for up and down reserves are shown Figure 4.7a and Figure 4.7b, respectively. The deployed values are based on the results of the MC simulations performed in Figure 4.4. For deployment, the solid bar represents the average quantity for all trials and the confidence interval (red) for one standard deviation, thus showing the variability. In Figure 4.7a, 47.8 MW over the course of the day was offered as up regulation, of which 40.7 MW (85.1%) was accepted by the SO, and of that 8 MW (27.2%) on average was deployed with a standard deviation of 4.9 MW (16.7%). On the other hand, down regulation yielded a total offering quantity of 2.2 MW, of which 1.1 MW (51%) was accepted, and 0.4 MW (37.9%) with a deviation of 0.24 MW (22.1%) was deployed in the RT. The aggregator favors up regulation because it allows both the capacity and exercise revenues to be obtained. Major reasons for lower quantities of down regulation is caused by the aggregator's commitment to procuring energy for transportation, which limits the EV fleets capacity for additional charging for down regulation, and also because only the capacity revenue can be obtained. On the other hand, STOPDSG portion of down regulation can only be activated if energy market discharging (EMDSG) occurs. However, because REGUP services are profitable, this limits EMDSG from occurring often and so STOPDSG is limited.

For purposes of simplicity, it was assumed the probabilities of acceptance and deployment were equal, *i.e.* $\pi^{\mathrm{a}} = \phi^{\mathrm{a}}$ and $\pi^{\mathrm{d}} = \phi^{\mathrm{d}}$. Different values, however, can be chosen for the down regulation which better resemble the outcome of Figure 4.7b. At the same time, this also shows the SO requires less down regulation.

4.4.4   System operator's perspective

Table 4.1 uses the MC trials to show the SO's expected operating cost, standard deviation of cost, and the startup cost of committing additional units in the RT, which is compared to the cost of DA commitments. The base case in Table 4.1 presents the costs in the power system without the aggregator. Next, the case when the aggregator participates in energy markets

		Base	Energy Market	Regulation and Energy Market
RT	Total costs (10^6 \$)	2.436	2.435	2.433
	Standard deviation of costs (\$)	32,755	32,690	32,282
	Start-up costs (\$)	4,521	4,490	3,940
DA	Start-up costs (\$)	163,780	162,800	152,020

Table 4.1: System Operator's Costs

only and finally, the case when aggregator partakes in both markets. From Table 4.1, the SO's expected costs in the RT are reduced when the aggregator provides services to the grid. Also, the startup costs in the DA and RT decrease. Even though the total quantitative cost savings seem low, *e.g.* 0.08% when the aggregator participates in energy market and 0.12% when performing in both markets the qualitative benefits are of importance [155], and these would be mirrored as large amounts of money over an operating year.

The decrease in the start-up costs shows that less cycling of conventional generation occurs in both the DA and RT [156]. Especially in the RT, the lower start-up costs indicate the SO requires less fast-starting units to be on stand-by in the case of deviations. This follows because the aggregator obtains energy when there is an abundance and less need for deployment, and then supplies it when there is a need, thus making it a viable alternative to conventional generation for reserve provision. As compared to the conventional generation, the aggregator has essentially no startup costs and also has lower operating costs, which only include the compensation of the battery degradation to the EVs owners.

4.5 Conclusion

EV aggregators are the required mediators between large fleets of EVs and the SO. This chapter proposed a framework to determine the optimal bidding/offering strategy in the energy and regulation reserve markets, which maximizes the aggregator's profits while observing the

incurred loss of utility for the EV batteries. In addition, the aggregator takes into account its expected probability of acceptances and deployments for up and down regulation. EVs can provide a new stream of services to the power system, however in order to incentivize the EVs' participation in energy and reserve markets, a fair compensation mechanism must in place such as discussed in Chapter 2.

Results show the aggregator benefits from the reserve market more than the energy market for two main reasons: 1) it collects capacity revenue for providing regulation, which does not incur degradation, and 2) it gains additional revenue if required to deploy in the real-time. When the battery costs are high, most of the revenue is obtained from the energy market, however, with low battery costs most of the revenues come from regulation reserve provision. This is because as the battery costs decrease, the provision of regulating reserve would result into two streams of revenue: capacity and deployment. The provision of these services from EVs is also beneficial to the SO, since it would reduce the total operating costs of the system.

By combining the works in Chapter 2, 3, and 4, a complete business and operating framework can be incorporated by an aggregator. This complete framework considers the methodology to control consumer loads, *e.g.* EWHs, HVAC, EVs, among others, manage the grid limits, *e.g.* lines, transformer aging, and the bidding/offering strategy in the wholesale markets to generate revenue. Such frameworks open business opportunities for new players to enter the market.

Chapter 5

OPTIMAL MARKET PARTICIPATION OF AGGREGATED ELECTRIC VEHICLE CHARGING STATIONS CONSIDERING UNCERTAINTY

5.1 Introduction

In Chapters 2-4, the focus was on an aggregator managing residential customers equipped with EVs and other loads in order to provide benefits, *i.e.* additional revenue, lower operating costs, among others. However, an aggregator is capable of not only managing ensembles of loads but also a fleet of electric vehicle charging stations (EVCS), which is the focus of this chapter.

As the EV penetration grows high-capacity charging infrastructure is required to provide energy needs for transportation. The infrastructures energy needs will be procured through a power utility, which may not have the capacity to provide such volatile and high-power needs on-demand and at the same time at the minimal cost. As a solution, the stations can resort to the day-ahead (DA) electricity markets, where they may obtain their energy needs at lower costs and ensure quality-of-service for their EV customers.

To participate in DA markets, market operators set forth minimum capacity requirements, *e.g.* 0.5 MW in CAISO [157] and 0.1 MW in ERCOT [158]. However, a single station will not be able to meet these minimum capacity requirements. On top of this, it would be extremely difficult to predict its daily load curve. Thus, a centralized aggregator can aggregate the power requirements of an ensemble of EVCS in order to effectively participate in the DA market and reduce the electricity procurement costs. To further reduce the costs, the aggregator can perform energy arbitrage with an energy storage system (ESS) it manages in conjunction with the charging station ensemble.

The work in this chapter proposes a framework for an aggregator to manage an ensemble of EVCSs to bid/offer into the wholesale electricity market with the primary goal of minimizing operating costs. The aggregator, to further reduce its costs, is equipped with an ESS that acts as a buffer which can provide flexibility to the market bids/offers, while considering the effect of battery degradation due to cycling. The aggregator DA optimization model incorporates uncertainty management of market prices, using robust optimization (RO), and of EVCS power demand, using stochastic optimization. For cost-effective operation, the aggregator must effectively manage uncertainty while considering the trade-off between potential cost reduction compared to degradation of its ESS. The main contributions of this work are:

- Aggregator DA optimization model managing aggregated power needs of EVCSs while considering demand and market price uncertainty.

- Complete ESS model that supplies energy to the grid or to the EVCSs, if economically profitable, while considering degradation costs.

- Realistic framework of an aggregator exploiting its ESS, power system market, and EVCSs.

5.2 Framework

Aggregator is a profit-seeking business entity who acts as a mediator between the EVCSs and the wholesale electricity markets and contains an ESS. Fig. 5.1 shows its interactions with the different entities: ensemble of EVCSs, power system, and electricity markets. The aggregator coordinates with each EVCS under its jurisdiction to obtain their charging demand requirements for the next day. The demand of each EVCS is then used to obtain the aggregated demand. The aggregator performs a DA optimization to schedule its operation at the least-cost, while exploiting its ESS asset. The ESS charges from the grid in grid-to-battery (G2B) mode when the price of electricity is low. During the periods of high electricity prices it can either supply the stations in battery-to-station (B2S) mode or inject energy back into
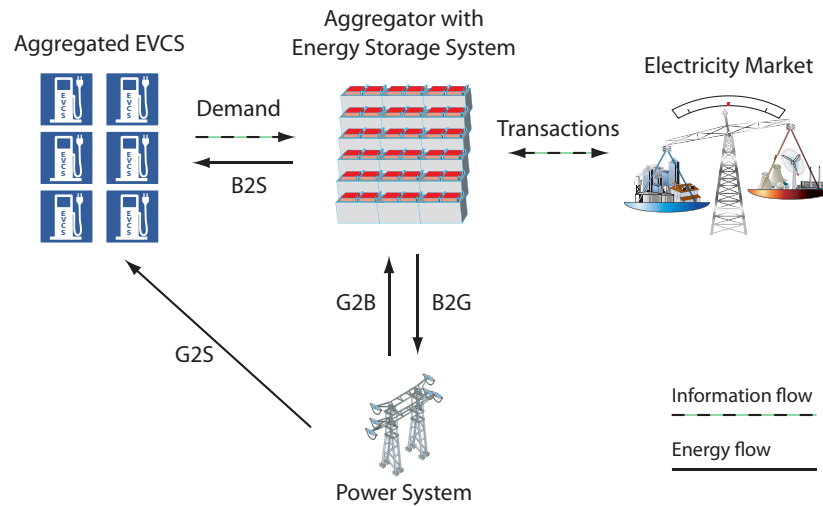
Figure 5.1: Aggregator's interaction with the EVCSs, electricity market, and power system.

the grid in battery-to-grid (B2G) mode. If the aggregator is unable to supply all of the energy needs from the ESS in B2S mode, it resorts to obtain the power directly from the grid in grid-to-station (G2S) mode. The aggregator's optimization determines the market bids (G2B and G2S services) and offers (B2G services) as a price-taker in the DA wholesale markets.

5.2.1 EVCS perspective

Without the intervention of an aggregator, each individual EVCS resorts to purchasing electricity directly from their local power utility company. From a business perspective, the average cost of retail energy is higher than in the wholesale electricity markets [159]. Each individual EVCS, however, may not meet the minimum energy requirements to participate in a wholesale market, and at the same time, their primary objective is to provide charging services to their EV customers. On the other hand, the purpose of the aggregator is to optimize its market performance and provide service to the individual EVCSs. Therefore, the aggregator should be reimbursed for its services by the EVCSs. However, this methodology is not in the scope of this work.

Within this framework, the EVCS are assumed to have in place an internal day-to-day operation for managing each individual EV customer. An interested reader is advised to refer to [97, 98, 99] for such methodologies. In this framework, each EVCS must provide its load curve for the following day. Note that internally, each EVCS may accommodate any pricing structure to expense individual EV charging and the resulting forecasted demand would be a by-product of that. Such communication hides proprietary information, for example, the number of EVs arriving at the stations, power requirements of EVs, type of charging protocols used, among others. The major benefit is that an EVCS is not required to change their internal business/operating procedures to conform to the aggregator's framework.

5.2.2   ESS

The ESS, which is owned by the aggregator, is beneficial when scheduling energy in the DA. Without the ESS, the aggregator has no other option but to blindly follow the aggregated demand curve. With the ESS at the disposal, however, it can charge and store energy which is either used to supply EVCSs in B2S mode or return to the grid in B2G mode, if economical. These operations by the ESS, however, cause battery degradation [10] and for them to be viable, the potential cost savings incurred must be higher than the cost of degradation.

The following section discusses the mathematical formulation of the optimization model considering the interactions of the aggregator shown in Fig. 5.1.

5.3   Optimization Model

5.3.1   Day-ahead model

In the DA model, an optimal charging/discharging schedule is determined for the EVCS to maximize its profit. The EVCS determines the amount of energy to sell p_t^{sell} and buy p_t^{buy} from the grid to meet the aggregated EVCS demand D_t. The objective function is formulated

as follows:

$$\min \quad \Delta t \sum_{t \in \mathcal{T}} \lambda_t \cdot (p_t^{\text{buy}} - p_t^{\text{sell}}) \tag{5.1}$$

where $p_t^{\text{buy}} = p_t^{\text{G2B}} + p_t^{\text{G2S}}$ and $p_t^{\text{sell}} = p_t^{\text{B2G}} \cdot \eta$ within the set of time periods T with index t. The aggregator sells energy (p_t^{sell}) by scheduling its ESS to perform in B2G mode, *i.e.* p_t^{B2G}, while considering battery discharge efficiency η. On the other hand, the aggregator purchases energy from the market (p_t^{buy}) to both charge the ESS (p_t^{G2B}) and directly supply the power consumption requirements of EVCSs (p_t^{G2S}). The buying and selling of energy is priced at the DA market prices λ_t with a timestep of Δt.

The objective function (5.1) is subject to several constraints. The first set of constraints (5.2) and (5.3) determine the energy state-of-charge (SoC) of the ESS. In (5.2), the SoC is dependent on its previous state, the charging power p_t^{G2B}, the discharging power p_t^{B2G}, and the amount of power discharged from the battery to supply the stations p_t^{B2S}. Constraint (5.3) ensures the SoC does not violate its preset minimum and maximum limits, and at the same time is below its rated capacity BC^{ES}.

$$soc_t = soc_{t-1} + \Delta t \left(p_t^{\text{G2B}} \cdot \eta - p_t^{B2G} - p_t^{\text{B2S}} \right) \quad \forall t \in \mathcal{T} \tag{5.2}$$

$$0 \leq \underline{SoC} \leq soc_t \leq \overline{SoC} \leq BC^{\text{ES}} \quad \forall t \in T \tag{5.3}$$

The aggregator obtains forecasts of the power consumption from each EVCS d_t which is then summed to obtain D_t, *i.e.* $D_t = \sum d_t$. This then must be met from a combination of the ESS discharging in B2S mode, p_t^{B2S}, or directly from the grid in G2S mode, p_t^{G2S}. This is managed by constraint (5.4).

$$p_t^{\text{B2S}} \cdot \eta + p_t^{\text{G2S}} = D_t \quad \forall t \in \mathcal{T} \tag{5.4}$$

The set of constraints (5.5)-(5.7) ensures the different services provided by the ESS are within their minimum and maximum power limits, $P^{\max}$. At the same time, these constraints also disallow B2S to occur simultaneously with B2G and G2B, where $x_t \in \{0, 1\}$ is an auxiliary binary variable. For example, if $x_t = 1$ then B2S is allowed whereas B2G and G2B

are disallowed. This is implemented to ensure the ESS system performs only charging or discharging, and not both simultaneously, which is physically not viable.

$$0 \leq p_t^{\text{B2S}} \leq P^{\max} \cdot x_t \quad \forall t \in \mathcal{T} \tag{5.5}$$

$$0 \leq p_t^{B2G} \leq P^{\max} \cdot (1 - x_t) \quad \forall t \in \mathcal{T} \tag{5.6}$$

$$0 \leq p_t^{\text{G2B}} \leq P^{\max} \cdot (1 - x_t) \quad \forall t \in \mathcal{T} \tag{5.7}$$

The last constraint (5.8) ensures the total energy in the ESS at the beginning of the optimization horizon is replenished by the end, *i.e.* $t = |\mathcal{T}|$.

$$soc_{t=|\mathcal{T}|} = SoC^{\text{init}} \tag{5.8}$$

5.3.2 Demand uncertainty

The aggregator obtains demand requirements of each EVCS for the next operating day, which is then aggregated into D_t. However, each EVCSs demand is prone to uncertainty thus rendering D_t to be uncertain. This is the case because the demand is based on predictable, yet uncertain arrival, departure, and charging times of EVs at EVCSs. Thus, the aggregator must take into consideration the effect of such demand uncertainty on its decision-making process for wholesale market participation. To hedge against this uncertainty, the technique of stochastic optimization [160] is implemented. This technique takes advantage of the known probability distributions of the uncertain parameters (*i.e.* D_t). With this, instead of using a single aggregated demand scenario D_t in the optimization, now a set of scenarios $\mathcal{S}$ with index s is considered, *i.e.* $D_{s,t}$. In addition, each demand scenario $D_{s,t}$ has an expected probability π_s to materialize in the real-time (RT). With this approach, the aggregator obtains the DA bidding/offering schedule that is optimal with respect to all the demand scenarios instead of only of them particularly.

The mathematical formulation of the aggregator's DA stochastic optimization is as follows:

$$\min \quad \Delta t \sum_{t \in \mathcal{T}} \lambda_t \cdot (p_t^{\text{buy}} - p_t^{\text{sell}}) + \Delta t \sum_{s \in \mathcal{S}} \pi_s \sum_{t \in \mathcal{T}} \lambda_t^{\uparrow} \cdot p_{s,t}^-$$

$$- \Delta t \sum_{s \in \mathcal{S}} \pi_s \sum_{t \in \mathcal{T}} \lambda_t^{\downarrow} \cdot p_{s,t}^+ \tag{5.9}$$

subject to:

$$soc_{s,t} = soc_{t-1} + \Delta t \left(p_t^{\text{G2B}} \cdot \eta - p_t^{B2G} - p_{s,t}^{\text{B2S}} \right) \quad \forall s \in \mathcal{S}, t \in \mathcal{T} \tag{5.10}$$

$$0 \leq \underline{SoC} \leq soc_{s,t} \leq \overline{SoC} \leq BC^{\text{ES}} \quad \forall s \in \mathcal{S}, t \in \mathcal{T} \tag{5.11}$$

$$p_{s,t}^{\text{B2S}} + p_t^{\text{G2S}} + p_{s,t}^- - p_{s,t}^+ = D_{s,t} \quad \forall s \in \mathcal{S}, t \in \mathcal{T} \tag{5.12}$$

$$0 \leq p_{s,t}^- \leq p_{s,t}^{\text{B2S}} + p_t^{\text{G2S}} \quad \forall s \in \mathcal{S}, t \in \mathcal{T} \tag{5.13}$$

$$0 \leq p_{s,t}^+ \leq p_{s,t}^{\text{B2S}} + p_t^{\text{G2S}} \quad \forall s \in \mathcal{S}, t \in \mathcal{T} \tag{5.14}$$

$$0 \leq p_{s,t}^{\text{B2S}} \leq P^{\max} \cdot x_t \quad \forall s \in \mathcal{S}, t \in \mathcal{T} \tag{5.15}$$

$$soc_{s,t=|T|} = SoC^{\text{init}} \quad \forall s \in \mathcal{S} \tag{5.16}$$

$$\text{Constraints } (5.6), (5.7) \tag{5.17}$$

The objective function (5.9) has two additional terms as compared to (5.1). The expected cost of purchasing additional energy in the RT market in scenario s is determined based on the power shortage $p_{s,t}^-$ and the buying price $\lambda_t^{\uparrow}$. Similarly, the expected revenue from selling surplus energy in the RT market in scenario s is determined based on the excess power $p_{s,t}^+$ and selling price $\lambda_t^{\downarrow}$. Both of these two terms contain probability π_s representing the chance of the demand scenario s to materialize in the RT.

The objective function is subject to the constraints similar to (5.2)-(5.8), however, with the addition of stochastic scenario index s. The decision variables that include index s are $soc_{s,t}$ and $p_{s,t}^{\text{B2S}}$, as they are wait-and-see decisions within the stochastic framework [160], and are determined after the demand materializes in the RT [160]. On the other hand, the variables representing G2B (p_t^{G2B}), B2G (p_t^{B2G}), and G2S (p_t^{G2S}) are here-and-now decisions, *i.e.* they have the same value regardless on the scenario. The bidding/offering decisions into

the markets, *i.e.* G2B, B2G, and G2S, are based on the weighed average values over all scenarios. Slack variables $p_{s,t}^-, p_{s,t}^+$ capture the shortage/excess at each scenario. The final energy balance is expected to be obtained from the RT market. On the other hand, B2S is the operation of the ESS to supply the EVCSs, which does not require interaction with markets and can be controlled by the aggregator as demand materializes in the RT.

5.3.3   Market price uncertainty

The aggregator, using its ESS, exploits electricity market prices λ_t by purchasing energy p_t^{buy} when prices are low and selling energy p_t^{sell} when prices are high. To participate in the DA market, however, the aggregator forecasts market prices which are uncertain. Such price uncertainties may cause the aggregator to incur monetary losses. For example, with forecasted prices λ_t, the aggregator's optimization will schedule and consequently bid into the DA market for large amounts of energy to be procured during the low-price periods. After the DA market clears, however, the realization of specific prices may be higher than forecasted, and thus may leave the aggregator with high monetary losses. To hedge against such uncertainty in the DA, the RO technique is implemented [161]. RO is an uncertainty modeling approach suitable for situations where the range of the uncertainty (*e.g.* range of electricity prices) is known and not necessarily the distribution.

Deviations of the market prices are modelled within the range $\left[\lambda_t^{\min}, \lambda_t^{\max}\right]$, where $\lambda_t^{\max} = \lambda_t^{\min} + \Delta\lambda_t$ and $\Delta\lambda_t$ is the highest expected price deviation in period t. To control the level of protection against uncertainty, parameter Γ is varied from $[0, J]$, where $[J = t|\Delta\lambda_t > 0]$. With $\Gamma = 0$, no price deviations are considered and the solution is equivalent to the deterministic case, *i.e.* no consideration of uncertainty. On the other hand, if $\Gamma = |J|$ the solution is the most conservative since price deviations at all time periods t are considered, *i.e.* prices at all time periods are equal to $\lambda_t^{\max}$. This solution is equivalent to the RO model proposed by [162]. However, the implemented RO procedure is based on [161] and it allows choosing any Γ from range $[0, J]$, thus fine-tuning the level of conservatism.

The RO-based DA model is formulated as follows:

$$\min \quad \Delta t \sum_{t \in \mathcal{T}} \lambda_t^{\min} \cdot (p_t^{\text{buy}} - p_t^{\text{sell}}) + \Gamma^{\text{RO}} \cdot z^{\text{RO}} + \sum_t y_t^{\text{RO}} \tag{5.18}$$

subject to:

$$\text{Constraints } (5.2) - (5.7) \tag{5.19}$$

$$z^{\text{RO}} + y_t^{\text{RO}} \geq \Delta t \cdot \Delta \lambda_t \cdot \left(p_t^{\text{G2B}} + p_t^{\text{G2S}} \right) \quad \forall t \in \mathcal{T} \tag{5.20}$$

$$y_t^{\text{RO}} \geq 0 \quad \forall t \in \mathcal{T} \tag{5.21}$$

$$z^{\text{RO}} \geq 0 \quad \forall t \in \mathcal{T} \tag{5.22}$$

In comparison to the deterministic DA objective function (5.1), the extended objective function (5.18) includes two additional terms containing variables z^{RO} and y_t^{RO} used to account for the known price bounds and parameter Γ. This objective is subject to the original constraints (5.2)-(5.7) along with constraints (5.20)-(5.22). Constraint (5.20) determines the worst set of time periods in which price deviations could materialize when interacting with the market in G2B and/or G2S. RO variables z^{RO} and y_t^{RO} are positive, which is imposed in constraints (5.21)-(5.22). The interested reader is encouraged to refer to [161] for details on how to obtain the robust counterpart.

5.3.4 Battery degradation management

As the battery cells within the ESS charge and discharge, they lose a fraction of their capacity, which is often referred to as battery degradation [10]. The aggregator incurs all costs related to the ESS and thus must consider costs of degradation in its DA optimization. Degradation management determines the optimal trade-off between revenue collected from services, *i.e.* B2G and B2S, and the cost of cycling the battery. Without degradation management, the ESS would be exploited to obtain the maximum revenue, however, it would experience excessive degradation that is not economically justified.

The formulation of the aggregator model that considers battery degradation is as follows:

$$\min \Delta t \sum_{t \in \mathcal{T}} \lambda_t \cdot (p_t^{\text{buy}} - p_t^{\text{sell}}) + \left| \frac{m}{100} \right| \frac{\sum_{t \in \mathcal{T}} soc_t^{\text{deg}}}{BC^{ES}} \cdot C^{ES} \cdot BC^{ES} \qquad (5.23)$$

subject to

$$\text{Constraint } (5.2) - (5.7) \qquad (5.24)$$

$$soc_t^{\text{deg}} \geq soc_{t-1} - soc_t \quad \forall t \in \mathcal{T} \qquad (5.25)$$

$$soc_t^{\text{deg}} \geq 0 \quad \forall t \in \mathcal{T} \qquad (5.26)$$

The second term in objective function (5.23) represents the degradation costs, where C^{ES} is the \$/kWh price of the ESS, which includes the balance-of-system costs, *e.g.* battery and labor [163]. In addition, soc_t^{deg} determines the amount of energy discharged from the battery in period t and m is a linear approximation of the battery life as a function of the number of cycles. Parameter m can be estimated based on datasheets of battery manufacturers [164]. The objective function is subject to constraints (5.2)-(5.7) and (5.25)-(5.26). In (5.25), the constraint models $\max\{0, soc_{t-1} - soc_t\}$, where the amount of energy discharged from periods $t-1$ to t is determined. It is assumed the same energy discharged was charged into the battery in previous time periods in order to complete one full cycle of degradation [10]. Constraint (5.26) imposes non-negativity on soc_t^{deg}.

5.3.5 Complete DA model

The complete aggregator's DA model that includes EVCSs demand uncertainty, market price uncertainty, and ESS degradation costs is formulated as follows:

$$
\begin{aligned}
\min \quad & \Delta t \sum_{t \in \mathcal{T}} \lambda_t \cdot (p_t^{\text{buy}} - p_t^{\text{sell}}) \\
& + \Delta t \sum_{s \in \mathcal{S}} \pi_s \sum_{t \in \mathcal{T}} \lambda_t^{\uparrow} \cdot p_{s,t}^- - \Delta t \sum_{s \in \mathcal{S}} \pi_s \sum_{t \in \mathcal{T}} \lambda_t^{\downarrow} \cdot p_{s,t}^+ \\
& + \Gamma^{\text{RO}} \cdot z^{\text{RO}} + \sum_t y_t^{\text{RO}} \\
& + \left| \frac{m}{100} \right| \frac{\sum_{t \in \mathcal{T}} soc_t^{\text{deg}}}{BC^{ES}} \cdot C^{ES} \cdot BC^{ES} \qquad (5.27)
\end{aligned}
$$
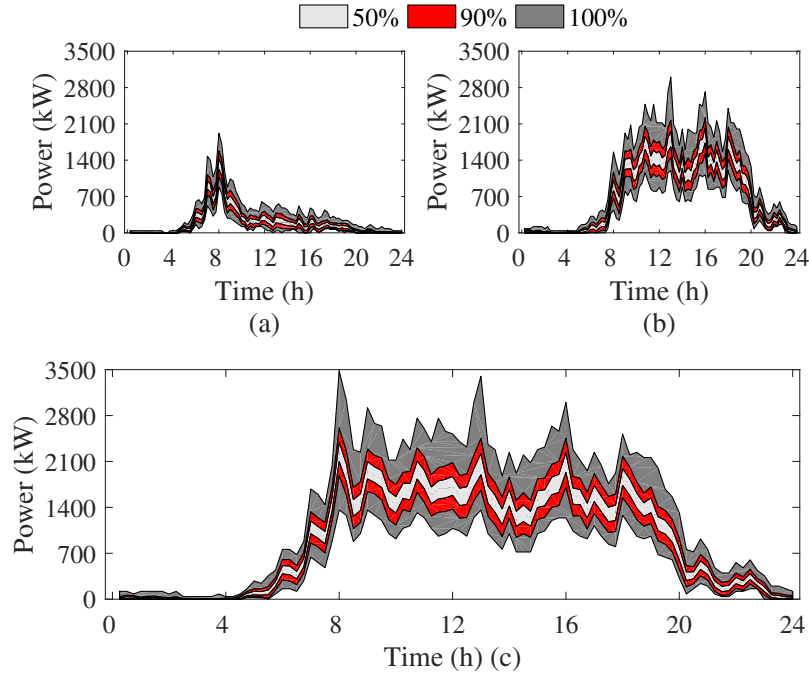
Figure 5.2: Day-ahead forecast of aggregated EVCS demand at the workplace location (a), commercial location (b), and the total sum of the two (c). The intervals 50%, 90%, and 100% are shown to represent the spread of the data. For example, 50% of the EVCS demand lies within the specified range.

The objective function (5.27) is subject to constraints (5.6), (5.7), (5.10)-(5.16), (5.20)-(5.22), and (5.25)-(5.26). Note in (5.25)-(5.26), the stochastic index s is included into the SoC, similar to (5.10)-(5.11).

5.4 Case Study

The proposed approach is applied to aggregated EVCS demand D_t obtained by implementing the methodology outlined in [42] using the vehicle data from the National Household Travel Survey (NHTS) [124]. A total of 5,000 EVs were tracked over 1000 days to obtain daily charging consumption profiles in the workplace and commercial (*e.g.* shopping and restaurants) locations equipped with EVCS. The EVCSs are assumed to be fast charging stations (FCS) using Level 3 charging protocol at 40 kW power rating [96]. Fig. 5.2 shows
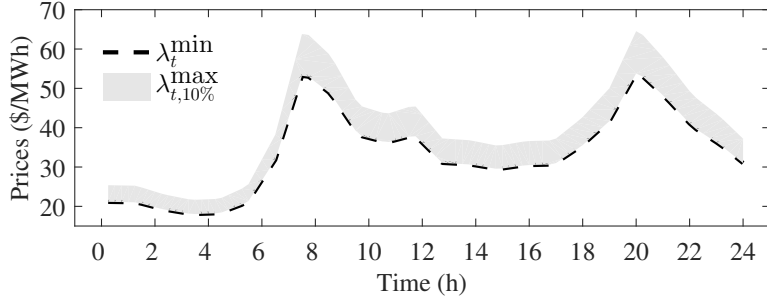
Figure 5.3: Day-ahead market price with deviation band for uncertainty

the aggregated EVCS charging profiles at workplace (a), commercial (b), and the total of the two locations (c). In Fig. 5.2(a)-(c), the light grey area represents the 50% band (*i.e.* 0.67 of the standard deviation from the mean consumption), the red is the 90% band (*i.e.* 1.645 of the standard deviation from the mean), and the dark grey is the 100% band, which represents the minimum/maximum of the data. One thousand EVCS charging demand profiles are reduced to a set of scenarios with their respective probabilities π_s using the K-medoids scenario reduction technique [165].

The capacity of the ESS is 1 MWh, however, the available SoC ranges from 15% to 95% of the rated capacity due to constraints on the batteries [127]. The charging and discharging power ratings are 500 kW, while the charging/discharging efficiencies are 95%. The initial ($t = 0$) SoC of the ESS is randomized. The ESS price is set to 300 $/kWh unless otherwise specified.

To represent a typical weekday DA market prices, the ERCOT historical data in the period January-March 2016 is used [166]. A typical price curve that best characterizes the data set is obtained using the K-medoids approach [165], and is shown in Fig. 5.3 as $\lambda_t^{\min}$. The upper bound prices $\lambda_t^{\max}$ used in RO are proportional to $\lambda_t^{\min}$. To discourage scheduling of bids/offer in the RT markets under the stochastic optimization framework, the buying $\lambda_t^{\uparrow}$ and selling $\lambda_t^{\downarrow}$ prices are assumed to be twice and half the DA typical prices $\lambda_t^{\min}$, respectively.
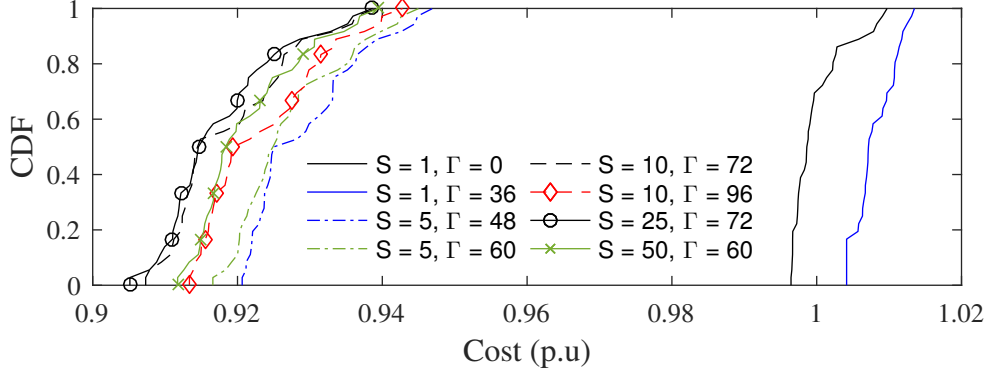
Figure 5.4: Normalized cost CDFs for combinations of stochastic scenarios and price robustness parameter.

5.4.1 Optimal combination of stochastic scenarios and RO parameters

To minimize its operating cost, the aggregator must determine its optimal bidding/offering strategy in the DA market. To do so, the uncertainty of energy prices and EVCS demand must be estimated using the RO parameter, Γ, and the number of scenarios $|S|$ in stochastic optimization, respectively.

To determine the best combination of parameters that yield the minimal operating cost, Monte Carlo (MC) simulations are performed [154]. The DA schedules are obtained for all discrete RO parameters in $\Gamma = [0, |T|]$, and stochastic scenarios, $|S| = [1, 5, 10, 25, 50, 100]$. For each combination of $|S|$ and Γ yielding a DA schedule, MC trials were performed to determine the actual cost of operation as the uncertainty materializes. The number of MC trials are set to $\min\{1000, N^{MC}\}$, where N^{MC} is the number of trials required to obtain a 95% confidence of an error less than 1% [154]. In the MC simulations, 32 price and 32 EVCS demand profiles are used totalling 1024 MC trials.

Fig. 5.4 shows the normalized CDF of the aggregator operating cost for different combinations of Γ and $|S|$. Cost of each MC trial is normalized against the mean cost of the deterministic MC trial, $i.e.$ $|S| = 1$ and $\Gamma = 0$. In other words, normalization occurs against cost realizations when uncertainty is not taken into consideration. While all combination of

$|S|$ and Γ are considered, Fig. 5.4 shows only select combinations for clarity.

From Fig. 5.4, the CDF curves to the left of the deterministic curve yield the lowest operating cost over all MC trials. In all combinations where $|S| > 1$ and $\Gamma > 0$, the aggregator sees cost savings. However, if only a single scenario, *i.e.* $|S| = 1$, is considered with $\Gamma > 0$, specifically the case shown in Fig. 5.4 where $|S| = 1, \Gamma = 36$, the costs are higher than in the deterministic case. This is caused by the RO, where it increases B2S and decreases B2G energy to protect against unforeseen price deviations that may materialize within the bounds shown in Fig. 5.3. Thus, it is more favorable to offset the demand needs of the EVCSs using the ESS to discharge in B2S, compared to selling energy back to the grid in B2G mode. Since B2S is highly-favored with respect to the set with a single scenario, *i.e.* $|S| = 1$, the operating cost is increased because once the demand materializes, the single demand scenario cannot capture the volatile demand variations thus requiring additional energy purchases.

On the other hand, the cases with $|S| > 1, \Gamma > 0$ outperform the deterministic case. This shows that both the demand and price uncertainty should be properly characterized in order to obtain the minimum operating cost. In addition, from Fig. 5.4, some combinations outperform others, *e.g.* $|S| = 10, \Gamma = 72$ and $|S| = 25, \Gamma = 72$. Thus, the price uncertainty parameter $\Gamma = 72$ yields the lowest cost. The major difference, however, between these two cases are the number of considered scenarios, *i.e.* 10 compared to 25 scenarios. In terms of computational complexity of stochastic optimization, larger number of scenarios requires additional computational time to obtain the optimal solution [160]. Thus, it is important to analyze the saturation point at which higher number of scenarios does not yield substantial cost savings. This is studied in Fig. 5.5, where the average normalized costs over all MC trials are shown against the number of stochastic scenarios $|S|$ for different values of Γ. In addition, the computation times for $\Gamma = 72$ over a select number of stochastic scenarios are shown in Table 5.1. As expected, the average cost experiences a significant decrease from a single scenario to five scenarios. If $\Gamma = 72$, there are clear cost savings between 10 and 25 scenarios (Fig. 5.4). However, the computational time increases from 34.3 to 806 seconds.
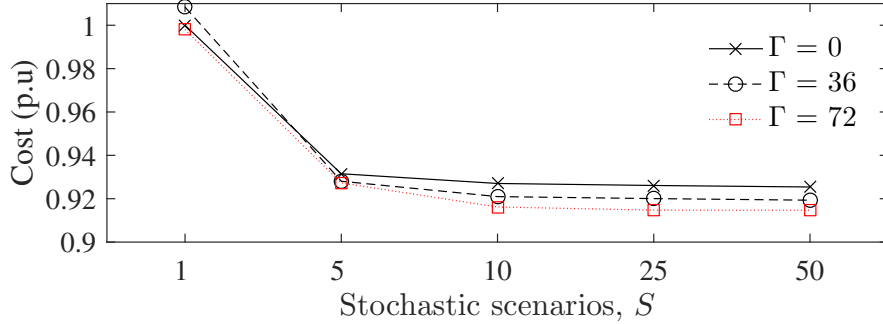
Figure 5.5: Normalized average cost as a function of the number of stochastic scenarios.

Table 5.1: Computational Times (seconds)

	Stochastic Scenarios, $|\mathcal{S}|$				
	1	5	10	25	50
$\Gamma = 72$	2.1	9.9	34.3	806	4486

This increase in computational time still keeps the problem tractable for market operations. On the other hand, moving from 25 to 50 scenarios, the cost savings is minimal but the computational time increases drastically to 4486 seconds.

The combination of the number of scenarios, $|S| = 25$, and the RO parameter, $\Gamma = 72$, yields a balance between the least operating cost over all MC trials and computational burden. This combination is used throughout the remainder of the test case.

5.4.2 Battery degradation effects

As the ESS is used, it experiences cycle-life degradation which can be translated into cost, as shown in equation (5.23). The ES price, normalized on a per-kWh basis, is varied from 800 \$/kWh to 300 \$/kWh to study the effect on the aggregator's G2B, B2S, and B2G actions. The degradation model, as shown in (5.23), is linear and represented by slopes $m = -[0.0017, 0.0006]$. The lower slope is the approximation of the current technology [164], and the higher slope indicates technological life cycle improvement.

The aggregator's daily total energy scheduled as a function of the ESS price is shown
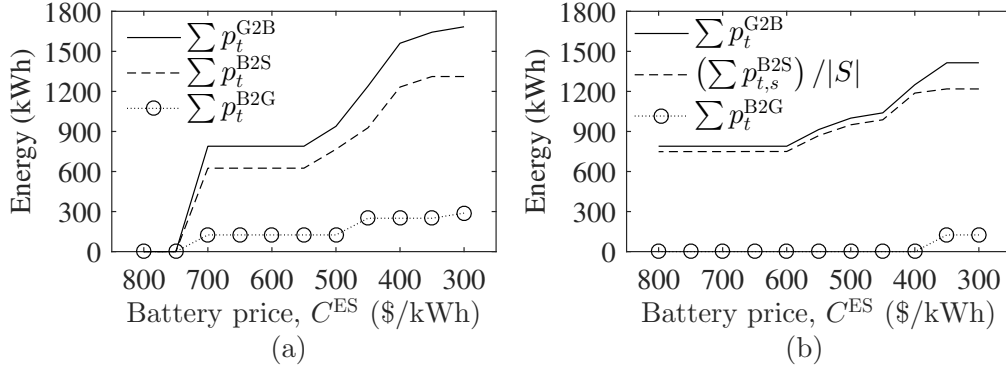
Figure 5.6: Total daily energy scheduled in the deterministic case (a) and with uncertainty management considered (b), as a function of varying ESS prices. Note in (b) the average B2S is shown since it is a function of scenario s.

in Fig. 5.6 for G2B, B2S, and B2G services. Fig. 5.6(a) shows the deterministic case, *i.e.* $|S| = 1, \Gamma = 0$, whereas Fig. 5.6(b) considers uncertainty with the best estimates. In both cases, as the ESS price decreases, the amount of energy scheduled for all operating modes monotonically increases because the potential revenue outweighs the degradation costs.

As for the specific modes, selling energy back to the grid in B2G mode is highly unfavorable when uncertainty is considered. For B2G to occur profitably, the aggregator must purchase energy in the low-price periods to charge the ESS (G2B) so it can sell back to the grid by discharging in the high-price periods. However, the uncertainty in market prices renders the potential arbitrage revenue to be lower than expected and thus as a result, less B2G is scheduled. However, if the price of the ESS is low enough, *i.e.* less than 400 \$/kWh, B2G is sporadically scheduled because the potential grid revenue obtained for such services outweighs the degradation costs, as shown in Fig. 5.6(b).

On the other hand, when considering uncertainty management in Fig. 5.6(b), the aggregator decreases B2G and increases B2S for all battery prices. This happens because by scheduling B2S, the aggregator offsets the need to purchase energy from the grid (G2S) exactly in periods when the EVCSs require it. Instead, the aggregator uses the energy purchased during low-price periods and stored in the ESS to discharge and supply the EVCS
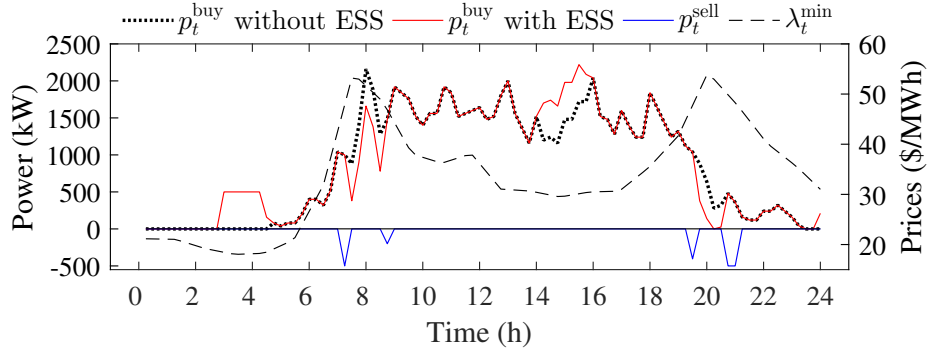
Figure 5.7: DA market buying and selling strategy in the deterministic case.

(B2S). The aggregator uses the ESS as a method to reduce monetary risks in the electricity markets.

5.4.3 Day-ahead schedules

The aggregator determines its bidding/offering schedule in the DA as shown in Fig. 5.7 for the deterministic case, and in Fig. 5.8 for the case considering uncertainty with the best estimates. The net power purchases p_t^{buy} with and without the ESS, the power sold p_t^{sell}, and DA market prices are shown in the figures. The net purchases with the ESS is equivalent to $p_t^{\text{buy}} = p_t^{\text{G2S}} + p_t^{\text{G2B}} - \left(\sum_{s \in \mathcal{S}} p_{t,s}^{\text{B2S}} \right) / |S|$, whereas without the ESS it is equivalent to $p_t^{\text{buy}} = p_t^{\text{G2S}}$. Also, $p_t^{\text{sell}} = p_t^{\text{B2G}}$ in both cases. If any period, the p_t^{buy} with ESS is greater than p_t^{buy} without ESS, then the ESS is performing in G2B and thus additional purchases are made. On the other hand, if the opposite is true (less than), then B2S is occurring which reduces purchases in the market (*i.e.* offsets G2S).

In the deterministic case ($|S| = 1, \Gamma = 0$), the aggregator exploits the low-price periods (03:00 to 04:30, and 14:15 to 15:45) by scheduling purchases in the form of G2B (p_t^{buy} with ESS in red is larger in these periods). During the high-price periods (07:15 to 08:45, and 19:30 to 21:00), the aggregator discharges the ESS to obtain revenue from the market (p_t^{buy} with ESS in red is lower in these periods). The discharging, however, is split between B2G (p_t^{sell}) with 526.3 kWh and B2S with 1074 kWh total. The total B2S energy is higher than B2G
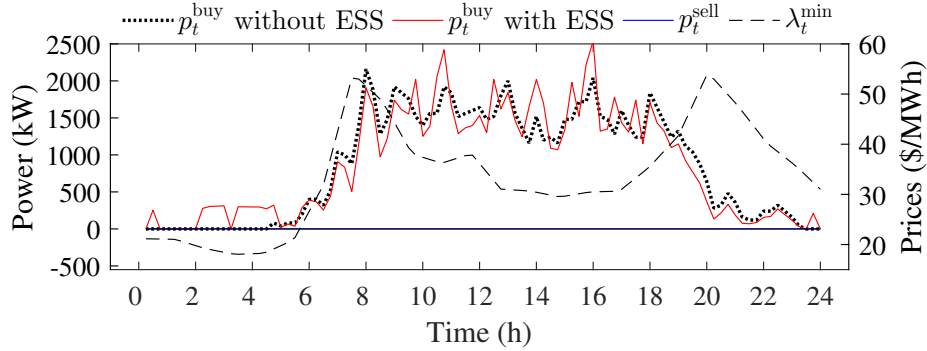
Figure 5.8: DA market buying and selling strategy when uncertainty management is considered. Note that the average B2S is used in p_t^{buy} with ESS since it is dependent on the scenario set.

because the demand needs of the EVCS, as shown in Fig. 5.2(c), correlate with the high-price regions. Thus, it is economical to discharge, while incurring degradation costs, to supply the EVCSs in B2S and offset purchases directly from the market in G2S. Furthermore, B2G is only exploited when the potential revenue that can be obtained by selling in the market outweighs both the degradation cost and the potential benefit of performing in B2S mode to offset G2S. This effect can be seen in Fig. 5.7 where B2G (p_t^{sell}) is scheduled to be sold during the high-price periods but not during the peaks, because it is more economical to perform B2S due to correlation with EVCS demand.

In Fig. 5.8, the DA schedule is shown considering the best estimates of uncertainty management, i.e. $|S| = 25, \Gamma = 72$. As compared to the deterministic case, G2B is spanned across more time periods (i.e. p_t^{buy} with ESS is larger). This occurs because the RO technique makes the aggregator hedge against the worst-case of unforeseen increase in market prices. As an example, in Fig. 5.7, the lowest-price period is 03:15 hours, and the maximum power of 500 kW is scheduled by the aggregator. However, potential uncertainty exists in the estimate of the market price, and thus the aggregator is risk-averse by scheduling 212 kW in that time period as shown in Fig. 5.8.

When considering uncertainty (Fig. 5.8), the aggregator does not schedule any B2G

($p_t^{\text{sell}} = 0$ in all periods). Instead, it increases the average B2S to 2161 kWh compared to the 1074 kWh in the deterministic case in Fig. 5.7. An example of this can be seen from periods 18:00 to 23:30, where B2S is performed consistently (p_t^{buy} with ESS is lower). This occurs because in the worst-case the market prices may be higher than expected, and thus there might be an adverse effect on the overall cost caused by excessive purchasing in G2S mode from the market. In addition, since the aggregator also considers multiple scenarios of demand that may materialize, the B2S is scheduled as an average response across all scenarios, as opposed to only a single scenario. Therefore, B2S is not only increased significantly, but also spread across multiple time periods that correlate with the EVCS demand (see Fig. 5.2(c)) to offset G2S purchases.

5.4.4   Yearly cost/benefit analysis

The aggregator must obtain a monetary benefit when participating in the grid markets and scheduling the ESS. A yearly cost/benefit analysis is performed for two cases: 1) day-ahead market (DAM) case where the aggregator schedules the aggregated EVCSs without the ESS, and 2) DAM including the ESS. The results are summarized in Table 5.2.

In the first case (1), the aggregator manages the EVCSs and participates in the DAM, which incurs a cost of \$311,092 which is solely based on purchases from the market in G2S mode. Furthermore, if the aggregator uses an ESS in conjunction with the market scheduling, it obtains revenue benefits of \$47,321 by performing in B2S/B2G mode. However, this introduces additional costs related to purchasing energy in the markets in G2B mode and the respective degradation costs when charging/discharging as shown in Table 5.2. By implementing an ESS, the total costs are reduced from the DAM case by 5.31%. It is important to emphasize that the ESS installation cost, cost of market participation, bidirectional metering cost, or any other auxiliary costs that arise in the cases are not considered. Therefore, the presented comparison of yearly revenue should be used as a basis for a detailed cost/benefit analysis.

Table 5.2: Yearly Cost/Benefit Analysis

	Costs ($)			Benefit ($)	Total ($)
	G2S	G2B	ES deg.	B2S/B2G	
1) DAM	311,092	-	-	-	311,092
2) DAM + ESS	311,092	27,185	3,627	47,321	294,583

5.5   Conclusion

This chapter developed a framework for an aggregator to manage an ensemble of electric vehicle charging stations to participate in the day-ahead electricity market to minimize energy procurement costs. To further reduce costs, the aggregator exploits its energy storage system to charge during the low-price periods in G2B mode, and then to discharge and either supply the stations directly in B2S mode or to inject power to the grid in B2G mode. However, since the charging/discharging of the ESS causes degradation, this effect is translated into an economic index and taken into consideration. To manage uncertainty, a stochastic and robust optimization approach are employed for the charging station power needs and market prices, respectively. The employment of robust optimization for market price uncertainty allows fine-tuning the conservativeness of the solution by varying the parameter Γ. On the other hand, weighed stochastic scenarios capture the expected cost of operations over demand scenarios that are estimated probabilistically. The benefit of this framework is twofold. First, the volatile and high-power needs of the charging stations are now procured in the day-ahead market, and second, the charging stations can now focus on their primary role to provide services to electric vehicle customers as opposed to attempting to reduce energy procurement costs.

Results show that the aggregator provides extensive benefits to the charging stations by managing their energy procurement from the wholesale market. The cost savings, however, are only experienced if uncertainty is properly characterized. The total cost savings are 5.31% if both DA market participation and uncertainty management is implemented with

an ESS, as compared to ignoring the ESS.

While it is expected that charging stations will provide the necessary infrastructure for EVs, other infrastructures are needed that provide on-demand service for EVs. The concept of battery swapping stations have been discussed in the literature and also in commercial applications. The next chapter develops a business and operating framework for such swapping stations.

Chapter 6

OPTIMAL OPERATION AND SERVICES SCHEDULING FOR AN ELECTRIC VEHICLE BATTERY SWAPPING STATION

6.1 Introduction

The frameworks in Chapter 2, 3, and 4 are methods that tackle EV issues of upfront costs by providing streams of revenue to owners. However, the issues of range anxiety, slow charging times, and lack of public infrastructure cannot be solved directly by extracting services from EVs. Battery swapping stations (BSS) are poised as effective means of eliminating these issues [9].

Since the BSS is a new player that aggregates and operates a large number of EV batteries in its stock, it can directly participate in the wholesale power markets without the need of a mediator, *e.g.* aggregagor. As an objective, the BSS seeks to maximize its profits, by participating in markets and providing services, such as demand response, energy storage, and reserves. The storing capabilities of the BSS are scheduled based on time-varying electricity prices, *e.g.* RTP. The BSS maximizes its profits by exploiting the low-price periods of the day to purchase electricity and charge batteries in Grid-to-Battery mode (G2B), and sell during the high-price periods by discharging batteries to the grid in Battery-to-Grid mode (B2G). Additionally, BSS can perform Battery-to-Battery (B2B) services in order to charge certain batteries using the energy stored in other batteries.

The BSS mimics a traditional gasoline station in its operations. Consumer's arrive at the BSS with depleted batteries and the batteries are swapped with fully-charged ones. Such swapping relieves the stress of range anxiety and slow charging times of EV owners. In addition, the BSS would lease the batteries to EV owners and thus reduce the overall operating cost in maintaining the battery. The motivation behind this chapter is to present
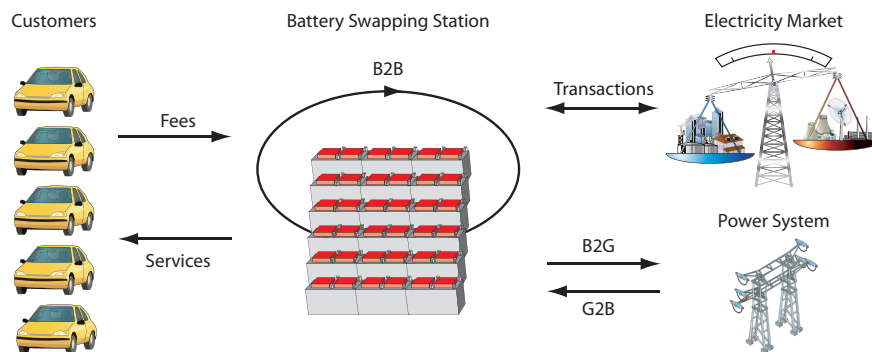
Figure 6.1: BSS interactions with customers, market, and the power system.

a complete BSS framework that benefits the BSS itself, EV consumers, and the power grid. The main contributions of this chapter are:

- A realistic framework of a BSS in the DA scheduling process in order to take advantage of G2B and B2G services.
- Complete BSS operating model including battery degradation, market price uncertainty, and battery demand uncertainty. The impact of each feature is individually analyzed.
- The model exploits the ability to transfer energy among batteries in B2B mode, if there is an economic benefit.

6.2 Business Case

6.2.1 Operations

The operation of the BSS is shown in Figure 6.1 [167]. The BSS's goal is to supply the battery demand while maximizing its profits. The BSS requires a stock of batteries with different capacities to serve its customers. It is assumed the batteries are owned by the BSS and leased to the customers. The customers benefit from this arrangement since all the costs related to the batteries, including degradation and maintenance, are accrued by the BSS. The customer is not concerned with the battery lifetime nor with the way in which the

battery was charged (rapid, high power charging or slow charging). To recoup these costs and to make a profit, the BSS charges customers a fixed fee for the service of swapping.

The BSS decides the optimal battery charging/discharging schedules and purchases/sells electricity by submitting bids and offers in the electricity market. By exploiting the time-dependencies of wholesale electricity prices, the BSS can take advantage of buying electricity (in G2B mode) during the low-price periods, selling electricity (in B2G mode) during the high-price periods, and shifting energy within its stock of batteries (in B2B mode).

As an example of B2B mode, consider a scenario of two 24 kWh batteries with current state-of-charges 18 kWh and 21 kWh, in which one of them is to be swapped in the near future, and the price of electricity is high. If we assume the power rating is 3 kW, and ignore the efficiencies for the sake of simplicity, then the BSS has three choices: it can purchase 3 kWh in the market and charge the 21 kWh battery (G2B mode), it can purchase 6 kWh in the market and charge the 18 kWh battery (G2B mode), or it can discharge 3 kWh from the 18 kWh battery to fully charge the 21 kWh battery (B2B mode). Since the electricity price is high, it is more economical to perform B2B and thus postpone G2B to low-price time periods. The proposed optimization model takes advantage of these scenarios in order to maximize profits for the BSS.

6.2.2   Customer perspective

From the customers' perspective, the largest cost of owning an EV is the battery. In 2012, the replacement cost of a 24 kWh battery ranged from $12,000 to $14,400 (*i.e.* 500-600 $/kWh) [34]. However, in the proposed BSS scheme, the customers would lease the battery from the BSS and avoid a lump investment.

The other aspects that concern potential EV owners are the long charging times, the costs of upgrading household installations to high power chargers, and the limited number of public charging stations. Typical EVs are equipped with standard 1.6 kW level I chargers (see Table 1.2) that connect directly to a household outlet [168]. At this charging level, it would take about 15 hours to fully charge a 24 kWh battery. Owners, however, can install

upgraded level II chargers [168], with a power level of 3.3 kW and thus reduce the charging time to about 7 hours. However, the upgraded charger comes at an extra cost, which is approximately \$849 in 2013 [31]. Even if these additional expenses are acceptable to the owners, they may not be able to install upgraded chargers due to limits in their current electric supply installations, or the regulations of the housing structure they reside in (*e.g.* apartments).

Another concern of the EV owners is the limited range due to the relative small capacity of the batteries. In order to ease this concern, the owners would need to have access to public charging stations, which are translated into requiring heavy infrastructure investments. These concerns could be eliminated if an EV owner has access to BSSs in the areas where they usually travel.

6.2.3   Power system benefits

As the penetration of EVs increases [169], and if instead of resorting to the BSS, the consumers favor high-power charging, they would need to install upgraded chargers to accommodate their daily energy needs for transportation. This may require upgrades not only of the electric installations at the household level, but also of the distribution system itself, in order to successfully accommodate the increased power demand. On the other hand, if BSSs are installed, some of the investments would be avoided, and the only required upgrades would be at the site at which the BSSs are located.

Furthermore, the BSS is an aggregator of batteries, and these stations could also be used to provide services to the system as a whole. The BSS can inject power back into the power system to smooth the net daily demand curve, if the BSS perceives a benefit in doing so. In addition to acting as a storage device, the BSS can also provide a share of the required ancillary services in different intervals, *e.g.* frequency regulation, load following, and voluntary reserve provisions [170].

6.3   Optimization Model

6.3.1   Assumptions

In the DA scheduling, the BSS estimates the market price λ_t^{DA} and the battery demand $N_{g,t}$. With this information, the DA optimization takes place. In this process, the discounts for swapping only partially charged batteries to the customers are incorporated. These discounts are a form of compensation for the inconvenience caused to the customers, and can be adjusted based on the BSS business. The DA model determines the battery charging, discharging and swapping schedules as well as the offering/bidding schedule to the market.

6.3.2   Day-ahead model

In the DA, the model determines the amount of electricity to buy em_t^{buy}, and to sell em_t^{sell}, in the market to meet the battery demand $N_{g,t}$. An optimal charging/discharging schedule is derived to maximize profits for the BSS. The DA model is formulated as:

$$
\begin{aligned}
\text{maximize} \quad & BSR \sum_{(t\in T)} \sum_{(i\in I)} x_{i,t} \\
& - \sum_{(t\in T)} \lambda_t^{\mathrm{DA}} \left(em_t^{\mathrm{buy}} - em_t^{\mathrm{sell}} \right) \\
& - VoCD \sum_{(t\in T)} \sum_{(g\in G)} bat_{g,t}^{\mathrm{short}} \\
& - BSR \sum_{(t\in T)} \sum_{(i\in I)} \beta_{i,t}
\end{aligned}
\tag{6.1}
$$

In equation (6.1), the first term is the revenue collected from customers for swapping priced at BSR. The binary variable $x_{i,t}$ is equal to 1 if battery i is swapped at the beginning of time period t, and 0 otherwise. The second term is the energy purchased and sold in the DA market at price λ_t^{DA}. The objective function also considers the BSS's inability to supply battery demand $bat_{g,t}^{\mathrm{short}}$, which is penalized at the cost of value-of-customer-dissatisfaction,

$VoCD$. The last term is the discount $\beta_{i,t}$ given on the revenue BSR collected from consumers for a battery swap if a 100% charged battery cannot be supplied.

The $VoCD$ is a monetary value the BSS business places on the inability to supply a customer with a battery. This value is determined by performing research studies and surveys of its customers. A parallel can be drawn between the $VoCD$ and the value-of-lost-load ($VoLL$), which is used in operating and planning models for power systems, *e.g.* [153]. $VoLL$ represents the value customers place on the loss of 1 MWh of supply, which is dependent on interruption duration, time of day, location, and cause of interruption [171]. The BSS has two criteria when estimating the $VoCD$: i) the monetary loss of swapping revenue that could have been obtained at present and potentially in the future from the dissatisfied customer, and ii) the monetary loss due to new customer acquisition. However, the estimation of $VoCD$ is beyond the scope of this work.

This objective function is subject to several constraints as discussed and shown below.

$$soc_{i,t} = \left(soc_{i,t-1} + bat_{i,t}^{\text{chg}}\eta^{\text{chg}} - \frac{bat_{i,t}^{\text{dsg}}}{\eta^{\text{dsg}}} \right)(1 - x_{i,t}) + SOC_{i,t}^{\text{init}} \cdot x_{i,t} \quad \forall i \in I, t \in T \qquad (6.2)$$

Equation (6.2) is the energy state-of-charge $soc_{i,t}$ of each battery i. This energy state-of-charge takes into account the state-of-charge at the previous time period, the charging power $bat_{i,t}^{\text{chg}}$, discharging power $bat_{i,t}^{\text{dsg}}$, and efficiencies. Thus, in (6.2), if $x_{i,t}$ is equal to 1, the $soc_{i,t}$ is not updated. Instead, the battery is swapped with a different one with the incoming energy state-of-charge, $SOC_{i,t}^{\text{init}}$. Constraint (6.2) performs multiplication of continuous and binary variables, which are linearized with the approach discussed in [123] and further explained in Appendix B.2.

$$soc_{i,t-1} + soc_{i,t}^{\text{short}} \geq BC_g^{\text{max}} \cdot S_{i,g} \cdot x_{i,t} \quad \forall i \in I, g \in G, t \in T \qquad (6.3)$$

Constraint (6.3) captures the battery swapping mechanics. If battery i is swapped to an EV, the state-of-charge should be at the maximum battery capacity BC_g^{max}, for the battery group g it belongs to. Binary parameter $S_{i,g}$ is used to identify the appropriate battery group g, which battery i belongs to. If the maximum battery capacity cannot be met, the

remainder is captured in the energy shortage variable $soc_{i,t}^{\text{short}}$.

$$\sum_{(i \in I)} S_{i,g} \cdot x_{i,t} + bat_{g,t}^{\text{short}} = N_{g,t} \quad \forall g \in G, t \in T \tag{6.4}$$

In (6.4), The BSS seeks to meet the battery demand $N_{g,t}$. Battery shortage is captured in variable $bat_{g,t}^{\text{short}}$, which is penalized in (6.1). To meet the demand, energy needs to be purchased from the market and the excess can be sold back if this results in profit for the BSS, as shown in (6.5).

$$em_t^{\text{buy}} - em_t^{\text{sell}} = \sum_{(i \in I)} \left(bat_{i,t}^{\text{chg}} - bat_{i,t}^{\text{dsg}} \right) \quad \forall t \in T \tag{6.5}$$

Each battery has a maximum charging/discharging power limit P_i^{max}, enforced by constraints (6.6) and (6.7). The batteries energy state-of-charge and energy state-of-charge shortage are constrained by maximum and minimum battery capacities in constraints (6.8) and (6.9). The energy state-of-charge ceiling is below the nominal value in order to avoid the risk of setting the battery on fire, and the minimum avoids rapid degradation of the battery, as explained in [127]. Constraints (6.10) and (6.11) disallow charging and discharging to occur simultaneously at any given period of time, while (6.12) and (6.13) disallow activating the purchasing and selling variables simultaneously. Constraint (6.14) ensures the total stored energy is the same as it was at the beginning of the day.

$$0 \leq bat_{i,t}^{\text{chg}} \leq (1 - x_{i,t}) P_i^{\text{max}} \quad \forall i \in I, t \in T \tag{6.6}$$

$$0 \leq bat_{i,t}^{\text{dsg}} \leq (1 - x_{i,t}) P_i^{\text{max}} \quad \forall i \in I, t \in T \tag{6.7}$$

$$\sum_{(g \in G)} BC_g^{\text{min}} \cdot S_{i,g} \leq soc_{i,t} \leq \sum_{(g \in G)} BC_g^{\text{max}} \cdot S_{i,g} \quad \forall i \in I, t \in T \tag{6.8}$$

$$\sum_{(g \in G)} BC_g^{\text{min}} \cdot S_{i,g} \leq soc_{i,t}^{\text{short}} \leq \sum_{(g \in G)} BC_g^{\text{max}} \cdot S_{i,g} \quad \forall i \in I, t \in T \tag{6.9}$$
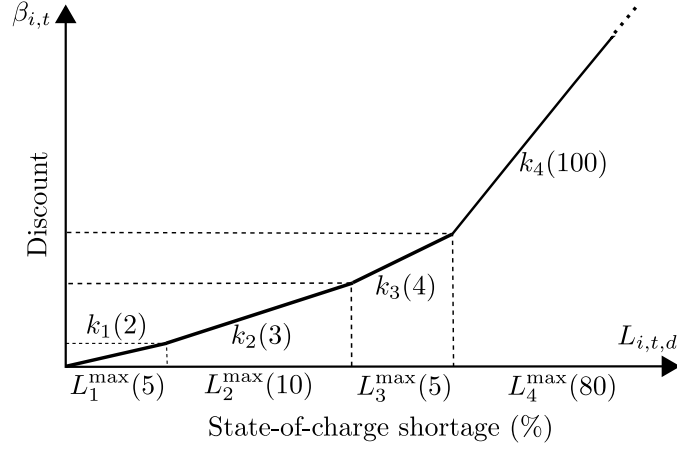
Figure 6.2: Piecewise discount function. The values in (·) are used in the case studies in Section IV.

$$bat_{i,t}^{\mathrm{dsg}} \leq P_i^{\max} \cdot a_{i,t} \quad \forall i \in I, t \in T \tag{6.10}$$

$$bat_{i,t}^{\mathrm{chg}} \leq P_i^{\max} \left(1 - a_{i,t}\right) \quad \forall i \in I, t \in T \tag{6.11}$$

$$em_t^{\mathrm{sell}} \leq M \cdot c_t \quad \forall t \in T \tag{6.12}$$

$$em_t^{\mathrm{buy}} \leq M \left(1 - c_t\right) \quad \forall t \in T \tag{6.13}$$

$$soc_{i,t=|T|} = SOC_{i,t=0}^{\mathrm{init}} \quad \forall i \in I \tag{6.14}$$

If the BSS cannot manage to fully charge a battery that potentially could be swapped to a customer, it has two alternatives. The first is to offer a discount on the price of the battery swap, BSR. The second alternative is not to swap the battery incurring the $VoCD$ penalty. The discounts are modeled as a piecewise linear curve in Figure 6.2 and they increase as the battery energy shortage increases. The piecewise curve needs to incorporate the discount due to the energy shortage in the swapped battery and the perceived inconvenience of the customer having to return to the BSS sooner due to the energy shortage. This is modeled

through constraints (6.15)-(6.17). Constraint (6.15) calculates the normalized energy state-of-charge shortage and distributes it among the discrete energy state-of-charge shortage segments $L_{i,t,d}$. The discount $\beta_{i,t}$ in (6.16) is calculated as the product of the slope of each discount segment k_d and the respective shortage segment L_d. Lastly, constraint (6.17) limits the state-of-charge shortage segments to their preset limits $L_d^{\max}$. An example is shown in Figure 6.2. For the first 5% ($L_1^{\max}$) of the missing energy, the BSS gives up to 10% discount ($k_1 \cdot L_1^{\max}$) on the price of the battery swap, BSR. For the next 10% ($L_2^{\max}$) of the missing energy, the BSS gives up to an additional 30% discount ($k_2 \cdot L_2^{\max}$). This rationale follows for the remaining segments.

$$\frac{soc_{i,t}^{\text{short}}}{\sum_{(g \in G)} S_{i,g} \cdot BC_g} = \sum_{(d \in D)} L_{i,t,d} \quad \forall i \in I, t \in T \tag{6.15}$$

$$\beta_{i,t} = \sum_{(d \in D)} k_d \cdot L_{i,t,d} \quad \forall i \in I, t \in T \tag{6.16}$$

$$0 \leq L_{i,t,d} \leq L_d^{\max} \quad \forall i \in I, t \in T, d \in D \tag{6.17}$$

6.3.3   Demand uncertainty with inventory robust optimization

At the DA stage, battery demand intervals $[N_{g,t}^{\min}, N_{g,t}^{\max}]$ represent the bounds of the expected battery demand for the next day. If the battery demand is high, the BSS will need to resort to purchasing energy in the volatile real-time market to meet the demand. Furthermore, the BSS might need to offer discounts for non-fully charged batteries or it might even be unable to supply some customers. On the other hand, if the battery demand realization is low, the excess electricity can either be sold in the real-time market or stored in the batteries for later use. However, having a battery stock fully charged would prevent the BSS to take advantage of possible low prices in the real-time market. This uncertainty is managed using the robust inventory theory [172]. In such approach, a sub-optimal solution is obtained if the demand realizations are within the defined interval that belongs to $[N_{g,t}^{\min}, N_{g,t}^{\max}]$, where $N_{g,t}^{\max} = N_{g,t}^{\min} + \Delta N_{g,t}$ and $\Delta N_{g,t}$ is the battery demand deviation. The DA model (6.1)-(6.17)

extended to account for demand uncertainty is formulated as follows:

$$\text{maximize} \quad BSR \sum_{(t\in T)} \sum_{(i\in I)} x_{i,t} - \text{DA}\left(em_t^{\text{buy}} - em_t^{\text{sell}}\right)$$

$$- VoCD \sum_{(t\in T)} \sum_{(g\in G)} bat_{g,t}^{\text{short}}$$

$$- BSR \sum_{(t\in T)} \sum_{(i\in I)} \beta_{i,t}$$

$$- \sum_{(g\in G)} y_g \tag{6.18}$$

This objective function is subject to the constraints shown below:

$$\text{Constraints} \quad (6.2), (6.3), (6.5) - (6.17) \tag{6.19}$$

$$\sum_{(i\in I)} S_{i,g} \cdot x_{i,t} + bat_{g,t}^{\text{short}} = N_{g,t}^{\text{min}} + bat_{g,t}^{\text{add}} \quad \forall g \in G, t \in T \tag{6.20}$$

$$y_g \geq VoCD \left(-\sum_{(t\in T)} bat_{g,t}^{\text{add}} + \Gamma_g \cdot q_g + \sum_{(t\in T)} r_{g,t}\right) \quad \forall g \in G \tag{6.21}$$

$$q_g + r_{g,t} \geq \Delta N_{g,t} \quad \forall g \in G, t \in J_g \tag{6.22}$$

The robust objective function is shown in (6.18). The last term represents the penalty cost y_g imposed by the inventory RO for each battery group g. Equation (6.20) ensures the minimum battery demand ($N_{g,t}^{\text{min}}$) is met. Variable $bat_{g,t}^{\text{add}}$ represents the additional number of batteries charged on top of $N_{g,t}^{\text{min}}$. Constraint (6.21) determines the worst time periods in which additional battery demand could materialize. Parameter Γ_g is used to control the level of robustness of the solution taking values in $[0, |J_g|]$, where $J_g = \{t|\Delta N_{g,t} > 0\}$. If $\Gamma_g = 0$, no deviations are considered and the solution is equivalent to the deterministic one, whereas if $\Gamma_g = |J_g|$, deviations at all time periods are considered, acquiring the most conservative solution (*i.e.* demand at all time periods is equal to $N_{g,t}^{\text{max}}$). Variables q_g and $r_{g,t}$ are non-negative auxiliary variables used to account for the known demand bounds. Variable $r_{g,t}$ is incorporated in constraints (6.21)-(6.22) as the dual variable of constraint (6.4) and
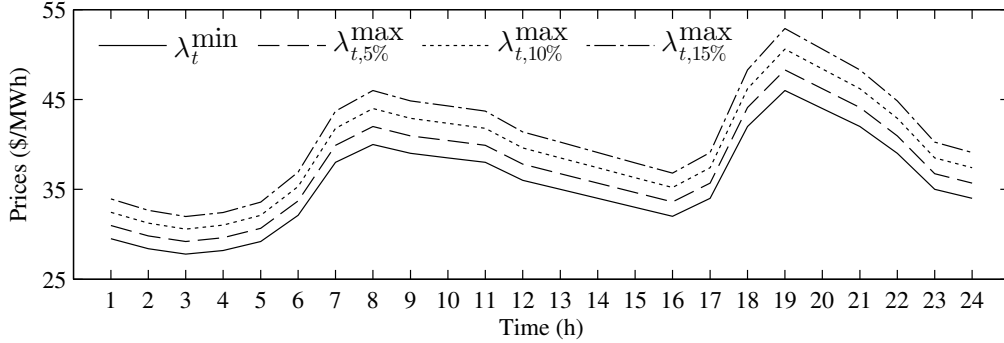
Figure 6.3: DA price deviations with multiple bands.

q_g is used to preserve linearity. A detailed explanation of how to obtain the inventory RO problem is given in [172].

6.3.4 Price uncertainty with multi-band robust optimization

The BSS can interact with electricity markets by purchasing energy when it is inexpensive and injecting it back when the price is high, at a profit. Profit opportunities may be missed or the BSS could incur losses if uncertainty of market prices is not appropriately accounted for. To hedge against this uncertainty, the multi-band RO approach is used [173].

In [173], deviations in prices are modeled within the range $[\lambda_t^{\min}, \lambda_{t,b}^{\max}]$, where $\lambda_{t,b}^{\max} = \lambda_t^{\min} + \Delta\lambda_{t,b}$ and $\Delta\lambda_{t,b}$ is the market price deviation for each band b. Unlike inventory RO used for the battery demand uncertainty, the multi-band approach uses multiple deviation bands controlled by robustness parameter θ_b, which takes values in $[0, |U_b|]$, where $U_b = \{t|\Delta\lambda_{t,b} > 0\}$. However, the total number of deviations over the optimization horizon must be $\sum_{(b \in B)} |\theta_b| \leq |T|$. As an example, Figure 6.3 shows three uncertainty bands. The band $\lambda_{t,5\%}^{\max}$ represents all the uncertainty materializations that are 5% above $\lambda_t^{\min}$. Similar rationale applies to $\lambda_{t,10\%}^{\max}$ and $\lambda_{t,15\%}^{\max}$. The formulation of the model that manages price uncertainty

using multi-band RO is:

$$\text{maximize} \quad BSR \sum_{(t \in T)} \sum_{(i \in I)} x_{i,t} - \sum_{(t \in T)} \lambda_t^{\min} \left(em_t^{\text{buy}} - em_t^{\text{sell}} \right)$$

$$- VoCD \sum_{(t \in T)} \sum_{(g \in G)} bat_{g,t}^{\text{short}}$$

$$- BSR \sum_{(t \in T)} \sum_{(i \in I)} \beta_{i,t}$$

$$- \sum_{(b \in B)} \theta_b \cdot v_b$$

$$- \sum_{(t \in T)} z_t \tag{6.23}$$

This objective function is subject to the following constraints:

$$\text{Constraints} \quad (6.2) - (6.17) \tag{6.24}$$

$$v_b + z_t \geq \Delta \lambda_{t,b} \cdot em_t^{\text{buy}} \quad \forall b \in B, t \in U_b \tag{6.25}$$

The objective function (6.23) includes additional variables v_b and z_t, and parameter θ_b, which controls the robustness of the solution. If $\theta_b = 0$, the effect of price deviations is ignored and the solution is deterministic. On the other hand, for $\theta_b = |U_b|$ all price deviations are considered, which results in the most conservative solution. Equation (6.25) ensures feasibility for any deviation $\Delta \lambda_{t,b}$. The non-negative variable z_t is the dual variable of the DA objective function (6.1) and the non-negative variable v_b is used for linear equivalency. A detailed explanation of how to obtain the multi-band RO problem is discussed in [173].

6.3.5 Battery degradation costs

Charging cycles reduce batteries' lifetime. Since the BSS incurs all costs related to batteries, it needs to incorporate the costs resulting from battery degradation. In this work, degradation characteristic is highly sensitive to the number of cycles and virtually insensitive to the depth-of-discharge, as explained in [10]. However, other chemistries with higher sensitivity

to the depth-of-discharge can be modeled as proposed in [10]. The formulation of the BSS model that manages battery degradation is:

$$\text{maximize} \quad BSR \sum_{(t \in T)} \sum_{(i \in I)} x_{i,t} - \sum_{(t \in T)} \lambda_t^{\text{DA}} \left(em_t^{\text{buy}} - em_t^{\text{sell}} \right)$$

$$- VoCD \sum_{(t \in T)} \sum_{(g \in G)} bat_{g,t}^{\text{short}}$$

$$- BSR \sum_{(t \in T)} \sum_{(i \in I)} \beta_{i,t}$$

$$- \sum_{(t \in T)} \sum_{(i \in I)} C_{i,t}^{\text{deg}} \tag{6.26}$$

Subject to:

$$\text{Constraints}(2) - (17) \tag{6.27}$$

$$C_{i,t}^{\text{deg}} = \left| \frac{m_i}{100} \right| \frac{bat_{i,t}^{\text{chg}} + bat_{i,t}^{\text{dsg}}}{\sum_{g \in G} S_{i,g} \cdot BC_g} C_i^{\text{bat}} \quad \forall i \in I, t \in T \tag{6.28}$$

The objective function (6.26) explicitly includes the cost of degrading the battery C_i^{deg}, due to charging/discharging cycles undergone. C_i^{deg} is calculated in (6.28), where m_i is the slope of the linear approximation of battery life as a function of the number of cycles, and C_i^{bat} is the cost of the battery. The value of m_i is approximated from manufacturer datasheets [174].

6.3.6 Complete day-ahead model

The complete DA model that incorporates battery demand uncertainty, market price uncertainty, and battery degradation costs is as follows:

$$\text{maximize} \quad BSR \sum_{(t \in T)} \sum_{(i \in I)} x_{i,t} - \sum_{(t \in T)} \lambda_t^{\min} \left(em_t^{\text{buy}} - em_t^{\text{sell}} \right)$$

$$- VoCD \sum_{(t \in T)} \sum_{(g \in G)} bat_{g,t}^{\text{short}}$$

$$- BSR \sum_{(t \in T)} \sum_{(i \in I)} \beta_{i,t}$$

$$- \sum_{(g \in G)} y_g - \sum_{(b \in B)} \theta_b v_b - \sum_{(t \in T)} z_t$$

$$- \sum_{(t \in T)} \sum_{(i \in I)} C_{i,t}^{\text{deg}} \quad (6.29)$$

subject to:

$$\text{Constraints} \quad (6.2), (6.3), (6.5) - (6.17), (6.20) - (6.22), (6.25), (6.28) \quad (6.30)$$

6.4 Case Study

The proposed approach is applied to two case studies over a 24 hour period. The charging/discharging efficiencies are 90% with maximum charging/discharging power of 3.3 kW. The energy state-of-charge variable $(soc_{i,t})$ is bounded within 15% and 95% of the nominal capacities in order to protect the batteries [127]. The initial energy state-of-charge $(SOC_{i,t=0}^{\text{init}})$ of the batteries are uniformly randomized between 15% and 95%, and the incoming energy state-of-charge $(SOC_{i,t>0}^{\text{init}})$ is randomized within 30% and 60% of the nominal capacity. Parameter $SOC_{i,t=0}^{\text{init}}$ represents the energy stored in each battery in the BSS stock at the beginning of the day, whereas $SOC_{i,t>0}^{\text{init}}$ represents the energy in the customer's battery when they arrive to the BSS for swapping. The BSR is set to $70, as used in [13], and the $VoCD$ is $200. The piecewise discount curve is designed with four segments: 1) $k_1 = 2$ and $L_1^{\max} = 5\%$, 2) $k_2 = 3$ and $L_2^{\max} = 10\%$, 3) $k_3 = 4$ and $L_3^{\max} = 5\%$, and 4) $k_4 = 100$ and $L_4^{\max} = 80\%$, and is shown in Figure 6.2.
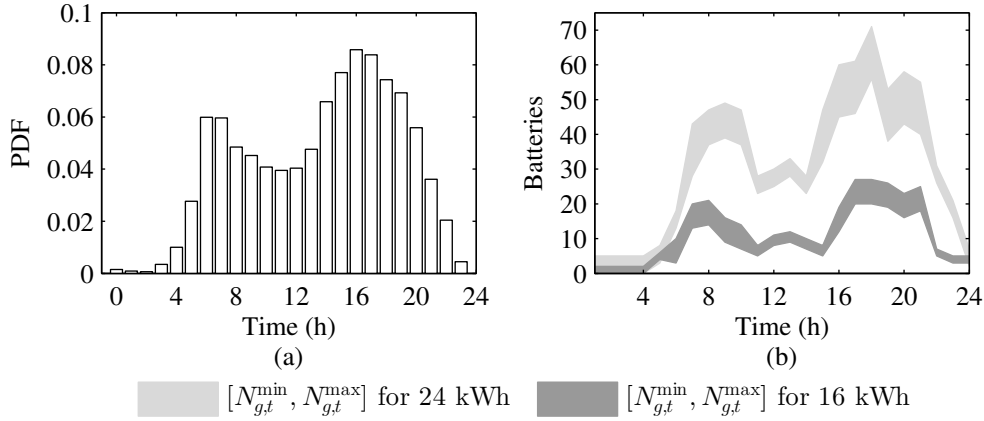
Figure 6.4: Distribution of demand at BSS in (a), and uncertainty bounds in (b).

In order to represent a typical weekday, the historical data of every Thursday in the period January-March 2013 from the PJM market [125] was used. The typical weekday curve was obtained using the K-means clustering approach [139] to identify a price profile that best characterizes the data. The upper bound prices $\lambda_{t,b}^{\max}$ are proportional to the derived typical weekday curve which is equivalent to $\lambda_t^{\min}$, as shown in Figure 3. The arrival times for swapping are assumed to follow the probability distribution function (PDF) shown in Figure 6.4a, which is derived from [124]. This assumption is justifiable since there is no historical data available for any existing BSS. The demand range $[N_{g,t}^{\min}, N_{g,t}^{\max}]$ for battery group 24 kWh is shown in Figure 6.4b in light grey, and for 16 kWh batteries in dark grey.

A discussion on the software and techniques used to solve these models is presented in Appendix A.

6.4.1 Small battery stock with a single battery type

This study assesses the individual effects of price uncertainty, demand uncertainty, and battery degradation. A single battery group is used with a stock of 200 batteries with nominal capacities of 24 kWh, as shown in Figure 6.4b in light grey area.
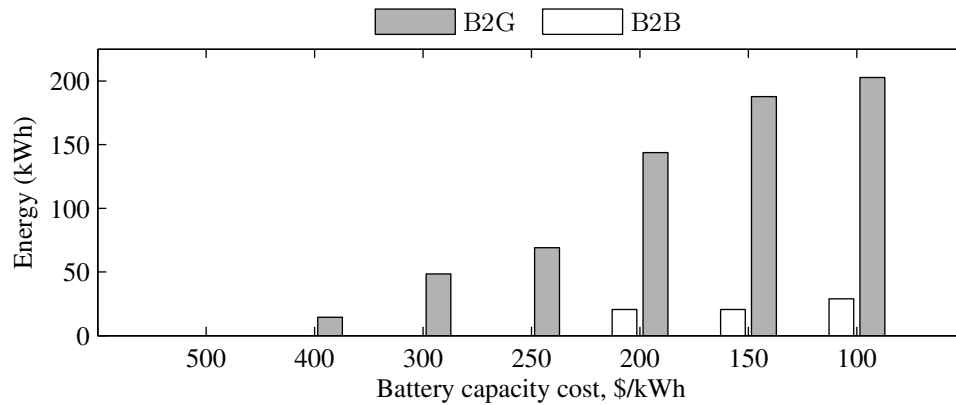
Figure 6.5: Impact on B2G and B2B as battery capacity cost decreases.

6.4.1.1 *Effect of battery degradation*

By varying the battery capacity cost from 500 (cost in 2012) to 100 \$/kWh, accounting for the advancement of battery technologies as time progresses, the effect on B2G and B2B is studied. The degradation model of the batteries is linear and represented by equation (6.28) with slopes $m_i = [-0.0158, -0.0009]$. The lower slope is the linear approximation of the 2012 technology [34], and the higher slope represents a technological improvement in the battery cycle-life of three times the current value. Figure 6.5 shows the energy transfer in B2G and B2B modes for different values of battery capacity cost. When the battery capacity cost is 500 \$/kWh, the battery performs no B2G or B2B. However, these services become attractive as the battery capacity cost decreases, reaching a maximum for the lowest battery capacity cost. If B2G and B2B are not present, the BSS purchases only the electricity needed to supply the battery demand. B2B is significantly lower than B2G since B2B requires a battery to discharge in order to charge another battery. This causes degradation of both batteries and thus, the overall cost increases. However, B2G supplies electricity to the system by discharging a battery and thus, only degrading a single battery during the optimization horizon. Figure 6.5 shows that as the battery technology improves, the provision of services to the grid, and internal energy transfers in B2B result in economic benefits to the BSS.
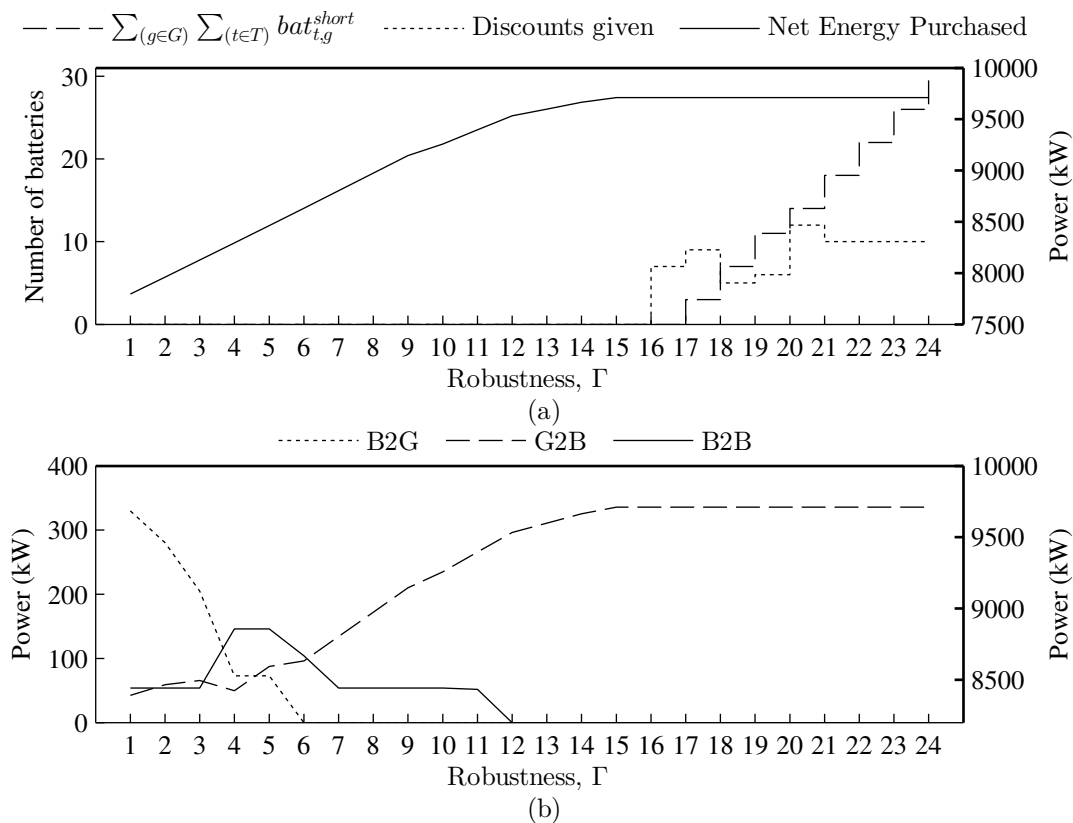
Figure 6.6: (a) Effect on battery shortage, discounts, and net energy purchased, and (b) effect on B2G, G2B, and B2B services. B2G and B2B are referred to the left-side-axis and G2B to the right-side-axis.

6.4.1.2   Effect of uncertainty in battery demand

As discussed, the parameter Γ controls the level of robustness in the objective. Figure 6.6a shows the battery shortage, discounts given (dashed line), and net energy purchased (solid line) to charge batteries as a function of Γ. Figure 6.6b shows the total energy in B2G, G2B, and B2B modes as a function of Γ. The net energy purchased is defined as the energy required to meet the battery demand over the optimization horizon.

In Figure 6.6a, it can be seen that as Γ increases, the net energy purchased to charge batteries increases, because the BSS needs to schedule additional batteries for the worst-

case realizations (within the ranges shown in Figure 6.4b) without having to resort to offer discounts, or incur $VoCD$. This figure shows that the net energy purchased saturates after $\Gamma = 15$, since the BSS has insufficient stock to offer fully charged batteries, and thus needs to give discounts and even is unable to serve all the customers. The battery stock is the limiting factor because additional batteries cannot be scheduled above $\Gamma = 15$.

Figure 6.6b shows B2G, G2B and B2B as a function of Γ. This figure shows that B2G decreases until $\Gamma = 6$, because additional batteries are scheduled in order to cope with the uncertainty. This results in energy that used to be sold to the grid to be used for swapping purposes. On the other hand, B2B reaches the maximum for $\Gamma = 4$ and $\Gamma = 5$ because the demand increase requires more energy. However, before resorting to buying energy from the grid, B2B is a less expensive option. This is because stand-by batteries pre-charge during the low-price periods, and supply other batteries in the BSS stock when they require energy during the high-price periods. For Γ values from 6 to 12, B2B reduces because the batteries that used to pre-charge are now required to be swapped. Thus, they store their pre-charged energy rather than transferring to other batteries. For $\Gamma \geq 12$, B2G and B2B do not occur because the additional batteries scheduled for swapping has increased up to the point where the BSS cannot exploit the advantages of selling and transferring energy, but has to store energy for swapping.

Battery demand uncertainty reduces the attractiveness of B2G and B2B services at the benefit of protection against the worst-case demand realizations. The BSS needs to decide what level of robustness is desired in the DA scheduling by weighing the benefits of B2G and B2B against incurring discounts and $VoCD$ if it is not able to meet the demand.

6.4.1.3 Effect of uncertainty in market prices

In general, the BSS tries to purchase electricity during the lowest-price periods. However, with market price uncertainty, electricity purchases span over multiple time periods to protect against price deviations. The robustness parameters $\theta_{10\%}$ and $\theta_{15\%}$, are varied between $[0, |U_b|]$ for price deviations of 10% and 15% above $\lambda_t^{\min}$ as shown in Figure 6.3. The varia-
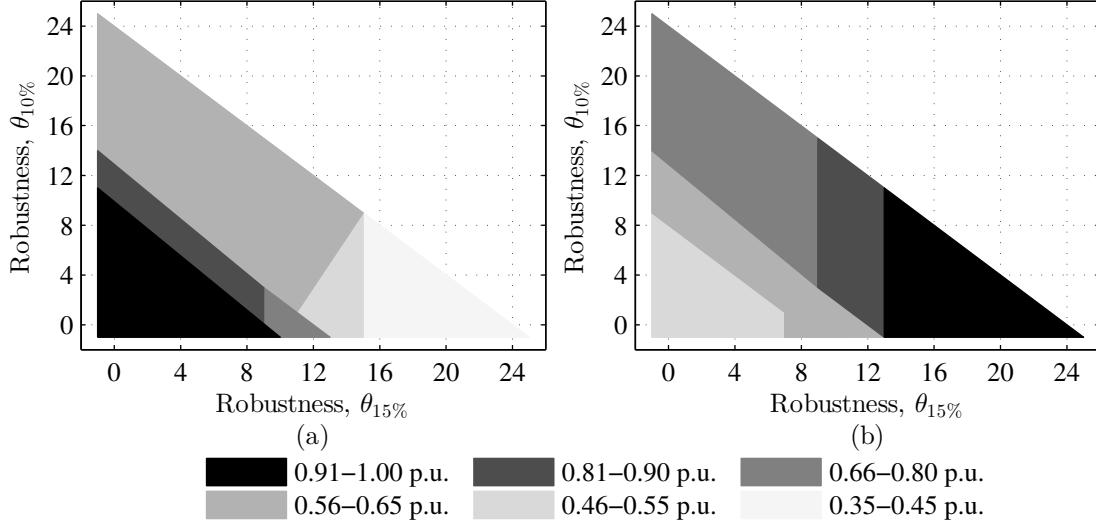
Figure 6.7: Effect of price uncertainty on the energy injected in B2G (a) and B2B (b) in p.u. (*i.e.* normalized over kWh).

tions, however, need to follow the rule $|\theta_{10\%}| + |\theta_{15\%}| \leq |T|$ [173]. The model is solved for these combinations of robustness parameters and the effect on B2G and B2B are shown in Figure 6.7. Quantities in Figure 6.7a are normalized to the maximum energy in B2G mode of 463.16 kWh, and in Figure 6.7b to the maximum energy in B2B mode of 120.60 kWh.

As an example, if the BSS decides to protect against eight deviations in the 10% band and four deviations in 15% band, *i.e.* $\theta_{10\%} = 8$ and $\theta_{15\%} = 4$, the B2G would be approximately 0.81-0.90 p.u and B2B would be 0.56-0.65 p.u. In Figure 6.7a, B2G decreases as the robustness parameter is increased. However, B2G decreases faster to its minimum of 0.45-0.35 p.u. for increases in $\theta_{15\%}$ as compared to $\theta_{10\%}$. This is the case because 15% price deviations are associated to larger price increments as compared to 10%. There are two reasons for the decreasing trend of B2G as a result of the price uncertainty. First, B2G requires excess electricity to be purchased and stored in batteries. By decreasing B2G, the amount of electricity purchased decreases, minimizing the potential impact of high-price materializations. Second, the large electricity purchases that were concentrated in the low-price periods, in order to minimize costs, are spread over multiple periods. This causes higher-price periods

to purchase rather than sell energy to cope with the uncertainty.

Since the RO approach spans the energy purchases over time, resulting even in purchases during the high-price periods, B2B is an economic alternative to the expensive market purchases. By exercising B2B, pre-charged batteries supply the batteries that require energy for swapping. From Figure 6.7b, it can be seen that if the robustness parameters are set to zero ($\theta_{10\%} = \theta_{15\%} = 0$), B2B is at its minimum of 0.46-0.55 p.u. As the robustness parameters increase, B2B increases as well. As in the B2G case, a higher increase in B2B occurs for 15% price deviations as compared to the 10% price deviations.

6.4.2   Large battery stock with two battery types

In the large-scale case study, 16 kWh and 24 kWh battery groups are used with 100 and 200 battery stock, respectively, as shown in Figure 6.4b. From Figure 6.5, battery capacity cost is set to 200 \$/kWh to denote a trend towards cheaper batteries in the future, where the benefits of B2G and B2B will be more evident. This study uses the complete DA model.

To determine the optimal combination of RO parameters, MC simulations were performed [154]. The DA schedules for all combinations of Γ_g for 16 and 24 kWh batteries, and θ_b for 10% and 15% price deviation bands are simulated against MC trials. The number of MC trials is set to the min $\{1000,\ N^{\mathrm{MC}}\}$, where N^{MC} is the number of MC trials required to ensure a 95% confidence of an error less than 1% [154]. All combinations of demand robust parameters Γ_g and price robust parameters θ_b were simulated against 32 market price and 32 battery demand profiles, totaling 1024 MC trials.

In order to create price profiles, the difference between the typical curve, shown in Figure 6.3, and the historical data from the PJM market for each time period was calculated, which represents the error. Next, the CDF of the error is obtained for each time period considering the inter-hour correlation. Finally, price profiles are created using the error distribution. The distribution function in Figure 6.4a is used to create the demand profiles.

Figure 6.8 shows the normalized CDFs of the BSS profits for different combinations of robustness parameters. Although the MC simulations were performed for all combination of
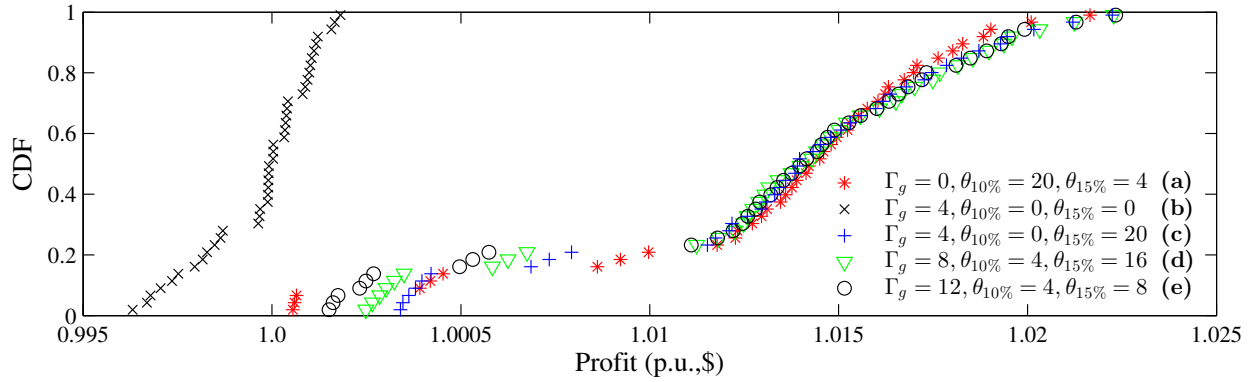
Figure 6.8: CDF for combination of robustness parameters for price and demand.

parameters, only selected CDFs are shown for clarity. Each MC trials' DA profit is obtained for the robustness combination without uncertainty, $i.e.$ $\Gamma_g = 0$ and $\theta_b = 0$, and these profits are used as the base-case, in which all other combination MC trials' profits are normalized against.

In general, the combination that yields the right-most CDF performs best, since it obtains the highest profits. From Figure 6.8, the lower tails of the right-most group of CDFs show differences in profit, where case (c) (labelled in Figure 6.8) yields the highest. However, there is no distinct CDF that can be determined as the optimal combination. This is the case because the right-most CDFs do not yield a large difference in profit for the majority of the MC trials, apart from the lower-tail. Since the right-most CDFs are similar, the BSS has less risk in determining an optimal combination of robust parameters for battery demand uncertainty. Therefore, to analyze the remainder of the results, Γ_g is chosen as 4 for both the 16 and 24 kWh battery groups.

On the other hand, if price uncertainty is ignored as in the case labeled (b) in Figure 6.8, the CDF is the one that has lowest profits (left-most) with some trials' profit below 1 p.u. Therefore, price uncertainty parameters (θ_b) need to be properly chosen otherwise a decrease in profits may occur. To determine θ_b combinations, MC simulations are performed but this time each MC trial is characterized by a fixed demand profile ($N_{g,t}^{\min}$ from Figure
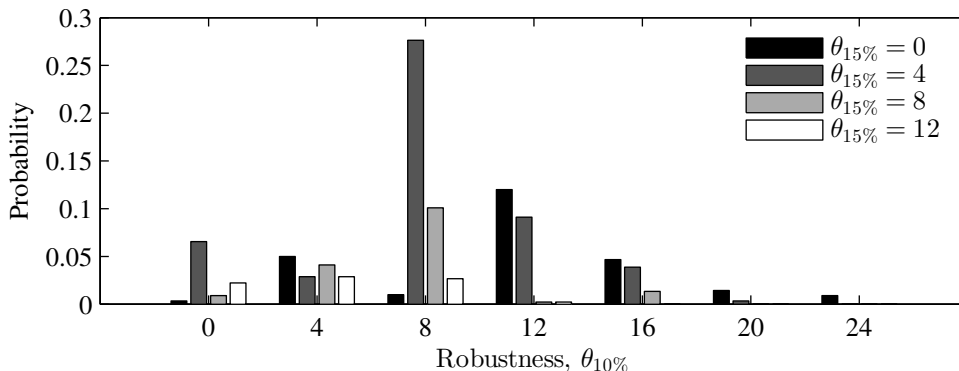
Figure 6.9: Probability of resulting in the highest overall profit for all combinations of $\theta_{10\%}$ and $\theta_{15\%}$.
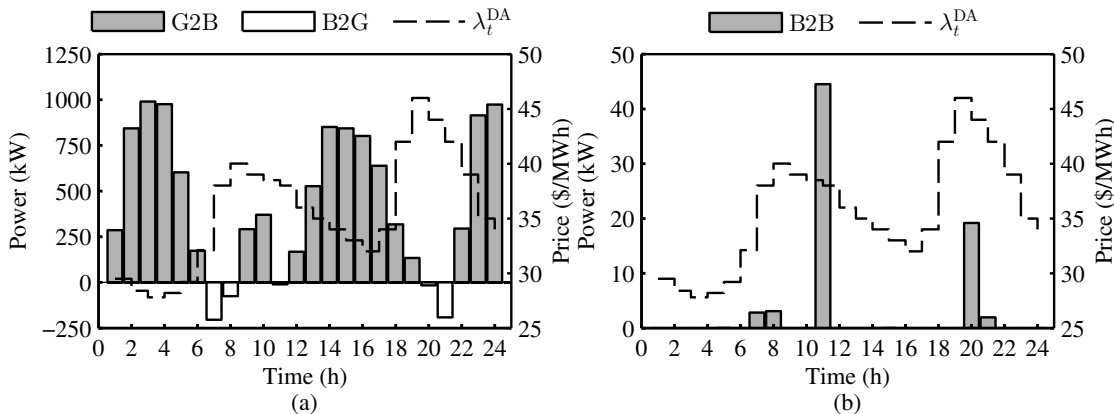
Figure 6.10: G2B and B2G (a), and B2B (b) services in the deterministic case.

6.4b), with different price profiles. The combination of robust parameters that result in the highest overall profit was identified for each MC trial. Figure 6.9 shows the probability of yielding the highest overall profit for different combinations of robustness parameters $\theta_{10\%}$ and $\theta_{15\%}$. The chances of incurring the highest profit for $\theta_{10\%} = 0$ and $\theta_{15\%} = 0$ is less than 1%, because no protection against price uncertainty is used. The optimal combination of $\theta_{10\%}$ and $\theta_{15\%}$ is 8 and 4, which results in probability of 27% for obtaining the highest profits. This combination of price robustness parameters is used while analyzing the remainder of the results.
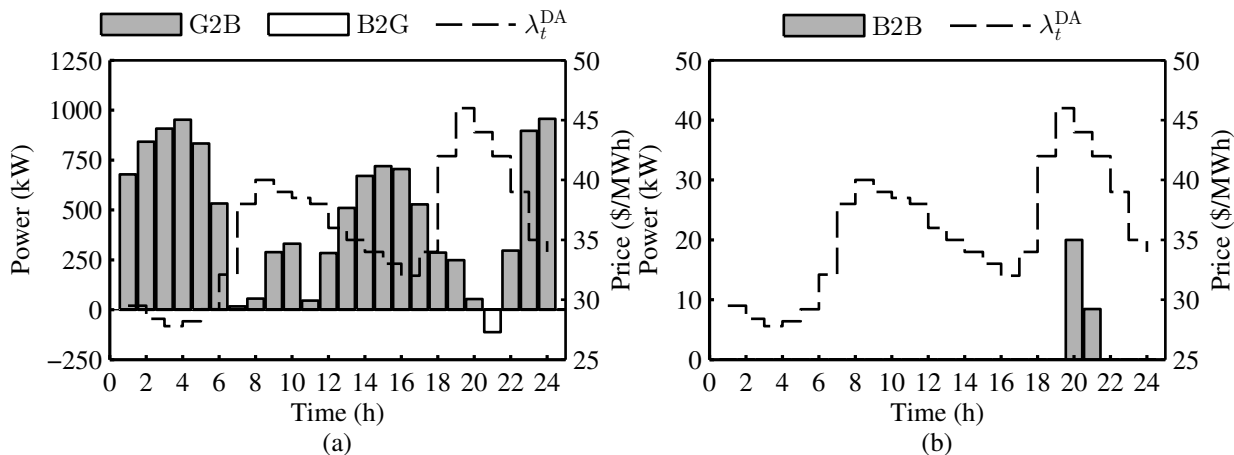
Figure 6.11: G2B and B2G (a), and B2B (b) services in the uncertainty case.

At the DA stage, the BSS determines its energy bidding and offering schedules which are equivalent to G2B and B2G mode, as shown in Figure 6.10a for the deterministic case when battery demand and market price uncertainty are not included. If the market price is high, the BSS sells electricity whereas during the low-price periods it purchases electricity. Figure 6.10b shows the energy transfer between batteries in B2B mode, which occurs during the high-price periods. The figure shows that B2B can occur simultaneously with B2G. Since battery demand and market prices are high during periods in which B2B occurs, the BSS uses stand-by batteries to discharge and charge other batteries. This way, they can be swapped and the remaining energy is sold in the market in B2G mode. B2B mode counteracts electricity to be purchased in G2B mode during the high-price periods. The total electricity scheduled in B2G mode is 499.40 kWh, and in B2B mode is 71.51 kWh.

With market price and battery demand uncertainty included, as shown in Figure 6.11, the BSS is more conservative by purchasing more electricity to supply the uncertain battery demand in G2B mode. Battery demand uncertainty decreases B2G services because the energy that was used for pre-charging batteries to be sold in later periods is instead being used to supply the battery demand. Market price uncertainty also decreases B2G because it limits the electricity that can be purchased at a competitive price during low-price periods.

Both of these effects can be seen in Figure 6.11a where the total energy purchased increases caused by the uncertain battery demand. However, the purchasing is spread between periods in order to minimize losses caused by realization of high prices.

Battery degradation further limits B2G since this service comes at a cost of additional charging in order to discharge later on, which degrades the battery life. From Figure 6.11a, B2G decreases by 77% to 112.56 kWh as compared to the deterministic case. Due to market price uncertainty, B2B decreases by 60% to 28.46 kWh in Figure 6.11b as compared to the deterministic case. The uncertainties decrease B2G and B2B, however it also protects against the worst-case materialization of prices and demand.

In the deterministic case, the total profit over the 24 hour period is \$55,648 and costs are \$352.20, of which \$323.44 correspond to electricity costs and \$28.76 to degradation costs. When considering uncertainty, the profit is \$55,609, while costs are \$421.63, of which electricity costs are \$361.1 and degradation costs are \$30.26. The remainder totaling to \$30.27 indicates the cost of including uncertainty in the model. The profit is lower and losses are higher when considering the battery demand and price uncertainty because the BSS purchases more energy and minimizes the purchases during the low-price periods.

The losses the BSS incurs do not include any discounts in the deterministic and uncertain cases, because the battery demand is met and the excess energy is sold in the market in B2G mode. If cases occur where the battery demand increases, the amount of energy in B2G mode would decrease until only G2B mode takes place at all time periods. Any further increase in the battery demand will require discounts to be given to customers, since the BSS is purchasing at maximum capacity of all the batteries in G2B mode. In the worst case, when even discounts cannot satisfy the demand, then it is because battery stock is too small and $VoCD$ would be incurred by the BSS for each battery not supplied.

6.5   Conclusion

A detailed operating model of the BSS is presented in this chapter. The BSS can schedule batteries to operate in G2B, B2G, or B2B modes. The model employs robust optimization

techniques to manage uncertainty of electricity prices and battery demand. In addition, the effect of battery degradation due to the charging/discharging cycling is taken into account as well as their economic losses.

Results show that accounting for battery demand uncertainty, electricity price uncertainty, and battery degradation costs, decreases B2G and B2B services. Electricity price uncertainty has a major impact on the profits of the BSS and it needs to be managed properly in order to avoid poor economic performance. On the other hand, the impact of battery demand uncertainty is less severe, but proper management of this uncertainty results into better operating strategies for the BSS.

The order of priority for the services that the BSS can perform are dependent on the excess energy, in addition to battery swapping needs, obtained in G2B mode. Then, depending on the market conditions (*e.g.* high energy prices), the BSS schedules some of the batteries to transfer energy to other batteries in B2B mode. Lastly, if there is an economic benefit, the BSS sells the excess energy in B2G mode to the market.

The proposed model and the results that can be obtained by it will:

- help inform stakeholders on the design and operation of BSS stations

- allow more efficient short-run and long-run market decisions that can exploit storage capabilities of the BSS

- enhance the environmental sustainability of the power sector by allowing further introduction of renewable energy sources

Chapter 7

OPTIMAL ENERGY STORAGE MANAGEMENT SYSTEM: TRADE-OFF BETWEEN GRID ECONOMICS AND HEALTH

7.1 Introduction

Energy storage is expected to change the operating paradigm of the power grid. They are expected to be available in EVs providing not only the transportation needs of customers, but also grid services, and available in stationary applications. In all frameworks developed in this work, energy storage was at the forefront. Specifically, battery ES systems consisting of Lithium-ion (Li-ion) chemistries were studied since they are especially poised to provide grid services due to their high power and energy density and relatively low cost per unit of energy.

Research on battery ES systems has typically been segregated into focus on the chemistry and material properties, *e.g.* [115, 116, 117, 118, 119], and focus on the grid integration, operation, and economic performance, *e.g.* Chapters 2-6. This gap is notorious in both the research community and in commercial usage of batteries; especially for grid applications where the DA market-based decision-making tools use simplified models that limit the operations of the battery because cycle-life degradation (capacity fade [118]) and charging/discharging efficiencies are not properly characterized. In addition, empirical/theoretical degradation models developed, *e.g.* [115, 116, 117, 118, 119], are typically highly non-linear and thus introduce computational burden when optimizing over a multi-period time horizon. By combining the economic exploitation of ES systems for grid services with data-driven characterization of chemical properties, the decision-making processes can be improved.

The work in this chapter proposes a data-driven methodology to characterize battery ES systems embedded into a decision-making optimization model. Such data-driven approaches

enable the major battery characteristics along with grid economics to be co-optimized as a MILP, which benefits from low computational burden and optimality. As for characteristics, the ES system undergoes cycle-life degradation as a function of how it is operated in terms of C-rate charging/discharging, *i.e.* amount of energy that is charged/discharged in a certain timestep. Additionally, the internal resistance of the ES system leads to charging/discharging power losses which are also functions of the battery operation. These two mechanisms, variable C-rates and variable efficiencies, are embedded into the model so that batteries may be scheduled at high-power (high C-rate) operations to capture additional grid revenues, only if economical against the cost of adverse effects on the ES system.

The main contributions of this work are:

- A complete MILP optimization model for battery ES systems considering the effect on cycle-life degradation and efficiency based on its operations.

- A data-driven methodology to transform variable C-rate degradation and efficiencies into economic indices to be optimized.

7.2   *Data Analytics of Li-Ion Batteries*

Lithium ion batteries are a popular energy storage technology due to their high energy density and coulombic efficiency. However, the capacity of these chemistries fades over time due to degradative processes occurring alongside the main electrochemical reactions [175]. This capacity fade determines the usable lifetime of the batteries and is a function of how that battery is operated. In addition to the long-term capacity fade of these batteries, the internal (ohmic) resistance of the cells leads to power losses during charging/discharging. These losses affect the coulombic efficiency of the battery and are also a function of the battery's operation [176]. To improve the accuracy of the optimization of this ES system, the effects of battery operation on the cycle-life and efficiency are considered.
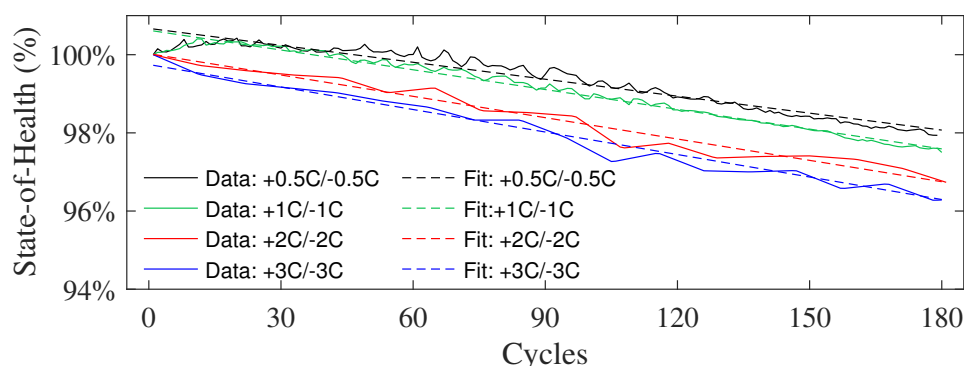
Figure 7.1: SoH measurements of a Samsung INR18650 Li-ion battery cell at various C-rates.

7.2.1 Variable C-rate degradation mechanism

Lithium-ion batteries undergo cycle-life degradation as a function of increased C-rates [118]. C-rate is defined as the charging/discharging current normalized by the current which would charge/discharge the nominal capacity of the battery in an hour, *e.g.* +1C and +3C are equivalent to charging the battery in 1 hour and 20 minutes, respectively.

In order to obtain representative cycle-life characteristics, Li-ion nickel-manganese-cobalt (Li-NMC) batteries, specifically 1.5 A-hr Samsung INR18650 cells [177], were cycled continuously at specified C-rates using a Maccor 4300M battery cycler [178]. In this context, a cycle is defined as a full constant current constant voltage (CC-CV) charge and constant current (CC) discharge using the manufacturer supplied voltage limits (2.5V to 4.2V with a 100mA cutoff for CV charging [177]). The capacity of the cells was measured every 10 cycles with a ±0.5C cycle for each of the C-rates studied. Fig. 7.1 shows the cycle-life degradation of the Samsung INR18650 at ±0.5C, ±1C, ±2C, and ±3C. From Fig 7.1, it can be seen higher C-rate operations lead to larger decreases in state-of-health (SoH) of the battery. Note that this process can be applied to any battery chemistry.
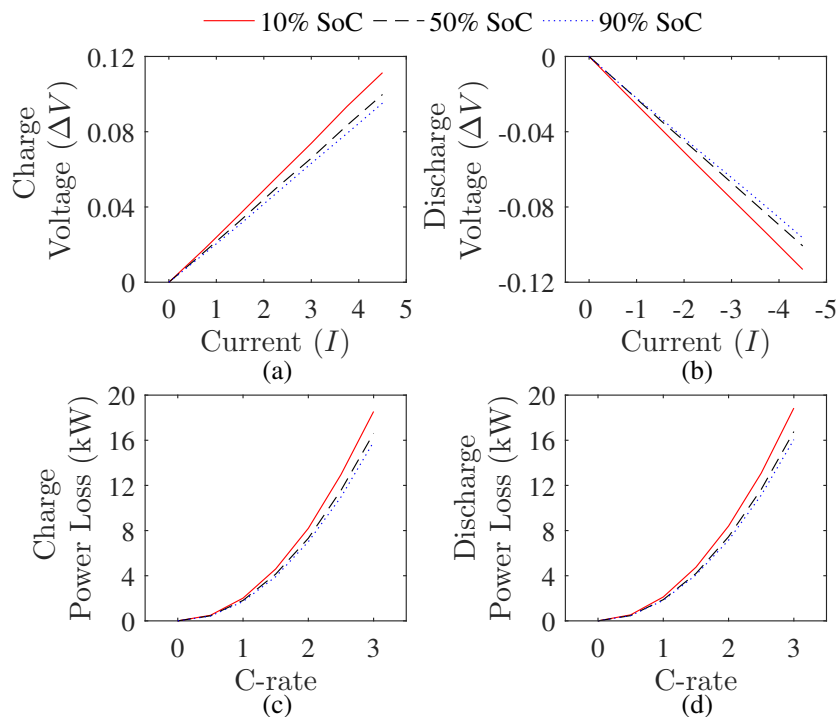
Figure 7.2: The charge and discharge voltage deviation (ΔV) shown in (a) and (b), respectively, for a single cell Li-ion battery. The charging and power losses are shown in (c) and (d), respectively, for an ES system with 200 kWh capacity.

7.2.2   Variable efficiency mechanism

The internal resistance of the electrodes and electrolytes within Li-ion battery chemistries lead to heat dissipation, which is correlated to power losses when charging or discharging the battery [121, 116]. Such power loss can be mathematically written as $P^{\text{loss}} = \Delta V \cdot I$, where a positive current $I > 0$ means the battery is charging. Furthermore, as I increases/decreases, the voltage sees an immediate change, as captured by the voltage drop ΔV.

ΔV is related to the current I by the internal resistance of the cell, *i.e.* higher currents lead to higher voltage drops. The following step-by-step process is applied to measure ΔV as a function of the current I and state-of-charge (SoC) in order to obtain the charging power

losses using an Autolab PGSTAT128N potentiostat[1] [179]:

1. Slowly charge/discharge the battery to specified SoC.
2. Induce current I to the battery cell
3. Measure the instantaneous (0.01 sec) voltage drop ΔV
4. Calculate power losses for the ES system, *i.e.* $P^{\text{loss}} = n \cdot \Delta V \cdot I$, where n is the number of Li-ion batteries used in the ES system.
5. Repeat step 1 with a new SoC level

The same rational follows for measuring the discharging power losses, however, instead current is withdrawn from the battery, *i.e.* $I < 0$. Fig. 7.2 shows the measured voltage drop for charging and discharging in (a) and (b), respectively, and the corresponding calculated power loss for charging and discharging in (c) and (d), respectively, as well.

7.3 Energy Storage Optimization

The ES system optimal charging/discharging model is developed by first introducing the standard model, and then embedding variable C-rate degradation and efficiency mechanisms to improve the operations.

7.3.1 Standard model

The objective function minimizing the costs of operating the ES system is formulated as follows

$$\min \quad \Delta t \cdot \sum_{t \in \mathcal{T}} \tau_t \cdot \left(p_t^{\text{ES+}} - p_t^{\text{ES-}} \cdot \eta^- \right) \tag{7.1}$$

where Δt is the time step, τ_t is the price of electricity, $p_t^{\text{ES+}}$ is the charging power, and $p_t^{\text{ES-}}$ is the discharging power of the ES system with η^- discharge efficiency.

---

[1]A potentiostat is an instrument that measures and controls the voltage difference between two electrodes.

The objective function (7.1) is subject to several constraints (7.2)-(7.6). The energy state-of-charge (SoC) of the ES system is tracked over time t and is formulated as

$$soc_t^{\text{ES}} = soc_{t-1}^{\text{ES}} + \Delta t \cdot p_t^{\text{ES}+} \eta^+ - \Delta t \cdot p_t^{\text{ES}-} \quad \forall t \in \mathcal{T} \tag{7.2}$$

where soc_t^{ES} is the SoC of the ES system. The current periods's SoC soc_t^{ES} as shown in (7.2) is dependent on its previous period's SoC, the amount of energy charged by the battery $\Delta t \cdot p_t^{\text{ES}+}$ with η^+ charging efficiency, and the amount of energy discharged by the battery $\Delta t \cdot p_t^{\text{ES}-}$. The SoC, however, must be within bounds and is formulated as

$$0 \leq \underline{SoC}^{\text{ES}} \leq soc_t^{\text{ES}} \leq \overline{SoC}^{\text{ES}} \leq BC^{\text{ES}} \quad \forall t \in \mathcal{T} \tag{7.3}$$

where BC^{ES} is the rated capacity of the ES system, and $\underline{SoC}^{\text{ES}}$ and $\overline{SoC}^{\text{ES}}$ are the minimum and maximum useable SoC, respectively. The SoC must lie below the rated capacity to avoid the risk of fire, whereas it must also lie above zero to avoid rapid degradation [127]. In addition to the SoC being within limits, the charging and discharging powers must also be within limits, which is expressed as

$$0 \leq p_t^{\text{ES}+} \leq \overline{P}^{\text{ES}} \cdot x_t \quad \forall t \in \mathcal{T} \tag{7.4}$$

$$0 \leq p_t^{\text{ES}-} \leq \overline{P}^{\text{ES}} \cdot (1 - x_t) \quad \forall t \in \mathcal{T} \tag{7.5}$$

where $\overline{P}^{\text{ES}}$ is the maximum power of the ES system. The charging and discharging actions, however, cannot occur simultaneously as managed by binary variable x_t, *i.e.* if $x_t = 1$ then $p_t^{\text{ES}+}$ is enabled, otherwise $p_t^{\text{ES}-}$ is enabled. Constraint (7.6) ensures the energy available in the ES at the start of the day is at least recouped by the end of the day.

$$soc_{t=|T|}^{\text{ES}} \geq SoC_{t=0}^{\text{ES}} \tag{7.6}$$

7.3.2   *Variable C-rate degradation*

7.3.2.1   *Piecewise degradation model*

A piecewise approximation of the variable C-rate degradation shown in Fig. 7.1 is performed to ensure the optimization considers continous C-rates, *i.e.* it is assumed the degradation at
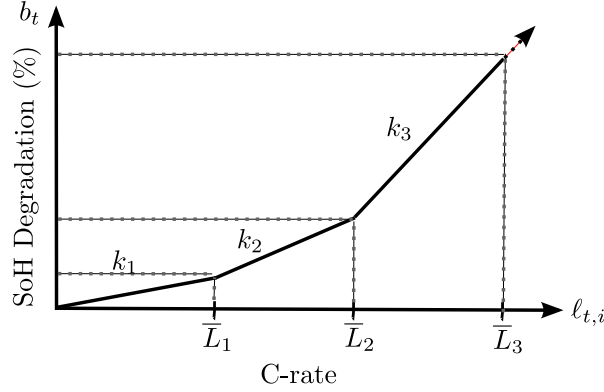
Figure 7.3: Piecewise approximation of the SoH degradation as a function of C-rates the ES system charges or discharges at in period t.

± 2.5C falls within the pre-measured ± 2C and ± 3C curves.

To develop the piecewise curves, linear fits are done on the data as shown in Fig. 7.1, and their respective slopes, k, with units of $\frac{\%}{cycle}$ degradation are determined. Next, with these slopes, a piecewise linear curve is created with multiple blocks i as shown in Fig. 7.3, where each block includes the slope of the piecewise curve k_i and a C-rate maximum for that block $\overline{L}_i$. The outcome of Fig. 7.3 is the percent degradation on the battery state-of-health (SoH). This curve is embedded into the DA optimization to determine the optimal C-rate operation in each period t.

7.3.2.2   DA optimization model

The optimization considering variable C-rate degradation has the objective (7.7), while similar to (7.1), includes an additional term determining the degradation costs and is formulated as

$$\min \quad \Delta t \sum_{t \in \mathcal{T}} \tau_t \cdot \left(p_t^{\text{ES}+} - p_t^{\text{ES}-} \cdot \eta^- \right) + C^{\text{ES}} \cdot BC^{\text{ES}} \cdot \sum_{t \in \mathcal{T}} b_t \tag{7.7}$$

where C^{ES} and BC^{ES} is the price and capacity of the ES system, respectively, and b_t is the percent state-of-health (SoH) loss due to cycling of the battery in period t. For example, if

in a period t, the SoH loss is 1% ($b_t = 0.01$), then the degradation cost is 1% of the purchase cost of the ES system.

The objective function (7.7) is subject to constraints (7.2)-(7.6) in addition to the following constraints. Constraints (7.8) and (7.9) capture the amount of energy charged or discharged, respectively. For example, in (7.8), $soc_t^{\text{ES+}}$ will be greater than 0 if the SoC in the current period t increases from the previous period $t-1$, $i.e.$ it is in the charge cycle. The same rationale applies to the discharge cycle with equation (7.9).

$$soc_t^{\text{ES+}} \geq soc_t^{\text{ES}} - soc_{t-1}^{\text{ES}} \quad \forall t \in \mathcal{T} \tag{7.8}$$

$$soc_t^{\text{ES-}} \geq soc_{t-1}^{\text{ES}} - soc_t^{\text{ES}} \quad \forall t \in \mathcal{T} \tag{7.9}$$

The next set of constraints (7.10) and (7.11) determines the how much the battery is cycled in period t. In (7.10), the amount cycled, defined as the total energy over the rated capacity in a period, is matched to the piecewise C-rate $\ell_{t,i}$ in each block i. In other words, it is attempting to determine where on the x-axis of Fig. 7.3 the ES C-rate lies. The C-rate in each block $\ell_{t,i}$, however, must be within the maximum pre-defined C-rates, $\overline{L}_i$, in each block i as shown in Fig. 7.3. As an example, if an ES system is rated at 200 kWh with a max power of 600 kW ($i.e.$ equivalent to a 3C rate), then to achieve a 1C rate in a time interval of $\Delta t = 15$ min, the ES system must charge at 200 kW resulting in 50 kWh entering the battery and thus performing one-fourth of a cycle. This process is determined in equation (7.10)-(7.11).

$$\Delta t \cdot \sum_{i \in I} \ell_{t,i} = \frac{soc_t^{\text{ES-}} + soc_t^{\text{ES+}}}{BC^{\text{ES}}} \quad \forall t \in \mathcal{T} \tag{7.10}$$

$$\ell_{t,i} \leq \overline{L}_i \quad \forall i \in \mathcal{I}, t \in \mathcal{T} \tag{7.11}$$

To obtain the SoH degradation b_t (as shown in Fig. 7.3) due to cycling of the battery at C-rate $\ell_{t,i}$, constraint (7.12) is used as shown below

$$b_t = \sum_{i \in I} \frac{k_i}{100} \cdot \ell_{t,i} \quad \forall t \in \mathcal{T}. \tag{7.12}$$

7.3.3   Variable efficiency

7.3.3.1   Charging/discharging power loss model

The charging and discharging power losses, shown in Fig. 7.2(c) and Fig. 7.2(d), respectively, can be modelled quadratically as a function of C-rate and SoC. To preserve tractability and linearity under a linear optimization framework, the power losses are averaged over all SoCs, such that they are recast into quadratics as a function of C-rate. This allows the recasted quadratics to be approximated using special-ordered-sets-of-type 2 (SOS2) [123, 180], which is discussed in detail in Appendix B.

The charging $\alpha_t^{\text{ES+}}$ and discharging $\alpha_t^{\text{ES-}}$ power losses, as a function of C-rate, are modelled as:

$$\alpha_t^{\text{ES+}} = a^+ \cdot \left(\frac{soc_t^{\text{ES+}}}{BC^{\text{ES}}} \right)^2, \quad \alpha_t^{\text{ES-}} = a^- \cdot \left(\frac{soc_t^{\text{ES-}}}{BC^{\text{ES}}} \right)^2 \tag{7.13}$$

where a^+ and a^- are the second-degree polynomial coefficients for charging and discharging, respectively. As the charging/discharging C-rates increase in a period t, the power losses quadratically increase which can also be seen as variable efficiencies of the ES system. These functions are embedded into the DA optimization to schedule the ES system.

7.3.3.2   DA optimization model

The objective function considering variable efficiencies is formulated as follows

$$\min \quad \Delta t \cdot \sum_{t \in \mathcal{T}} \tau_t \cdot \left(p_t^{\text{ES+}} - \left[p_t^{\text{ES-}} - \alpha_t^{\text{ES-}} \right] \right) \tag{7.14}$$

where the term $\left[p_t^{\text{ES-}} - \alpha_t^{\text{ES-}} \right]$ represents the total power sold to the grid in period t including the variable discharging losses ($\alpha_t^{\text{ES-}}$ obtained from the process in Section 7.2.2). Compared to the standard ES system model in Section 7.3.1 where power losses are modelled by fixed efficiency percentages, *i.e.* η^+ and η^-, in this case efficiency is modelled indirectly as $\eta^+ = \left(p_t^{\text{ES+}} - \alpha^{\text{ES+}} \right) / \overline{P}^{\text{ES}}$ and $\eta^- = \left(p_t^{\text{ES-}} - \alpha^{\text{ES-}} \right) / \overline{P}^{\text{ES}}$. The objective function is subject to
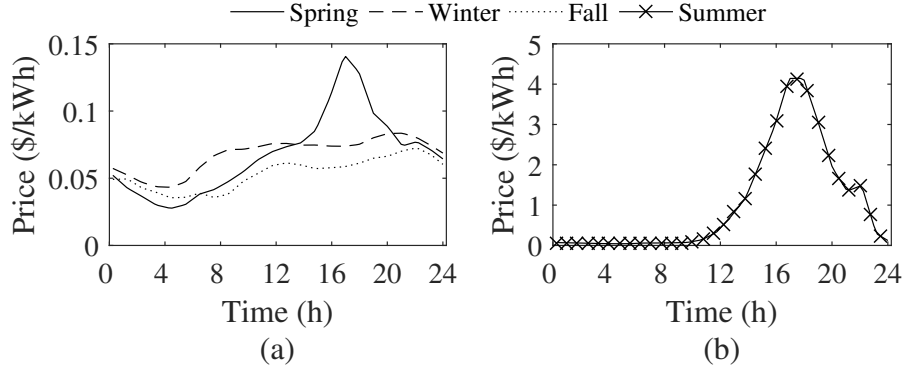
Figure 7.4: RTP tariffs based on time of the year and weather, *i.e.* normal or high temperatures, obtained from [2].

(7.3)-(7.6) in addition to

$$soc_t^{ES} = soc_t^{ES} + \Delta t \cdot \left(p_t^{ES+} - \alpha_t^{ES+} \right) - \Delta t \cdot p_t^{ES-} \quad \forall t \in \mathcal{T} \tag{7.15}$$

Constraint (7.15), similar to equation (7.2), updates the SoC in period t considering the charging power losses α_t^{ES+}. The quadratic terms α_t^{ES-} and α_t^{ES+} render the optimization problem to be non-linear. These terms are linearized using the technique of special ordered sets-of-type-2 (SOS2). The interested reader is encouraged to refer to Appendix B.

7.4   Case Study

The ES system optimization model was solved for an operating day of 24 hours, with a timestep Δt of 15-min. The ES system was subject to retail real-time electricity tariffs obtained from Southern California Edison [2], which are based on outdoor temperatures in the region during a day. Using data from [2], representative price curves were categorized for the seasons of spring, winter, fall and summer shown in Fig. 7.4.

The ES system is rated at 200 kWh, which is compromised of 37,000 Samsung INR18650 cells rated at 3.6 V and 1.5 Ah each [177]. The ES power rating was taken as 600 kW allowing it to perform up to ±3C rates. The measured data for the Samsung INR18650's cycle-life degradation is shown in Fig. 7.1 and its charge and discharge power losses are shown in Fig.
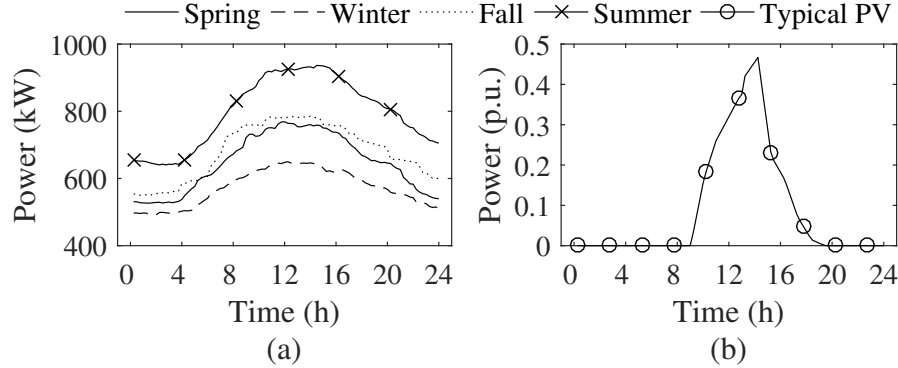
Figure 7.5: Typical base demand in the winter, spring, summer, and fall seasons shown in (a), and power output of PV (p.u.) shown in in (b).

7.2(a) and Fig. 7.2(b), respectively. The measured cycle-life degradation data in Fig. 7.1 was transformed into a piecewise approximation, as shown in Fig. 7.3, that consists of four blocks with degradation slopes of $k_i = [0.0145, 0.016, 0.0182, 0.0192] \frac{\%}{cycle}$ and pre-set C-rates of $L_i = [0.5, 0.5, 1, 1]$, where $\sum L_i = 3C$. As an approximation, it is assumed charge and discharging both have equal effect on degradation, thus the measured degradation slopes are halved, *i.e.* $k_i = \frac{k_i}{2}$. The round-trip efficiency is set to 95%, if variable efficiencies are not considered. The ES price was set to 300 \$/kWh unless otherwise specified.

7.4.1 ES system operations

7.4.1.1 Illustrative example

The effect of variable C-rate and efficiency mechanisms on the power schedule of the ES system is shown in Fig. 7.6 as an example for the spring tariff. In Fig. 7.6(a), the optimal schedule is shown in which both variable C-rate degradation and efficiencies are not considered. On the other hand, Fig. 7.6(b) shows the optimal schedule where both mechanisms are included in the optimization. In Fig. 7.6(a), the optimization exploits the low- and high-price periods at close to maximum power. This occurs because the total arbitrage profit is increased if energy is obtained at the lowest price and then sold at the highest price. On the
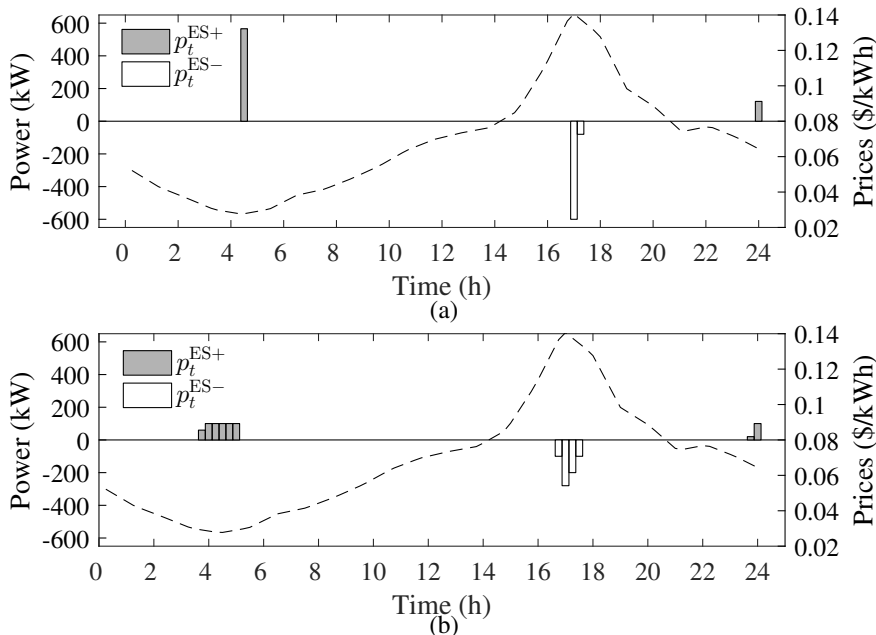
Figure 7.6: ES system's DA power schedule in (a) and (b) for the case where variable C-rate and efficiency mechanisms are ignored and considered, respectively.

other hand, in Fig. 7.6(a) when both mechanisms are considered, the high C-rate behavior is sub-optimal because it causes increased degradation (see Fig. 7.1), and thus the C-rate is maintained below ± 1C (below 200 kW in a period) to operate at the least cost. However, in the high-price region (1615-1730) the ES system increases beyond -1C for discharging, because the revenue collected from the grid is higher than the incurred degradation cost. Although, this increase beyond -1C (-200 kW) is still significantly lower than in Fig. 7.6(a).

The power schedules shown in Fig. 7.6 have a profound effect on both the monetary benefits and cycle-life loss of the ES system. For cycle-life loss, 0.0145% compared to 0.0127% is experienced by the ES system during the operating day when the mechanisms are ignored and included in the model, respectively. The mechanisms increase the effective lifetime of the ES system. In Fig. 7.6(a), such a power schedule has adverse monetary effects, where the potential grid revenue is reduced by the actual cost of degradation that is not modelled. In this case, the grid revenue totals $17.73 for the operating day. However, the actual cost of
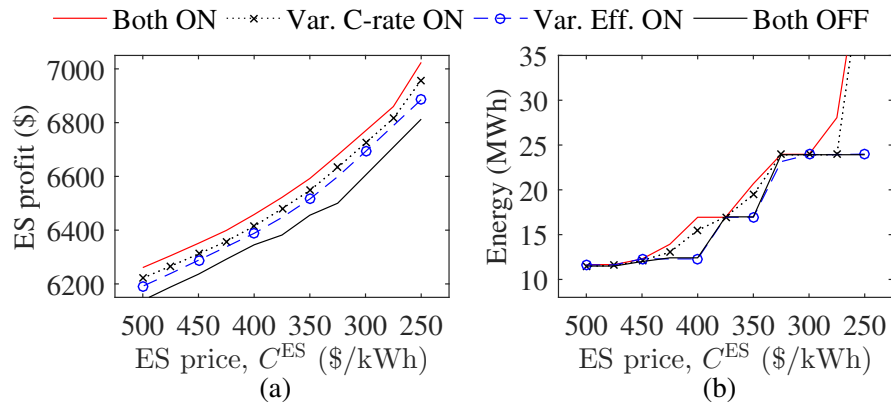
Figure 7.7: Yearly profit potential of the ES system in (a) and yearly energy discharged in (b) while the ES price is varied.

degrading the ES system is $8.71 thus leaving an actual profit of $9.02. On the other hand, with both mechanisms in Fig. 7.6(b), the revenue is $17.47 with a degradation cost of $7.62, and thus a profit of $9.85. It can be seen the revenue is higher in the Fig. 7.6(a) compared to Fig. 7.6(b) because high C-rate operations are favored. However, the actual degradation cost is also higher. Therefore, it is beneficial to operate the system with both mechanisms because profits are increased from $9.02 to $9.85, and SoH loss is decreased.

7.4.1.2 Yearly profit with ES system mechanisms

Using the realistic real-time tariffs for each day based on the time of the year (see Fig. 7.4(a)), the yearly profit potential and discharge energy of the ES system is explored while varying the ES price from 500 $/kWh to 250 $/kWh. The results are shown in Fig. 7.7, where (a) shows the the yearly profits and (b) shows the total discharge energy. The yearly profit and discharge energy are shown for four cases: 1) both mechanisms ON, 2) only variable-C rate degradation ON, 3) only variable efficiency ON, and 4) both mechanisms OFF.

As the ES price decreases from 500 to 250 $/kWh, both profits and discharge energy to the grid increase. This is the case because the potential grid revenues outweigh the degradation costs, which are a function of ES price. For any given ES price in Fig. 7.7(a),

using both mechanisms generates the maximum profit and deactivating both generates the least. In between these profit curves are the cases where only one mechanism (variable C-rate degradation or efficiency) is ON. When only variable C-rate mechanisms is ON, it obtains higher profit than compared to when variable efficiency is ON. This is because high C-rate operations cause a decrease in SoH (see Fig. 7.1) resulting in high degradation costs. Consequently, according to Fig. 7.2, the efficiency of the ES system is quadratic function of the C-rate. Therefore, by lowering the C-rates to preserve the SoH, consequently, the efficiency is also improved. However, if variable efficiency is only ON, then it under-performs because while it does reduce high C-rates, it does not characterize the degradation costs.

For the total discharge energy shown in Fig. 7.7(b), the case where both mechanism are OFF and only variable efficiency is ON, provide the same energy discharge to the grid. When both mechanisms are OFF, the optimization exploits charging/discharging at high C-rates to maximize profit with usage of the standard fixed efficiencies. To this point, however, the profits are smaller when both mechanisms are OFF as shown in Fig. 7.7(a). This occurs because the quadratic power losses shown in Fig. 7.2 are inherently affecting the ES system but ignored in the model. Additionally, activation of both mechanisms optimally schedules the most energy and achieves the maximum profits.

In summary, it is of benefit to implement both mechanisms in the ES system model so that maximum energy is provided for grid services and maximum profit is generated in return.

7.5   *Conclusion*

In this chapter, an optimal decision-making model was developed to perform tradeoff between potential grid revenue that can be collected and the effect of degrading the battery. This model used a data-driven methodology to consider the effect of variable C-rate operations on both the cycle-life and charging/discharging efficiencies of the system. By considering the effect of variable C-rates, the grid revenue potential is increased significantly while considering the effect on the state-of-health and efficiencies. The implementation of the mechanisms

on a day-to-day basis may require revamped hardware, *e.g.* inverters, to manage the high C-rate operations. On a yearly basis, results show a 3.1% improvement on the potential profits of the ES system using the improved optimization model.

The proposed model and the results that can be obtained by it will:

- allow economic exploitation beyond the current operating paradigm of ES systems in grid-scale and EV applications,

- enabled in-depth economic analysis to be performed on the viability of ES systems, and

- allow further introduction of renewable energy sources since ES systems are operated in a more optimal manner.

Chapter 8

CONCLUSION

EVs are poised as alternatives to traditional internal combustion engine vehicles due to using electricity as opposed to gasoline for transportation. EVs can be used to provide a plethora of grid services by charging and discharging their batteries and in return, the owners can receive revenue. To take advantage of EVs as grid resources, however, their needs to be widespread adoption. In the current market, potential consumers may be hindered due to range anxiety, slow charging times, lack of public infrastructure, and upfront costs in regards to owning an EV. With the proposed frameworks developed in this dissertation, the effect of these issues is decreased and thus can assist the adoption of EVs in the market. The frameworks developed are summarized below:

1. In the first framework developed in Chapter 2, a decentralized methodology is developed in which an aggregator can obtain demand response from consumers with calculated monetary incentives. The consumers optimize their load schedules based on a set of incentives. The aggregator then runs an optimization to determine the least-cost allocation of demand response to meet certain objectives. Results show the aggregator can effectively control EV consumers with proper incentives, however, it needs to consider the rebound of the loads in future periods of the day as that may cause issues in the grid. In addition, large benefits were obtained in terms of avoided costs in the distribution grid. Overall, this methodology can be applied to any scenario where a hierarchical agents desires control of a large fleet of consumers loads, *e.g.* EVs and appliances.

2. In the second framework developed in Chapter 3, the aggregator's operating and busi-

ness framework is further developed at the residential sector. As the EV penetration grows, they are expected to obtain their energy from their homes which are connected to pole-top distribution transformers. This will cause accelerated aging of the transformer assets. An aggregator, on behalf of the DSO or it can be the DSO itself, can manage the EV charging/discharging behavior to ensure transformer life aging is minized. Results show that by managing the tradeoff between EV revenue potential from energy arbitrage and the transformer aging, the potential aging can be maintained at expected values and in some cases, it can even be further improved. The incentives-based framework developed in Chapter 2 can be implemented with this framework to motivate EV owners to participate.

3. In the third framework developed in Chapter 4, a model is developed that optimizes the bidding/offering strategy for a fleet of EVs managed by an aggregator in both the day-ahead energy and regulation markets, while considering the cost of degrading EV batteries. The results showed that an aggregator, even while considering battery degradation, obtained a profit on a day-to-day basis. In addition, the avoided costs to the power system was significant if EVs bid/offer into the markets since some traditional power plants were not required to cycle. Such a framework, partnered with the first developed framework of incentives, provides an approach to generate revenue for consumers on a day-to-day basis to offset the upfront costs of owning an EV.

4. In the fourth framework developed in Chapter 5, the focus was on the charging infrastructure, specifically charging stations. These stations' power profiles are both large in magnitude and volatile. A local power utility, from which they are expected to obtain such energy, may not be able to supply it at the minimal cost. In this context, an aggregator manages an ensemble of charging stations to participate in wholesale electricity markets in order to reduce operating costs. Results show that the aggregator can provide significant cost savings, while also taking into consideration uncertainties in market prices and the volatile demand needs of the stations.

5. In the fifth framework developed in Chapter 6, a similar hierarchical entity is developed like the aggregator that takes advantage of EV batteries to generate profits. This entity is a battery swapping station that alleviates issues of range anxiety, slow charging times, and lack of public infrastructure. Specifically, the role of a battery swapping station is to swap consumers' depleted EV battery with fully-charge ones from its battery stock. In return, consumers pay for this swap similar to a traditional gasoline station. The swapping station optimizes its operations to take advantage of the EV battery stock it owns to meet consumer demand and bid/offer into the energy market.

6. A common element in Chapters 2-6 is energy storage, either mobile in EVs or stationary. In the sixth framework developed in Chapter 7, a data-driven methodology and an optimal decision-making tool is developed to exploit energy storage to its fullest potential. In this chapter, energy storage systems are exploited to perform at high-power (high C-rate), while characterizing the adverse degradation effects via two mechanisms: 1) effect of variable C-rate degradation on life cycle-loss, and 2) effect on the charging/discharging efficiencies. These mechanisms are characterized with by a data-driven methodology which includes real-life testing of Li-ion batteries. Then, these mechanisms are transformed into economic costs along with the potential grid revenues and a tractable optimization model is developed. Results show additional grid revenues are obtained with these improved models when performing energy arbitrage, while considering the cost of degradation. When applied, the additional revenue obtained from the improved model can reduce upfront costs, and allow fast-charging capabilities while considering its effect on degradation.

These frameworks provide solutions to assist further EV adoption. Several entities will benefit from such frameworks which are discussed in the following subsection.

8.1 Beneficiaries of the developed frameworks

The developed frameworks, while orientated towards the research community, also provides numerous benefits to others, *e.g.* the industry. The benefits of these frameworks to different entities are summarized below:

- **Research community**: the frameworks can lay groundwork for future research undertaken by universities, laboratories, and the industry. Further research is required to tackle the four main issues with EVS: range anxiety, slow charging times, infrastructure, and upfront costs.

- **Industry**: the industry can develop technologies employing the principles in these frameworks. The industry is split into three sub-groups and benefits of each are explained further.

  - Power Industry: the power grid player, *e.g.* utilities, system operators, among others, may use these frameworks as a basis to understand the challenges and benefits EVs bring to the grid. The frameworks can quantify these benefits so that changes can be made to the current operating paradigm to more easily accept EVs.

  - Large Companies: The developed frameworks require new products to be developed, *e.g.* management systems, smart appliances, among others. Companies can use these frameworks to understand the type of products that must be developed. For example, one of the underlying assumptions in these frameworks is that all the EVs are equipped with V2G technology and without such technology, discharging of the battery is not possible. This is one such technology the large players in the technology industry may develop so that the power grid and consumers can benefit.

  - Startups: the power grid industry will see new startups enter the market that will introduce innovative technologies and business models to the power grid. Many

of these startups are currently and will in the future focus on the advent of EVs. These frameworks can provide a starting reference for these startups.

- **Investors**: for these frameworks to be deployed in the real-world, large investments will be required. Investors can use these frameworks as guidelines to understand the revenue potential of such businesses.

8.2 Suggestions for future work for other researchers

In this section, a few ideas are discussed to further use EVs as grid resources.

- With regards to aggregator business and operating model frameworks developed in this dissertation (see Chapter 2-5), it was assumed that the arrival, departure, and travel time of EVs were known with 100% certainty. This was assumed because if a large enough fleet of EVs are considered then the uncertainties would be small. However, uncertainty management techniques should be developed for proper characterization and to determine the full revenue potential.

- In all power systems, ancillary services are important for the well-being of the system. However, such services have usually been provided from the supply side as opposed to the demand side. As the demand side becomes more flexible, they are poised to provide such services. The works in Chapters 2, and 5-7 only considered energy arbitrage as a primary revenue stream from wholesale markets. However, additional revenue can be obtained by participating in the ancillary markets, *e.g.* secondary regulation, as was shown in Chapter 4 with an aggregated fleet of EVs. Further work is required to cater the frameworks to optimize the bidding and offering strategy in the ancillary markets as well.

- An aggregator provides many opportunities for EVs and the power grid to benefit. It is expected, however, that many aggregators will co-exist in a system. Therefore,

questions remain unanswered on the revenue potential when numerous aggregators are participating in wholesale markets. Also, it is unknown the impact of several aggregators on distribution grid assets, since each aggregator may have different objectives that may not align to meet a certain global objective.

- As for EV infrastructures, further work is needed on the optimal allocation of combined battery swapping and charging stations in a city. It is expected that a swapping station will be more expensive in terms of infrastructure as opposed to a charging station. Therefore, their is a tradeoff on the number of swapping verses charging stations, while considering EVs' driving behavior. Such work can assist city planners determine where, how many, and type of stations to install.

Appendix A

MIXED-INTEGER LINEAR PROGRAMMING (MILP)

An integer program is a mathematical optimization in which some or all variables are integers. A MILP is a sub-problem of integer programming where some variables are allowed to be continuous while others integer. The work in this dissertation uses MILP as a tool to find optimal solutions to problems.

A typical MILP problem can be formulated as follows:

$$\text{minimize} \quad c^T \cdot x \tag{A.1}$$

subject to

$$A \cdot x = b \tag{A.2}$$

$$l \leq x \leq u \tag{A.3}$$

where c^T and b are vectors, A is a matrix, and l and u are the lower and upper bound vectors on variable x. In this model, some or all of x must take on integer values, which may be in the form of binary $\{0,1\}$. A typical MILP problem can have several equality and inequality constraints to model real-life applications.

A.1   General Algebraic Modeling System (GAMS)

GAMS is a high-level programming language that connects to solvers to perform mathematical optimization [180]. In this dissertation, GAMS is used to develop the model and then passed onto the solver, IBM CPLEX [181], which obtains the MILP solution.

The feasibility gap of all the MILP problems are set to less than 0.01% to obtain an optimal solution.

Appendix B

LINEARIZATION TECHNIQUES

B.1 Special Ordered Sets of Type 2 (SOS2)

MILP problems require linearity in equations. However, by introducing variables and constraints, the SOS2 technique can piecewise approximate functions, *e.g.* x^2, x^3, $x \cdot y$, among others, in order for them to be present in MILP problems.

This technique will be demonstrated on the framework developed in Chapter 2. From the power flow constraints in Chapter 2, equation (2.5) is non-linear and must be linearized and must be linearized in order to obtain an optimal solution under the MILP framework. For simplicity, the indices are removed from equation (2.5) and thus can be written as:

$$\ell \geq \frac{(p^{\text{flow}})^2 + (q^{\text{flow}})^2}{e} \tag{B.1}$$

The following steps are taken to simplify equation (B.1):

$$e \cdot \ell \geq (p^{\text{flow}})^2 + (q^{\text{flow}})^2 \tag{B.2}$$

Where the term $e \cdot \ell$ can be represented quadratically as:

$$e \cdot \ell = \frac{(e + \ell)^2 - e^2 - \ell^2}{2} \tag{B.3}$$

By combining equation (B.2) and (B.3), the simplified equation is represented as:

$$\frac{(e + \ell)^2 - e^2 - \ell^2}{2} \geq (p^{\text{flow}})^2 + (q^{\text{flow}})^2 \tag{B.4}$$

The terms $(e+\ell)^2$, e^2, ℓ^2, $(p^{\text{flow}})^2$, and $(q^{\text{flow}})^2$ are non-linear and are linearized via SOS2 [123, 180]. For simplicity, the process to linearize $(e+\ell)^2$ is shown. The same rationale applies to the remaining non-linear terms. The SOS2 technique is used for modelling piecewise

approximations of functions of a variable. The piecewise linear approximation is defined by the x- and y-coordinates (O_m, Y_m) of M points, with $m = 1, ..., M$. Note that with M points there are $M - 1$ piecewise segments. This is modelled as follows:

$$\sum_{m=1}^{M} O_m \cdot \theta_m = (e + \ell) \tag{B.5}$$

$$\sum_{m=1}^{M} Y_m \cdot \theta_m = \rho \tag{B.6}$$

$$\sum_{m=1}^{M} \theta_m = 1 \tag{B.7}$$

These three equations involve only two unknowns: θ_m, ρ. On the other hand, $(e + \ell)$ is known. O_m are the preset values that linearly map to $(e + \ell)$. The value ρ represents the approximate value of $(e + \ell)^2$, which is linearly mapped by the preset values Y_m. The continuous variable θ_m is used to determine over which points the value is within. However, to guarantee the non-zero θ_m variables correspond to only two adjacent points, additional constraints are required:

$$\theta_1 \leq \mu_1 \tag{B.8}$$

$$\theta_m \leq \mu_m + \mu_{m-1} \quad \forall m \in 2 \ldots M - 1 \tag{B.9}$$

$$\theta_M \leq \mu_{M-1} \tag{B.10}$$

$$\sum_{m=1}^{M-1} \mu_m = 1 \tag{B.11}$$

Where μ_m is a binary variable, such that $\mu_m = 1$ if $(e + \ell)$ lies within two points representing a segment, and $\mu_m = 0$ otherwise. The same rationale can be applied for the other non-linear terms. The interested reader is advised to refer to [123] and [180] for more details.

B.2 Multiplication of continous and binary variables

The multiplication of binary variable g and continuous variable x renders an optimization problem non-linear. The linearization is performed by introducing a new continuous variable

y that takes on the resulting value of the multiplication, as shown in (B.12):

$$y = g \cdot x \qquad\qquad (B.12)$$

In order to linearize (B.12), the following constraints are needed:

$$y \leq x \qquad\qquad (B.13)$$

$$y \geq x - M \cdot (1 - g) \qquad\qquad (B.14)$$

$$y \leq M \cdot g \qquad\qquad (B.15)$$

where M is a large number. For example, if $g = 0$, then according to (B.15), $y = 0$. However, if $g = 1$, then equation (B.15) is non-binding. In addition, in (B.13), $y \leq x$ and in (B.14), $y \geq x$, and thus $y = x$ is obtained. By using constraints (B.13)-(B.15), the variable y can either take on the value of 0 or x.

Constraints (B.13)-(B.15) can be used to linearize each multiplication of binary and continuous variables present in equations (4.3)-(4.6). In (4.3)-(4.6), the binary variables are $w_{t,b}^{\text{up}}$, $w_{t,b}^{\text{dn}}$, $v_{t,b}^{\text{up}}$, and $v_{t,b}^{\text{dn}}$, and the positive continuous variables are p_t^{up}, p_t^{dn}, $e_{t,g}^{\text{regup}}$, and $e_{t,g}^{\text{stopdsg}}$.

BIBLIOGRAPHY

[1] "Fueling a better future," Union of Concerned Scientists, Report, 2013.

[2] "Southern california edison: Tariffs," 2015. [Online]. Available: www.sce.com/wps/portal/home/regulatory/tariff-books/rates-pricing-choices/business-rates

[3] "Fuel economy of cars," 2015. [Online]. Available: https://www.fueleconomy.gov/

[4] "Plug-in electric vehicle handbook for consumers," U.S. Department of Energy, Report, 2015.

[5] "Inventory of u.s. greenhouse gas emissions and sinks: 1990-2013," 2015. [Online]. Available: http://www.epa.gov/climatechange/Downloads/ghgemissions/US-GHG-Inventory-2015-Main-Text.

[6] "Global ev outlook: Understanding the electric vehicle landscape to 2020," International Energy Agency, Report, 2013. [Online]. Available: www.iea.org/publications/globalevoutlook_2013.pdf

[7] J. A. P. Lopes, F. J. Soares, and P. M. R. Almeida, "Integration of electric vehicles in the electric power system," *Proceedings of the IEEE*, vol. 99, no. 1, pp. 168–183, 2011.

[8] M. Sarker, M. Ortega-Vazquez, and D. Kirschen, "Optimal coordination and scheduling of demand response via monetary incentives," *IEEE Transactions on Smart Grid*, vol. 6, no. 3, pp. 1341–1352, May 2015.

[9] M. R. Sarker, H. Pandzic, and M. A. Ortega-Vazquez, "Optimal operation and services scheduling for an electric vehicle battery swapping station," *IEEE Trans. on Power Systems*, vol. PP, no. 99, pp. 1–10, 2014.

[10] M. A. Ortega-Vazquez, "Optimal scheduling of electric vehicle charging and vehicle-to-grid services at household level including battery degradation and price uncertainty," *IET Gen., Trans. & Dist.*, vol. 8, no. 6, pp. 1007–1016, 2014.

[11] B. Zhang, A. Y. S. Lam, A. D. Dominguez-Garcia, and D. Tse, "An optimal and distributed method for voltage regulation in power distribution systems," *IEEE Transactions on Power Systems*, vol. 30, no. 4, pp. 1714–1726, 2015.

[12] H. Sekyung, H. Soohee, and K. Sezaki, "Estimation of achievable power capacity from plug-in electric vehicles for v2g frequency regulation: Case studies for market participation," *IEEE Transactions on Smart Grid*, vol. 2, no. 4, pp. 632–641, 2011.

[13] ——, "Development of an optimal vehicle-to-grid aggregator for frequency regulation," *IEEE Transactions on Smart Grid*, vol. 1, no. 1, pp. 65–72, 2010.

[14] E. Sortomme and M. A. El-Sharkawi, "Optimal scheduling of vehicle-to-grid energy and ancillary services," *IEEE Trans. on Smart Grid*, vol. 3, no. 1, pp. 351–359, 2012.

[15] J. Donadee and M. Ilic, "Stochastic optimization of grid to vehicle frequency regulation capacity bids," *IEEE Transactions on Smart Grid*, vol. 5, no. 2, pp. 1061–1069, March 2014.

[16] J. J. Escudero-Garzas, A. Garcia-Armada, and G. Seco-Granados, "Fair design of plug-in electric vehicles aggregator for v2g regulation," *IEEE Trans. on Vehicular Technology*, vol. 61, no. 8, pp. 3406–3419, 2012.

[17] W. Kempton, J. Tomic, S. Letendre, A. Brooks, and T. Lipman, "Vehicle-to-grid power: Battery, hybrid, and fuel cell vehicles as resources for distributed electric power in california," 2001. [Online]. Available: http://www.escholarship.org/uc/item/0qp6s4mb

[18] C. Guille and G. Gross, "A conceptual framework for the vehicle-to-grid (v2g) implementation," *Energy Policy*, vol. 37, no. 11, pp. 4379–4390, 2009. [Online]. Available: http://www.sciencedirect.com/science/article/pii/S0301421509003978

[19] L. Pieltain, Fernandez, T. G. S. Roman, R. Cossent, C. M. Domingo, and P. Frias, "Assessment of the impact of plug-in electric vehicles on distribution networks," *IEEE Transactions on Power Systems*, vol. 26, no. 1, pp. 206–213, 2011.

[20] J. Neubauer and E. Wood, "The impact of range anxiety and home, workplace, and public charging infrastructure on simulated battery electric vehicle lifetime utility," *Journal of Power Sources*, vol. 257, pp. 12 – 20, 2014.

[21] V. Silva, M. Entem, M. Aunedi, A. Shakoor, L. Glorieux, I. Bunzec, M. Bolczek, E. Plota, E. Szczechowicz, N. Vidal, M. Ortega-Vazquez, F. Pettersson, and P. Scuro, "D3.3: List of identified barriers and opportunities for large scale deployment of ev/phev and elaboration of potential solutions," 2011. [Online]. Available: www.g4v.eu/downloads.html

[22] P. Nelson, K. Amine, A. Rousseau, and H. Yomoto, "Advanced lithium-ion batteries for plug-in hybrid-electric vehicles: Argonne national laboratory: Argonne national laboratory," Report, 2013.

[23] S. Lowe, Marcy amd Tokuoka, T. Trigg, and G. Gereffi, "Lithium-ion batteries for electric vehicles: The u.s. value chain," Center on Globalization Governance & Competitiveness, Report, 2010.

[24] "Gas station statistics." [Online]. Available: www.statisticbrain.com/gas-station-statistics/

[25] "Electric vehicle charging station locations: U.s. department of energy." [Online]. Available: www.afdc.energy.gov/fuels/electricity_locations.html

[26] "Chargepoint: Ev charging network," 2015. [Online]. Available: http://www.chargepoint.com/network/

[27] "How do residential level 2 charging installation costs vary by geographic location?" Idaho National Laboratory, Report, 2015.

[28] "Bosch dc faster charger," 2015. [Online]. Available: www.chargepoint.com/files/BMW_i_DC_fast_charger_datasheet.pdf

[29] "Nissan leaf specifications." [Online]. Available: www.nissanusa.com/electric-cars/leaf/versions-specs/

[30] "Sae electric vehicle and plug in hybrid electric vehicle conductive charge coupler." [Online]. Available: http://standards.sae.org/j1772_201210/

[31] "General electric: Wattstation." [Online]. Available: www.geindustrial.com/products/static/ecomagination-electric-vehicles

[32] "Tesla motors supercharger stations." [Online]. Available: www.teslamotors.com/supercharger

[33] B. Nykvist and M. Nilsson, "Rapidly falling costs of battery packs for electric vehicles," *Nature Clim. Change*, vol. 5, no. 4, pp. 329–332, 2015. [Online]. Available: http://dx.doi.org/10.1038/nclimate2564

[34] "Battery technology charges ahead," 2012. [Online]. Available: www.mckinsey.com/insights/energy_resources_materials/battery_technology_charges_ahead

[35] "Crossing the line: Li-ion battery cost reduction and its effect on vehicles and stationary storage," Lux Research, Report, 2015. [Online]. Available: https://portal.luxresearchinc.com/research/report_excerpt/19123

[36] G. Heydt, "The impact of electric vehicle deployment on load management straregies," *IEEE Transactions on Power Apparatus and Systems*, vol. PAS-102, no. 5, pp. 1253–1259, May 1983.

[37] W. Kempton and S. E. Letendre, "Electric vehicles as a new power source for electric utilities," *Transportation Research Part D: Transport and Environment*, vol. 2, no. 3, pp. 157 – 175, 1997. [Online]. Available: http://www.sciencedirect.com/science/article/pii/S1361920997000011

[38] "Ac propulsion, inc." 2015. [Online]. Available: http://acpropulsion.com/about.html

[39] D. Tuttle and R. Baldick, "The evolution of plug-in electric vehicle-grid interactions," *IEEE Transactions on Smart Grid*, vol. 3, no. 1, pp. 500–505, March 2012.

[40] M. Yilmaz and P. Krein, "Review of battery charger topologies, charging power levels, and infrastructure for plug-in electric and hybrid vehicles," *IEEE Transactions on Power Electronics*, vol. 28, no. 5, pp. 2151–2169, May 2013.

[41] J. Tomi and W. Kempton, "Using fleets of electric-drive vehicles for grid support," *Journal of Power Sources*, vol. 168, no. 2, pp. 459 – 468, 2007. [Online]. Available: http://www.sciencedirect.com/science/article/pii/S0378775307005575

[42] K. Sun, M. Sarker, and M. Ortega-Vazquez, "Statistical characterization of electric vehicle charging in different locations of the grid," in *2015 IEEE Power Energy Society General Meeting*, July 2015, pp. 1–5.

[43] T. Wu, Q. Yang, Z. Bao, and W. Yan, "Coordinated energy dispatching in microgrid with wind power generation and plug-in electric vehicles," *IEEE Transactions on Smart Grid*, vol. 4, no. 3, pp. 1453–1463, Sept 2013.

[44] M. Vasirani, R. Kota, R. Cavalcante, S. Ossowski, and N. Jennings, "An agent-based approach to virtual power plants of wind power generators and electric vehicles," *IEEE Transactions on Smart Grid*, vol. 4, no. 3, pp. 1314–1322, Sept 2013.

[45] W. Hu, C. Su, Z. Chen, and B. Bak-Jensen, "Optimal operation of plug-in electric vehicles in power systems with high wind power penetrations," *IEEE Transactions on Sustainable Energy*, vol. 4, no. 3, pp. 577–585, July 2013.

[46] M. Khodayar, L. Wu, and M. Shahidehpour, "Hourly coordination of electric vehicle operation and volatile wind power generation in scuc," *IEEE Transactions on Smart Grid*, vol. 3, no. 3, pp. 1271–1279, Sept 2012.

[47] L. Cheng, Y. Chang, and R. Huang, "Mitigating voltage problem in distribution system with distributed solar generation using electric vehicles," *IEEE Transactions on Sustainable Energy*, vol. 6, no. 4, pp. 1475–1484, Oct 2015.

[48] S. Gunter, K. Afridi, and D. Perreault, "Optimal design of grid-connected pev charging systems with integrated distributed resources," *IEEE Transactions on Smart Grid*, vol. 4, no. 2, pp. 956–967, June 2013.

[49] M. Zhongjing, D. S. Callaway, and I. A. Hiskens, "Decentralized charging control of large populations of plug-in electric vehicles," *IEEE Transactions on Control Systems Technology*, vol. 21, no. 1, pp. 67–78, 2013.

[50] G. Binetti, A. Davoudi, D. Naso, B. Turchiano, and F. Lewis, "Scalable real-time electric vehicles charging with discrete charging rates," *IEEE Transactions on Smart Grid*, vol. 6, no. 5, pp. 2211–2220, Sept 2015.

[51] G. Lingwen, U. Topcu, and S. H. Low, "Optimal decentralized protocol for electric vehicle charging," *IEEE Transactions on Power Systems*, vol. 28, no. 2, pp. 940–951, 2013.

[52] E. Sortomme, M. Hindi, S. MacPherson, and S. Venkata, "Coordinated charging of plug-in hybrid electric vehicles to minimize distribution system losses," *IEEE Transactions on Smart Grid*, vol. 2, no. 1, pp. 198–205, March 2011.

[53] X. Luo and K. W. Chan, "Real-time scheduling of electric vehicles charging in low-voltage residential distribution systems to minimise power losses and improve voltage profile," *Generation, Transmission Distribution, IET*, vol. 8, no. 3, pp. 516–529, March 2014.

[54] H. Turker, S. Bacha, and A. Hably, "Rule-based charging of plug-in electric vehicles (pevs): Impacts on the aging rate of low-voltage transformers," *IEEE Transactions on Power Delivery*, vol. 29, no. 3, pp. 1012–1019, 2014.

[55] S. Weckx, R. D'Hulst, B. Claessens, and J. Driesensam, "Multiagent charging of electric vehicles respecting distribution transformer loading and voltage limits," *IEEE Transactions on Smart Grid*, vol. 5, no. 6, pp. 2857–2867, 2014.

[56] A. D. Hilshey, P. D. H. Hines, P. Rezaei, and J. R. Dowds, "Estimating the impact of electric vehicle smart charging on distribution transformer aging," *IEEE Transactions on Smart Grid*, vol. 4, no. 2, pp. 905–913, 2013.

[57] Q. Gong, S. Midlam-Mohler, V. Marano, and G. Rizzoni, "Distribution of pev charging resources to balance transformer life and customer satisfaction," in *Electric Vehicle Conference (IEVC), 2012 IEEE International*, Conference Proceedings, pp. 1–7.

[58] M. Humayun, M. Z. Degefa, A. Safdarian, and M. Lehtonen, "Utilization improvement of transformers using demand response," *IEEE Transactions on Power Delivery*, vol. 30, no. 1, pp. 202–210, 2015.

[59] W. Kersting, *Distribution System Modeling and Analysis.* Second Edition (Electric Power Engineering Series): CRC Press, 2001, doi:10.1201/9781420041736.fmatt.

[60] M. Farivar and S. H. Low, "Branch flow model: Relaxations and convexification: Part i," *IEEE Transactions on Power Systems*, vol. 28, no. 3, pp. 2554–2564, 2013.

[61] J. M. Sexauer, K. D. McBee, and K. A. Bloch, "Applications of probability model to analyze the effects of electric vehicle chargers on distribution transformers," *IEEE Transactions on Power Systems*, vol. 28, no. 2, pp. 847–854, 2013.

[62] H. Turker, S. Bacha, D. Chatroux, and A. Hably, "Low-voltage transformer loss-of-life assessments for a high penetration of plug-in hybrid electric vehicles (phevs)," *IEEE Transactions on Power Delivery*, vol. 27, no. 3, pp. 1323–1331, 2012.

[63] "Duke power - business." [Online]. Available: www.duke-energy.com/business.asp

[64] "Pacific northwest smart grid demonstration project," 2015. [Online]. Available: www.pnwsmartgrid.org/

[65] Z. Haiwang, X. Le, and X. Qing, "Coupon incentive-based demand response: Theory and case study," *IEEE Transactions on Power Systems*, vol. 28, no. 2, pp. 1266–1276, 2013.

[66] O. Erdinc, N. Paterakis, T. Mendes, A. Bakirtzis, and J. Catalao, "Smart household operation considering bi-directional ev and ess utilization by real-time pricing-based dr," *IEEE Transactions on Smart Grid*, vol. 6, no. 3, pp. 1281–1291, May 2015.

[67] Z. Tan, P. Yang, and A. Nehorai, "An optimal and distributed demand response strategy with electric vehicles in the smart grid," *IEEE Transactions on Smart Grid*, vol. 5, no. 2, pp. 861–869, March 2014.

[68] Y. He, B. Venkatesh, and L. Guan, "Optimal scheduling for charging and discharging of electric vehicles," *IEEE Transactions on Smart Grid*, vol. 3, no. 3, pp. 1095–1105, Sept 2012.

[69] C. Zhou, K. Qian, M. Allan, and W. Zhou, "Modeling of the cost of ev battery wear due to v2g application in power systems," *IEEE Transactions on Energy Conversion*, vol. 26, no. 4, pp. 1041–1050, Dec 2011.

[70] D. Pengwei and L. Ning, "Appliance commitment for household load scheduling," *IEEE Transactions on Smart Grid*, vol. 2, no. 2, pp. 411–419, 2011.

[71] L. Ning, "An evaluation of the hvac load potential for providing load balancing service," *IEEE Transactions on Smart Grid*, vol. 3, no. 3, pp. 1263–1270, 2012.

[72] M. Stadler, W. Krause, M. Sonnenschein, and U. Vogel, "Modelling and evaluation of control schemes for enhancing load shift of electricity demand for cooling devices," *Environmental Modelling & Software*, vol. 24, no. 2, pp. 285–295, 2009. [Online]. Available: http://www.sciencedirect.com/science/article/pii/S1364815208001321

[73] A. J. Conejo, J. M. Morales, and L. Baringo, "Real-time demand response model," *IEEE Transactions on Smart Grid*, vol. 1, no. 3, pp. 236–242, 2010.

[74] A. H. Mohsenian-Rad and A. Leon-Garcia, "Optimal residential load control with price prediction in real-time electricity pricing environments," *IEEE Transactions on Smart Grid*, vol. 1, no. 2, pp. 120–133, 2010.

[75] A. Agnetis, G. de Pascale, P. Detti, and A. Vicino, "Load scheduling for household energy consumption optimization," *IEEE Transactions on Smart Grid*, vol. 4, no. 4, pp. 2364–2373, 2013.

[76] M. Pipattanasomporn, M. Kuzlu, and S. Rahman, "An algorithm for intelligent home energy management and demand response analysis," *IEEE Transactions on Smart Grid*, vol. 3, no. 4, pp. 2166–2173, Dec 2012.

[77] "Nest," 2015. [Online]. Available: www.nest.com

[78] "Whirlpool: Smart electric water heaters." [Online]. Available: http://goo.gl/98ww62

[79] "opower," 2015. [Online]. Available: https://opower.com

[80] "Vivint, inc." 2015. [Online]. Available: www.vivint.com

[81] J. Fuller and G. Parker, "Modeling of ge appliances: Cost benefit study of smart appliances in wholesale energy, frequency regulation,and spinning reserve markets," Report, 2012. [Online]. Available: www.pnnl.gov/main/publications/external/technical_reports/PNNL-22128.pdf

[82] "Pjm manual 11: Energy & ancillary services market," 2015. [Online]. Available: http://www.pjm.com/~/media/documents/manuals/m11.ashx

[83] J. MacDonald, P. Cappers, D. Callaway, and S. Kiliccote, "Demand response providing ancillary services: A comparison of opportunities and challenges in the us wholesale markets," *Grid-Interop Forum 2012*, 2012.

[84] W. Di, D. C. Aliprantis, and Y. Lei, "Load scheduling and dispatch for aggregators of plug-in electric vehicles," *IEEE Transactions on Smart Grid*, vol. 3, no. 1, pp. 368–376, 2012.

[85] M. A. Ortega-Vazquez, F. Bouffard, and V. Silva, "Electric vehicle aggregator/system operator coordination for charging scheduling and services procurement," *IEEE Trans. on Power Systems*, vol. 28, no. 2, pp. 1806–1815, 2013.

[86] S. I. Vagropoulos and A. G. Bakirtzis, "Optimal bidding strategy for electric vehicle aggregators in electricity markets," *IEEE Trans. on Power Systems*, vol. 28, no. 4, pp. 4031–4041, 2013.

[87] E. Sortomme and M. A. El-Sharkawi, "Optimal combined bidding of vehicle-to-grid ancillary services," *IEEE Trans. on Smart Grid*, vol. 3, no. 1, pp. 70–79, 2012.

[88] R. J. Bessa, M. A. Matos, F. J. Soares, and J. A. P. Lopes, "Optimized bidding of a ev aggregation agent in the electricity market," *IEEE Trans. on Smart Grid*, vol. 3, no. 1, pp. 443–452, 2012.

[89] D. Kirschen and G. Strbac, *Fundamentals of Power System Economics*. John Wiley & Sons, 2004.

[90] F. Bouffard, F. D. Galiana, and A. J. Conejo, "Market-clearing with stochastic security-part i: formulation," *IEEE Trans. on Power Systems*, vol. 20, no. 4, pp. 1818–1826, 2005.

[91] G. Fox, "Electric vehicle charging stations: Are we prepared?" *Industry Applications Magazine, IEEE*, vol. 19, no. 4, pp. 32–38, July 2013.

[92] "Ev everywhere: Workplace charging challenge progress update 2014," U.S. Department of Energy: Energy Efficiency & Renewable Energy, Report, 2014.

[93] N. Neyestani, M. Yazdani Damavandi, M. Shafie-khah, J. Contreras, and J. Catalao, "Allocation of plug-in vehicles' parking lots in distribution systems considering network-constrained objectives," *IEEE Transactions on Power Systems*, vol. 30, no. 5, pp. 2643–2656, Sept 2015.

[94] A. Lam, Y.-W. Leung, and X. Chu, "Electric vehicle charging station placement: Formulation, complexity, and solutions," *IEEE Transactions on Smart Grid*, vol. 5, no. 6, pp. 2846–2856, Nov 2014.

[95] Z. Liu, F. Wen, and G. Ledwich, "Optimal planning of electric-vehicle charging stations in distribution systems," *IEEE Transactions on Power Delivery*, vol. 28, no. 1, pp. 102–110, Jan 2013.

[96] "Plug-in electric vehicle handbook for public charging station hosts," U.S. Department of Energy: Energy Efficiency & Renewable Energy, Report, 2012.

[97] P. Fan, B. Sainbayar, and S. Ren, "Operation analysis of fast charging stations with energy demand control of electric vehicles," *IEEE Trans. on Smart Grid*, vol. 6, no. 4, pp. 1819–1826, July 2015.

[98] P. You, Z. Yang, M. Y. Chow, and Y. Sun, "Optimal cooperative charging strategy for a smart charging station of electric vehicles," *IEEE Trans. on Power Systems*, vol. 31, no. 4, pp. 2946–2956, July 2016.

[99] O. Hafez and K. Bhattacharya, "Integrating ev charging stations as smart loads for demand response provisions in distribution systems," *IEEE Trans. on Smart Grid*, vol. PP, no. 99, pp. 1–1, 2016.

[100] D. Anand, R. de Salis, Y. Cheng, J. Moyne, and D. Tilbury, "A hierarchical incentive arbitration scheme for coordinated pev charging stations," *IEEE Transactions on Smart Grid*, vol. 6, no. 4, pp. 1775–1784, July 2015.

[101] J. Timpner and L. Wolf, "Design and evaluation of charging station scheduling strategies for electric vehicles," *IEEE Transactions on Intelligent Transportation Systems*, vol. 15, no. 2, pp. 579–588, April 2014.

[102] S. Negarestani, M. Fotuhi-Firuzabad, M. Rastegar, and A. Rajabi-Ghahnavieh, "Optimal sizing of storage system in a fast charging station for plug-in hybrid electric vehicles," *IEEE Trans. on Transportation Electrification*, vol. PP, no. 99, pp. 1–1, 2016.

[103] N. Machiels, N. Leemput, F. Geth, J. V. Roy, J. Bscher, and J. Driesen, "Design criteria for electric vehicle fast charge infrastructure based on flemish mobility behavior," *IEEE Trans. on Smart Grid*, vol. 5, no. 1, pp. 320–327, Jan 2014.

[104] I. S. Bayram, G. Michailidis, M. Devetsikiotis, and F. Granelli, "Electric power allocation in a network of fast charging stations," *IEEE Journal on Selected Areas in Communications*, vol. 31, no. 7, pp. 1235–1246, July 2013.

[105] "General electric - electric vehicle charging stations." [Online]. Available: www.geindustrial.com/products/electric-vehicle-charging-stations

[106] "Basic business concepts: Electric vehicle," G4V: Grid for Vehicles, Report, 2011.

[107] J. Lidicker, T. Lipman, and B. Williams, "Business model for subscription service for electric vehicles including battery swapping, for san francisco bay area, california," *Transportation Research Record: Journal of the Transportation Research Board*, vol. 2252, pp. 83–90, 2011.

[108] J. S. Neubauer and A. Pesaran, "A techno-economic analysis of bev service providers offering battery swapping services," National Renewable Energy Laboratory, Report, 2013, (U.S.) Title from title screen (viewed Dec. 9, 2013). "Published 04/08/2013." "Presented at the SAE 2013 World Congress & Exhibition." "2013-01-0500." Includes bibliographical references (p. 13-15). [Online]. Available: http://search.library.wisc.edu/catalog/ocn864890028

[109] "Tesla motors: Battery swap." [Online]. Available: www.teslamotors.com/batteryswap

[110] Z. Yu, D. Zhao Yang, X. Yan, M. Ke, Z. Jun Hua, and Q. Jing, "Electric vehicle battery charging/swap stations in distribution systems: Comparison study and optimal planning," *IEEE Transactions on Power Systems*, vol. 29, no. 1, pp. 221–229, 2014.

[111] O. Worley and D. Klabjan, "Optimization of battery charging and purchasing at electric vehicle battery swap stations," in *Vehicle Power and Propulsion Conference (VPPC), 2011 IEEE*, Conference Proceedings, pp. 1–4.

[112] G. Ya-jing, Z. Kai-xuan, and W. Chen, "Economic dispatch containing wind power and electric vehicle battery swap station," in *Transmission and Distribution Conference and Exposition (T&D), 2012 IEEE PES*, Conference Proceedings, pp. 1–7.

[113] "Better place: Battery switch stations (bss)." [Online]. Available: www.betterplace.com

[114] "China electric vehicle charging station market report, 2012-2013," Research in China, Report, 2013.

[115] B. Xu, A. Oudalov, A. Ulbig, G. Andersson, and D. Kirschen, "Modeling of lithium-ion battery degradation for cell life assessment," *IEEE Transactions on Smart Grid*, vol. PP, no. 99, pp. 1–1, 2016.

[116] O. Tremblay and L.-A. Dessaint, "Experimental validation of a battery dynamic model for ev applications," *World Electric Vehicle Journal*, vol. 3, no. 1, pp. 1–10, 2009.

[117] K. Thirugnanam, H. Saini, and P. Kumar, "Mathematical modeling of li-ion battery for charge/discharge rate and capacity fading characteristics using genetic algorithm approach," in *2012 IEEE Transportation Electrification Conference and Expo (ITEC)*, June 2012, pp. 1–6.

[118] G. Ning, B. Haran, and B. N. Popov, "Capacity fade study of lithium-ion batteries cycled at high discharge rates," *Journal of Power Sources*, vol. 117, no. 12, pp. 160 – 169, 2003. [Online]. Available: http://www.sciencedirect.com/science/article/pii/S0378775303000296

[119] P. Moss, G. Au, E. Plichta, and J. Zheng, "Study of capacity fade of lithium-ion polymer rechargeable batteries with continuous cycling," *Journal of the Electrochemical Society*, vol. 157, no. 1, pp. A1–A7, 2010.

[120] M. R. Sarker, Y. Dvorkin, and M. A. Ortega-Vazquez, "Optimal participation of an electric vehicle aggregator in day-ahead energy and reserve markets," *IEEE Transactions on Power Systems*, 2015.

[121] T. A. Nguyen and M. L. Crow, "Stochastic optimization of renewable-based micro-grid operation incorporating battery operating cost," *IEEE Trans. on Power Systems*, vol. 31, no. 3, pp. 2289–2296, May 2016.

[122] A. Hoke, A. Brissette, D. Maksimovi, A. Pratt, and K. Smith, "Electric vehicle charge optimization including effects of lithium-ion battery degradation," in *2011 IEEE Vehicle Power and Propulsion Conference*, Sept 2011, pp. 1–8.

[123] C. P. Christelle and M. Sevaux, *Applications of optimization with Xpress - MP*, 2002.

[124] "National household travel survey (nhts) data," NHTS, Report, 2009. [Online]. Available: www.nhts.ornl.gov

[125] "Day-ahead lmp prices," 2013. [Online]. Available: www.pjm.com/markets-and-operations/energy/day-ahead/lmpda.aspx

[126] "Ieee distribution test feeders." [Online]. Available: www.ewh.ieee.org/soc/pes/dsacom/testfeeders/index.html

[127] D. H. Doughty and A. Pesaran, "Vehicle battery safety roadmap guidance," National Renewable Energy Laboratory, Report, 2012.

[128] D. L. James, L. Xiaomin, E. M. James, W. Camilla Dunham, J. S. Leslie, and Q. T. McCure, "Modeling patterns of hot water use in households," Lawrence Berkeley National Laboratory, Report, 1996, formal Report, Energy and Buildings, v: 26, 2, 1997 LBL-37805R.

[129] "Ieee guide for determining the effects of high-temperature operation on conductors, connectors, and accessories," *IEEE Std 1283-2013 (Revision of IEEE Std 1283-2004)*, pp. 1–47, 2013.

[130] V. T. Morgan, "Effect of elevated temperature operation on the tensile strength of overhead conductors," *IEEE Transactions on Power Delivery*, vol. 11, no. 1, pp. 345–352, 1996.

[131] P. Musilek, J. Heckenbergerova, and M. M. I. Bhuiyan, "Spatial analysis of thermal aging of overhead transmission conductors," *IEEE Transactions on Power Delivery*, vol. 27, no. 3, pp. 1196–1204, 2012.

[132] "Ieee guide for loading mineral-oil-immersed transformers and step-voltage regulators," *IEEE Std C57.91-2011 (Revision of IEEE Std C57.91-1995)*, pp. 1–123, 2012.

[133] A. Seier, P. D. H. Hines, and J. Frolik, "Data-driven thermal modeling of residential service transformers," *IEEE Transactions on Smart Grid*, vol. 6, no. 2, pp. 1019–1025, 2015.

[134] P. Fox-Penner, *Smart Power: Climate Change, the Smart Grid, and the Future of Electric Utilities*. Island Press, 2010.

[135] P. J. Balducci, L. A. Schienbein, T. B. Nguyen, D. R. Brown, and E. M. Fatherlrahman, "An examination of the costs and critical characteristics of electric utility distribution system capacity enhancement projects," in *Transmission and Distribution Conference and Exhibition, 2005/2006 IEEE PES*, Conference Proceedings, pp. 78–86.

[136] "Residential electric service installation - comed." [Online]. Available: www.comed.com/documents/customer-service/service-request/redbook101007_inorder1.pdf

[137] "Pecanstreet: Energy dataport," 2015. [Online]. Available: https://dataport.pecanstreet.org/

[138] "Gridlab-d taxonomy feeders," 2015. [Online]. Available: http://sourceforge.net/p/gridlab-d/code/HEAD/tree/Taxonomy_Feeders/

[139] D. Arthur and S. Vassilvitskii, "k-means++: the advantages of careful seeding," pp. 1027–1035, 2007.

[140] "National oceanic and atmospheric administration (noaa): Temperature data," 2015. [Online]. Available: www.ncdc.noaa.gov/qclcd/QCLCD

[141] M. Humayun, A. Safdarian, M. Z. Degefa, and M. Lehtonen, "Demand response for operational life extension and efficient capacity utilization of power transformers during contingencies," *IEEE Transactions on Power Systems*, vol. PP, no. 99, pp. 1–10, 2014.

[142] R. Moyer, J. McGuigan, and R. Rao, *Contemporary Financial Management*. Cengage Learning, 2014. [Online]. Available: https://books.google.com/books?id=pFQ8AwAAQBAJ

[143] H. A. Gil and G. Joos, "On the quantification of the network capacity deferral value of distributed generation," *IEEE Transactions on Power Systems*, vol. 21, no. 4, pp. 1592–1599, 2006.

[144] "Ercot: The market guide." 2014. [Online]. Available: http://ercot.com/mktrules/bpm

[145] Y. V. Makarov, C. Loutan, M. Jian, and P. de Mello, "Operational impacts of wind generation on california power systems," *IEEE Transactions on Power Systems*, vol. 24, no. 2, pp. 1039–1050, 2009.

[146] Y. Dvorkin, D. S. Kirschen, and M. A. Ortega-Vazquez, "Assessing flexibility requirements in power systems," *Generation, Transmission & Distribution, IET*, vol. 8, no. 11, pp. 1820–1830, 2014.

[147] F. D. Galiana, F. Bouffard, J. M. Arroyo, and J. F. Restrepo, "Scheduling and pricing of coupled energy and primary, secondary, and tertiary reserves," *Proceedings of the IEEE*, vol. 93, no. 11, pp. 1970–1983, 2005.

[148] T. Zhen, "Real-time energy and reserve co-optimization," Report, 2011. [Online]. Available: www.iso-ne.com/support/training/courses/wem301/wem301_energy_reserve.pdf

[149] H. Pandzic, Y. Dvorkin, W. Yishen, Q. Ting, and D. S. Kirschen, "Effect of time resolution on unit commitment decisions in systems with high wind penetration," in *2014 IEEE PES General Meeting*, Conference Proceedings, pp. 1–5.

[150] D. Lew, G. Brinkman, E. Ibanez, A. Florita, M. Heaney, B.-M. Hodge, M. Hummon, and G. Stark, "The western wind and solar integration study phase 2," NREL, Report, 2013.

[151] E. Ela and M. O'Malley, "Studying the variability and uncertainty impacts of variable generation at multiple timescales," *IEEE Transactions on Power Systems*, vol. 27, no. 3, pp. 1324–1333, 2012.

[152] "Ercot day-ahead market." [Online]. Available: www.ercot.com/mktinfo/dam

[153] M. A. Ortega-Vazquez and D. S. Kirschen, "Optimizing the spinning reserve requirements using a cost/benefit analysis," *IEEE Trans. on Power Systems*, vol. 22, no. 1, pp. 24–33, 2007.

[154] G. J. Hahn and S. S. Shapiro, *Statistical models in engineering.* New York: Wiley, 1967.

[155] E. Karangelos and F. Bouffard, "Towards full integration of demand-side resources in joint forward energy/reserve electricity markets," *IEEE Trans. on Power Systems*, vol. 27, no. 1, pp. 280–289, 2012.

[156] N. Troy, E. Denny, and M. O'Malley, "Base-load cycling on a system with significant wind penetration," *IEEE Trans. on Power Systems*, vol. 25, no. 2, pp. 1088–1097, 2010.

[157] "Demand response frequently asked questions - caiso," 2016. [Online]. Available: www.caiso.com/Documents/DemandResponseandProxyDemandResourcesFrequentlyAskedQuestions

[158] "Load participation in the ercot nodal market," ERCOT, Report, 2016.

[159] S. Braithwait, D. Hanse, and M. O'Sheasy, "Retail electricity pricing and rate design in evolving markets," Edison Electric Institute, Report, 2007.

[160] A. J. Conejo, M. Carrión, and J. M. Morales, *Decision making under uncertainty in electricity markets.* Springer New York, 2010, vol. 1.

[161] D. Bertsimas and M. Sim, "The price of robustness," *Operations Research*, vol. 52, no. 1, pp. 35–53, 2004.

[162] A. L. Soyster, "Convex programming with set-inclusive constraints and applications to inexact linear programming," *Operations Research*, vol. 21, no. 5, pp. 1154–1157, 1973.

[163] R. Carnegie, D. Gotham, D. Nderitu, and P. V. Preckel, "Utility scale energy storage systems: Benefits, applications, and technologies," Report, 2013.

[164] "A123 apr18650 lithium ion cylindrical cell." [Online]. Available: www.a123systems.com/lifepo4-battery-cell.htm

[165] L. Kaufman and P. Rousseeuw, "Clustering by means of medoids," *Statistical Data Analysis Based on the L1-Norm and Related Methods*, pp. North–Holland, 1987.

[166] "Ercot market prices." [Online]. Available: www.ercot.com/mktinfo/prices/index.html

[167] M. Sarker, H. Pandzic, and M. Ortega-Vazquez, "Electric vehicle battery swapping station: Business case and optimization model," in *Connected Vehicles and Expo (IC-CVE), 2013 International Conference on*, Dec 2013, pp. 289–294.

[168] K. Morrowa, D. Karner, and J. Francfort, "Plug-in hybrid electric vehicle charging infrastructure review," U.S. Dep. Energy Veh. Technol. Program, Report, 2008 2008. [Online]. Available: http://avt.inl.gov/pdf/phev/phevInfrastructureReport08.pdf

[169] "Technology roadmap: Electric and plug-in hybrid electric vehicles," International Energy Agency, Report, 2009.

[170] A. J. Wood and B. F. Wollenberg, *Power generation, operation, and control / Allen J. Wood, Bruce F. Wollenberg.* Wiley New York, 1984. [Online]. Available: http://www.loc.gov/catdir/enhancements/fy0607/83001172-t.html

[171] K. K. Kariuki and R. N. Allan, "Evaluation of reliability worth and value of lost load," *Generation, Transmission and Distribution, IEE Proceedings-*, vol. 143, no. 2, pp. 171–180, 1996.

[172] D. Bertsimas and A. Thiele, "A robust optimization approach to inventory theory," *Operations Research*, vol. 54, no. 1, pp. 150–168, 2006. [Online]. Available: http://dx.doi.org/10.1287/opre.1050.0238

[173] C. Busing and F. D'Andreagiovanni, *New Results about Multi-band Uncertainty in Robust Optimization*, ser. Lecture Notes in Computer Science. Springer Berlin Heidelberg, 2012, vol. 7276, book section 7, pp. 63–74. [Online]. Available: http://dx.doi.org/10.1007/978-3-642-30850-5_7

[174] "Amp20 lithium ion prismatic cell." [Online]. Available: www.a123systems.com/prismatic-cell-amp20.htm

[175] J. Vetter, P. Novk, M. Wagner, C. Veit, K.-C. Mller, J. Besenhard, M. Winter, M. Wohlfahrt-Mehrens, C. Vogler, and A. Hammouche, "Ageing mechanisms in lithium-ion batteries," *Journal of Power Sources*, vol. 147, no. 1-2, pp. 269–281, Sep. 2005, 01124. [Online]. Available: http://linkinghub.elsevier.com/retrieve/pii/S0378775305000832

[176] B. University, "What causes lithium ion to die?" [Online]. Available: http://batteryuniversity.com/learn/article/what_causes_lithium_ion_to_die

[177] Samsung, "Specification of Product, INR18650-15M." [Online]. Available: http://www.batteryspace.com/prod-specs/9720.pdf

[178] "Maccor 4300m automated battery cycler," 2016. [Online]. Available: www.maccor.com/Products/Model4300.aspx

[179] "Autolab pgstat128n potentiostat," 2016. [Online]. Available: www.ecochemie.nl/Products/Echem/NSeriesFolder/PGSTAT128N

[180] "Gams - a user's guide." [Online]. Available: www.gams.com/dd/docs/bigdocs/GAMSUsersGuide.pdf

[181] "User's manual for cplex," Report, 2009.